HYDROGENATION CATALYSTS FROM SUPPORTED PALLADIUM COMPLEXES

UNIVERSITY
of
GLASGOW

By

GRAHAM R. CAIRNS

A Thesis Presented to the University of Glasgow for the Degree of Doctor of Philosophy

Department of Chemistry, April 1997

ProQuest LLC.
789 East Eisenhower Parkway
P.O. Box 1346
Ann Arbor, MI 48106 – 1346

To my family and friends

SUMMARY

In the course of this study, a series of mononuclear palladium phosphine complexes, trans-$[PdX_2(PMe_3)_2]$ and the binuclear analogues, trans-$[Pd_2X_4(PR_3)_2]$ (X=Cl, Br or I; R=Me, Et, Pr^i or Bu), were prepared. The purity of the complexes were confirmed using ^1H and ^{31}P NMR spectroscopy and microanalysis (M/A). These complexes were supported on silica by a wet impregnation technique and used as catalysts in the liquid phase hydrogenation of cinnamaldehyde. The results obtained were contrasted with those from a 5 % palladium-on-silica catalyst, which was shown to produce hydrocinnamaldehyde and then phenylpropanol sequentially. The reactions of all of these catalysts took place on a hydrocarbonaceous over-layer which formed rapidly from unsaturated aldehydes and alcohols. The presence of this over-layer was confirmed from mass balance calculations and elevated C and H % microanalysis measurements on used catalysts.

The binuclear bromo- and iodo-catalysts, which resulted from hydrogen reduction of the precursors, were 100 % selective for hydrocinnamaldehyde. The bromo-catalysts, however, were found to be far more active. Catalysts prepared from the chloro-containing precursors behaved differently and produced phenylpropanol along with hydrocinnamaldehyde. The reaction mechanisms, however, were different from that which operated with the palladium-on-silica catalyst. The rates of reaction were dependant on the nature of both the halide and phosphine substituents, but the selectivities were dependant primarily on the halide.

The catalysts and precursors were characterised by X-ray photoelecton spectroscopy (XPS), microanalysis (M/A), solid state ^{31}P magic angle

spinning nuclear magnetic resonance spectroscopy (MAS-NMR), thermogravimetric analysis (TGA) and neutron activation analysis (NAA).

XPS studies indicated that part of the binuclear chloro-complexes decomposed upon impregnation onto silica. Signals corresponding to Pd(II) as well as Pd(0) were observed and the proportion of Pd(0) increased with reaction time. A large amount of the halide and phosphine were lost from the chloro-catalysts over the same time period. For the binuclear bromo-catalysts, no decomposition was observed upon impregnation and no Pd(0) was observed until after several hours reaction. A higher proportion of halide was retained for the bromo- and iodo-catalysts although a drop in phosphorus content similar to the chloro-catalysts was recorded. The difference in selectivity was attributed to a difference in stability of the active species formed from the hydrogen activation of the precursors.

For the palladium-on-silica catalyst, Pd(0) was the active species for the hydrogenation of cinnamaldehyde to hydrocinnamaldehyde and also for the hydrogenation of hydrocinnamaldehyde to phenylpropanol. The majority of the hydrocinnamaldehyde formed from the binuclear palladium phosphine catalysts, however, was produced on Pd(II) sites.

The Pd(0) sites which formed on the binuclear palladium phosphine catalysts were associated primarily with the production of phenylpropanol, although hydrocinnamaldehyde may also have been produced to a limited extent. There are three possible modes of operation for this second site. It may have produced phenylpropanol directly from cinnamaldehyde from a single visit to the catalyst surface. The diminished amount of halide in the catalyst may have permitted the simultaneous co-ordination of a cinnamaldehyde molecule through both the C=C and C=O, which was

then hydrogenated prior to desorption. Secondly, this site type may have produced cinnamyl alcohol, some of which was rapidly further hydrogenated to phenylpropanol and the rest of which was isomerised to hydrocinnamaldehyde. Third, the sites could have been the same as those produced on [Pd/SiO_2]. The Pd(0) sites formed later in the reaction on the bromo- and iodo-catalysts appeared to be completely poisoned by decomposition products. For the chloro catalysts, however, a greater number of Pd(0) sites ensured the production of some phenylpropanol, although these sites were also poisoned with time.

The mononuclear complexes [$PdX_2(PR_3)_2$] (X=Cl, Br, or I; R=Me) were prepared, impregnated on silica and examined in the same way as for the catalysts discussed previously. The mononuclear bromo- and iodo-catalysts behaved in the same way as the binuclear analogues, and produced only hydrocinnamaldehyde, although the yield of hydrocinnamaldehyde produced for the mononuclear bromo-catalyst in comparison with the binuclear analogue was much reduced. The amount of halide retained by the mononuclear bromo-catalyst was found to be significantly greater than for the binuclear analogue, however, and the reduction in the observed reaction rate may have resulted from the increased halide retention. The behaviour of the mononuclear chloro-catalyst deviated from that of the binuclear analogue, but reproducible results could not be obtained. In all cases, no cinnamyl alcohol was formed.

The reaction of catalysts formed from the binuclear bromo-catalyst precursors [$Pd_2Br_4(PR_3)_2/SiO_2$] (R=Me or Pr^i) with 2-cyclohexene-1-one, resulted in a slow conversion of 2-cyclohexene-1-one to cyclohexanone. The reduced reaction rate was attributed to the increased stability of the

metal-olefin intermediate, which suggested that the geometric configuration of the substrate was important.

The nature of the active catalysts and the reactions involved are discussed.

ACKNOWLEDGEMENTS

Firstly, I would like to thank my supervisors Dr. R. J Cross and Dr D. Stirling for all the assistance they have provided me over the last three years, for putting up with me and for putting up with many of my 'daft' questions.

I would like to thank the technical Staff in the Chemistry Department for all their assistance, with special thanks going to Mrs Kim Wilson, Mr George McCulloch, Mrs Rose Kennedy and Ms. Vicky Yates.

I would like to thank all the occupants of the Inorganic Research Office, both past and present, who have always been a source of humour when 'stuff' went wrong (which happened frequently!). In particular, I would like to thank Paul Newman (the mad Welshie), David Kennedy (Dave-E Boy), Paul Lovatt (Serious scientist), Ian McBride (Santa), Phil Mackie (Postman Pat), Cambell Scott (Biker Dude), David Anderson (Thug), John McNamara, Simon Moore and Sarah Falconer. I would even like to thank all the 4th year students who have 'lived here' throughout the years and in particular Catherine Mcavoy for helping me through the more stressful moments of writing this thesis. Although they 'nicked' our glassware, life would have been dull without them.

I would like to thank our local pub 'The Rubiyat', for their large variety of potent alcoholic beverages, without which Friday nights might never have been the same.

I would like to thank my parents - my mum for running about 'daft' after me and for making the sandwiches without which I would have starved, and to my dad to whom I must have been an enormous financial burden. Without their help I would never have got this far.

Finally, I acknowledge 'The Engineering and Physical Science Research Council' for the grant award.

TABLE OF CONTENTS

Chapter 1

INTRODUCTION

1.0 INTRODUCTION

1.1 Catalysis

The phrase 'catalysis' is not a modern term. Indeed, it was first coined by one of the 'Founding Fathers' of modern day chemistry, Jons Jacob Berzelius in 1836 (1, 2). Literally, the phrase catalysis means 'to break down'. When this phrase was first coined, the field of chemistry was at a rudimentary stage of development and as knowledge and understanding progressed, a more precise definition came into being. Today, the acceptable definition of a catalyst is "a substance which increases the rate of attainment of equilibrium in a reacting system without causing any alteration in the free energy changes of the reaction" (3).

Catalysts work by lowering the activation energy of a reaction, often by providing an alternative path that avoids the slow, rate-limiting step of the uncatalysed reaction. This results in a higher reaction rate at the same temperature (Fig 1.1)

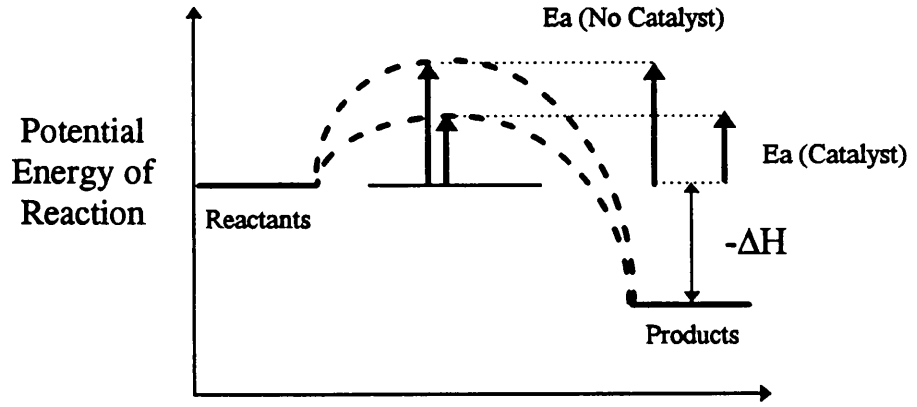

Fig 1.1

Simply reducing the energy barrier by a few kJ mol^{-1} results in a rate enhancement many orders of magnitude higher than in the uncatalysed example (Table 1.1).

The table below illustrates the effect of various catalysts on the activation energies of catalysed reactions.

Table 1.1.

Reaction	Catalyst	Ea (kJ mol^{-1})
$H_2 + I_2 \rightleftharpoons 2HI$	None	184
	Au	105
	Pt	59
$N_2 + 3H_2 \rightleftharpoons 2NH_3$	None	350
	W	162

Although catalysts work by lowering the activation energy of a particular reaction, their effects are purely kinetic in origin. The reaction itself must be thermodynamically feasible in the first place.

Quite often in the literature, catalysts are described as substances which speed up reactions but remain unchanged themselves after the reaction has ended. This statement, whilst being broadly true, comes apart upon close inspection. Using a variety of analytical techniques such as X-ray photoelectron spectroscopy (XPS), low energy electron diffraction (LEED), transmission electron microscopy (TEM) and atomic absorption (AA), processes such as surface etching, metal leeching and carbon

deposition can be observed. These processes alter the surface of the catalyst in small but important ways and over a period of time can affect catalyst activity. To this end, much of the time and effort put into the catalytic research of today has focused on trying to minimise such processes and thus preserve catalyst lifetimes.

The list below illustrates the great variety of reactions in which catalysts play a part. Almost the whole of the modern chemical industry depends on the development, selection and application of catalysts (4).

1. Metals such as Fe, Ni, Pt, Pd and Au have been used as hydrogenation and dehydrogenation catalysts.

2. Semiconducting oxides such as NiO and ZnO have been used as oxidation catalysts.

3. Insulating oxides such as Al_2O_3, SiO_2 and MgO, have been used as dehydration catalysts.

4. Acids such as H_3PO_4, H_2SO_4 and SiO_2/Al_2O_3, have been used as polymerisation, isomerisation, alkylation and cracking catalysts.

1.2 Catalytic Hydrogenation Reactions

The addition of hydrogen across the carbon-carbon double bond is one of the simplest catalysed reactions in which products and reactants are clearly different and it is for this reason that simple non-conjugated molecules such as ethene have been extensively studied (5, 6).

Although catalytic hydrogenation was discovered at the turn of the last century by Sabatier and Senderson (7), it was not until the 1940s, when isotopes of hydrogen became available, that the actual mechanistic aspects of hydrogenation became extensively studied. Since this time, literally scores of papers and books have been published. The variety and scope of hydrogenation reactions are enormous.

Groups 8-10 of the transition elements include those of atomic numbers 26-28 (Fe, Co, Ni), 44-46 (Ru, Rh, Pd) and 76-78 (Os, Ir, Pt). From these, the six elements of the platinum metals group, platinum, palladium, rhodium, ruthenium, osmium and iridium have been used most frequently as hydrogenation catalysts. The platinum metals make extremely active hydrogenation catalysts and will catalyse the reduction of most functional groups under mild conditions. In addition to these, other transition metal elements (and their oxides/sulphides) have been found to be useful in catalysing hydrogenation reactions. Cr, Mo, W, Cu and Zn have all been used; for example, copper chromite catalysts (Cu/Cr_2O_3) have been used to hydrogenate selectively a variety of polyunsaturated molecules (8, 9).

There are three main classifications of hydrogenation catalysts.

1. Supported heterogeneous catalyst.

Here, the catalyst is in a different phase from that of the reaction mixture, such as, for example, a solid catalyst and gaseous reactant system, or a solid catalyst and liquid reactant system.

Supported catalysts often have a number of advantages over their unsupported analogues. The use of a support results in greater efficiency in terms of metal use. Efficiency is improved by means of greater surface areas and also in terms of the ease of catalyst recovery. These two factors alone make them far more economically viable, considering the cost of precious and semi-precious metals. In addition to this, careful choice of support can provide further control over catalyst selectivity, as well as imparting greater resistance to poisoning.

Carbon, alumina, silica, magnesia and even silk are all examples of the broad range of materials used as catalyst supports (10). The relationship between the support chosen and catalyst performance is extremely complex and depends on such factors as the mode of catalyst preparation, the type of support used, the substrate to be hydrogenated and general experimental conditions. Physical properties of the support such as the total surface area, average pore size, pore size distribution and particle size are also important.

2. Unsupported heterogeneous catalysts.

Unsupported heterogeneous platinum metal catalysts are often used in the form of finely divided metals or metal oxides. Such metals are often referred to as blacks (or as colloidal catalysts if stabilised in solution). These types of catalyst have found use mainly in the form of fixed beds or slurry-type processes. They have been used in preference to supported catalysts in instances where a particular compound can be hydrogenated only with great difficulty, or when the catalyst support has bound the reaction products too strongly. Generally speaking, however, unsupported metal catalysts are less efficient than their supported analogues and there is the additional problem of metal recovery.

3. Homogeneous catalysts.

In this instance, the catalyst is in the same phase as the reaction mixture. Here, the platinum metal catalysts are often in the form of transition metal complexes (11, 12, 13, 14, 15). In heterogeneous systems, catalytic processes take place on the surface of the catalyst, which leads to certain diffusion limitations, whereas in the homogeneous case, since the reactants are in the same phase as the catalysts, a much greater proportion of the molecules is available for interaction at any given time. One of the most distinctive advantages which homogeneous catalysts have is high reaction specificity, such as in the asymmetric hydrogenation of organic compounds. One such example is the production of single enantiomers of organic compounds such as optically active amino acids (16). Such compounds are often produced in over 85 % enantiomeric excess (ee). This type of stereospecificity is rarely observed with heterogeneous catalysts.

Although many homogeneous transition metal compounds are used as catalysts, certain disadvantages remain. The main disadvantage lies with the difficulties which arise trying to separate them from the products. To overcome this problem, many attempts have been made to heterogenise the catalysts by attaching them to various supports such as montmorillonite (17), polymeric resins (18, 19) and silica (20). By heterogenising catalysts in this way, problems such as catalyst separation can be minimised, whilst retaining beneficial homogeneous catalyst merits such as high activity, selectivity and reproducibility.

This heterogenisation process can be carried out in three ways.

a. By attaching a metal complex to a carrier through the formation of chemical bonds. For example, π-allyl complexes have been anchored on oxidic surfaces such as silica by reaction with surface hydroxyl groups (21). Since most transition metal complexes can react to form stable complexes with phosphines, bifunctional phosphines have been used as 'linkers' between various supports and the complex itself (22).

Scheme 1.1

$$2Ph_2P(CH_2)_3Si(OEt)_3 + (COD)_2Ni \xrightarrow{-COD} (COD)Ni[Ph_2P(CH_2)_3Si(OEt)_3]_2$$

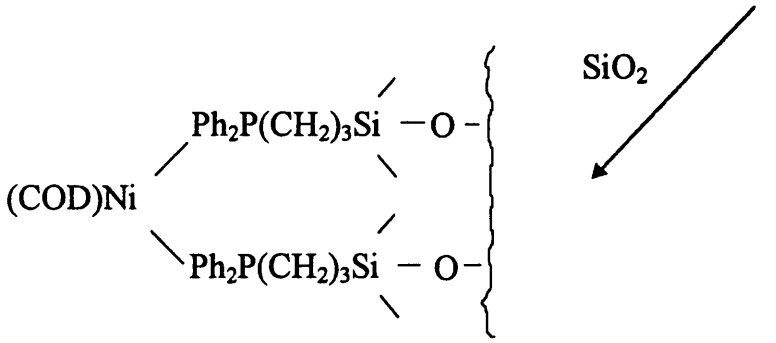

b. By physically dispersing the metal complex within the pore structure of a support by adding a solution of the complex to the support, stirring the support and complex for several hours to allow them to equilibrate and then evaporating the solvent. This technique is widely used and is known as wet impregnation.

c. By dispersing the complex in a similar manner as for (b), but with the additional presence of a relatively involatile solvent, which remains in the solid after the evaporation step and in which the complex is effectively dispersed. Supported liquid phase catalyst preparation (SLP), has been used to a much lesser extent than the two other methods listed above.

1.3 Aldehyde Hydrogenation over Platinum Metal Catalysts (23, 24)

The scope for change in the reactivity and selectivity of catalytic systems with small alterations in experimental conditions such as temperature, pressure and the method of catalyst preparation, makes the study of even simple substrate molecules often much more complicated than first would appear to be the case. This thesis is primarily concerned with the hydrogenation of cinnamaldehyde and for this reason discussion is largely limited to the literature surrounding aldehyde hydrogenation.

When hydrogenating aldehydes, the particular catalyst system chosen depends on the nature of the molecule: whether it is aliphatic or aromatic and whether it has additional unsaturation. Such factors as the addition of specific additives can influence the rate and course of reaction in one particular system, whilst having little or no effect on another.

1.3.1 Saturated Aliphatic Aldehydes.

Saturated aliphatic aldehydes can easily be reduced to the corresponding alcohol using hydrogen over platinum metal catalysts, with little risk of over-hydrogenation. The reaction rates are usually low, however, and elevated temperatures and pressures are often required. The platinum metal catalysts used frequently benefit from the addition of metallic salt promotors. The catalytic activity of platinum oxide is a typical example. It is shown to deactivate quickly when used to reduce aliphatic aldehydes, but when small amounts of metallic salts such as $FeCl_3$ are added, catalytic activity is enhanced (25, 26).

This effect is illustrated by (Fig 1.2) which shows the different rates of hydrogen uptake for platinum oxide catalyst doped with a variety of

different metal salts, in the reaction of valeraldehyde (n-pentanal) to pentanol.

Fig 1.2

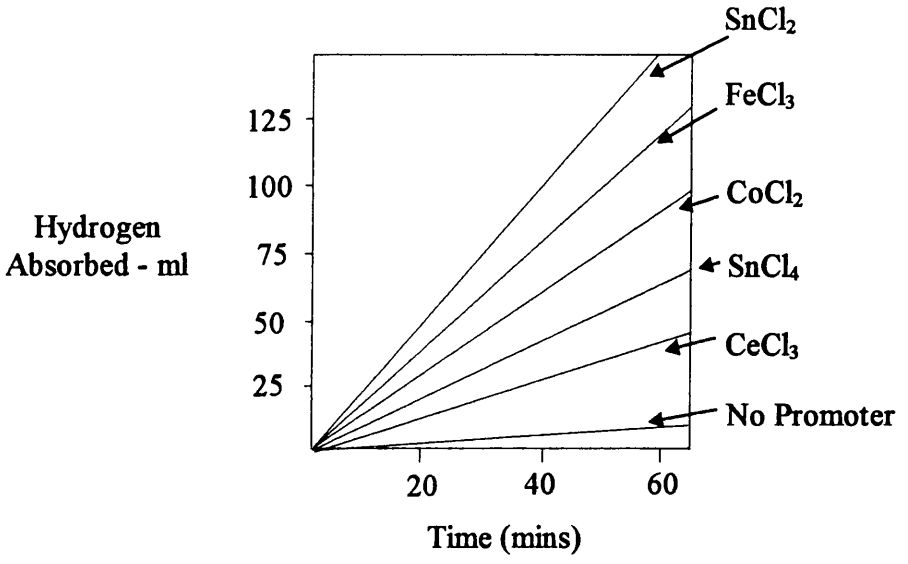

The reason for the increased hydrogen uptake was believed to be because the promotor was inhibiting the conversion of active platinum oxide to inactive platinum metal. Recent research however indicates that the increase in activity may be attributed to the metal component of the additive, polarising the CO bond and thus making it more susceptible to a weak nucleophilic reagent such as chemisorbed hydrogen (27). Supported catalysts such as 5 % Pt-on-carbon, and 5 % Ru-on-carbon also show a significant increase in the relevant rates of reaction when small quantities of promotors such as stannic chloride ($SnCl_4$) are added.

The three platinum group metals most used as catalysts in the hydrogenation of saturated aldehydes over the last few decades are palladium, platinum and ruthenium. These will be examined in turn.

1. Palladium Catalysts.

Palladium catalysts by themselves have not in general been proven to be particularly active for hydrogenating saturated aliphatic aldehydes. There have however been several specific examples where they have been used with considerable success. One such example was the use of supported palladium in the hydrogenation of the dialdehyde S-methoxy-S-hydroxy-methyldiglycolic aldehyde (Eq 1.1).

Eq 1.1

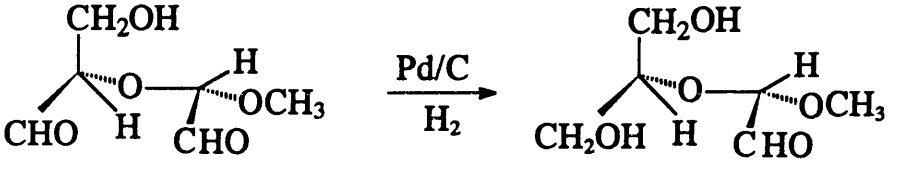

Preferential reduction of one aldehyde group takes place in ethanol solvent, at a pressure of 1200 psi g (23), as opposed to the reduction of both aldehyde groups over a Raney nickel catalyst under the same conditions.

2. Platinum Catalysts

Supported platinum catalysts are best used as hydrogenation catalysts when stabilised by additives as mentioned previously.

One example that illustrates the difference in activity between platinum and palladium is the hydrogenation of the aldehyde detailed overleaf (Eq 1.2).

Eq 1.2.

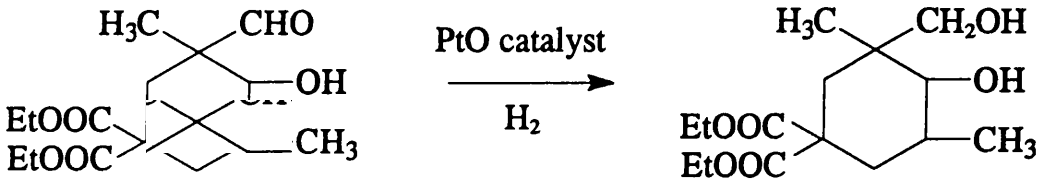

No reaction was observed on a 5 % palladium-on-carbon catalyst, whereas with platinum oxide exactly one mole of hydrogen was absorbed by the aldehyde, leading to the formation of the alcohol (28).

Another example of the successful use of a platinum catalyst is in the reduction of the aliphatic nitroaldehyde, 4-nitro-1-hexanal to 4-amino-1-hexanol. Using 1.3 g of platinum oxide in an ethanol solvent, a 78 % yield of the fully hydrogenated product was formed (29), (Eq 1.3).

Eq 1.3.

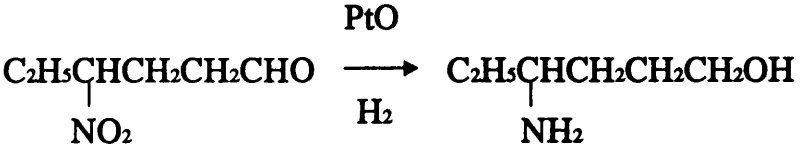

3. Ruthenium Catalysts

Ruthenium is an excellent catalyst in the hydrogenation of aliphatic aldehydes. Ruthenium catalysts are shown to work exceptionally well in an aqueous medium and because of this, have been used to produce polyhydric alcohols. Polyhydric alcohols are produced through the hydrolysis and simultaneous hydrogenation of polysaccharides, such as

cellulose (30). One example of such a reaction is the formation of sorbitol from glucose using a ruthenium-on-carbon catalyst promoted by palladium. At a pressure of 1000 psi g and a temperature of 130°C, a yield of 98 % sorbitol has been achieved (31).

1.3.2 Aromatic aldehydes

Aromatic aldehydes can be reduced readily to the corresponding alcohol and if the reduction is allowed to continue, then the alcohol can slowly be converted to the hydrocarbon. This suggests that production of the hydrocarbon arises primarily from the saturated alcohol and not in one step from the aldehyde. This is backed up by kinetic evidence relating to the hydrogenation of benzaldehyde (32).

1. Palladium Catalysts

Palladium catalysts are the most active catalysts for aromatic aldehydes. If the reaction products are not isolated at the alcohol stage, then further reduction can occur to produce the arene. This has been observed in the reduction of benzaldehyde, leading to the formation of toluene (33). This activity contrasts directly with their rather poor performance in hydrogenating saturated aliphatic aldehydes. Supported palladium-on-carbon catalysts were shown to be particularly active under mild conditions. In the reduction of β-naphthaldehyde over a ferric chloride promoted platinum catalyst, β-hydroxymethylnaphthalene was produced in 80 % yield, whereas, with a palladium-on-barium sulphate catalyst, β-methylnaphthalene was produced (34).

2. Platinum Catalysts

Platinum catalysts show valuable selectivities when hydrogenating halo-aldehydes. Reduction of the aldehyde function occurs readily, while little or no dehydrohalogenation is observed (35).

Eq 1.4.

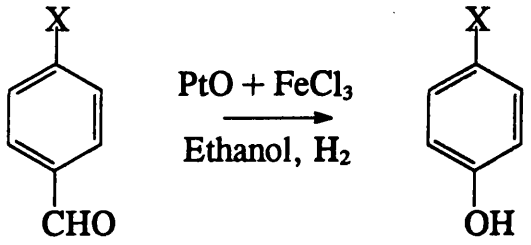

(X = Cl or Br. Yield of the corresponding alcohol = 96 %)

Other than for a few specific examples, however, the use of platinum catalysts in the reduction of aromatic aldehydes offers no real advantages over their palladium analogues.

3. Ruthenium Catalysts

Ruthenium is rarely used in the hydrogenation of aromatic aldehydes, as other platinum group metals such as palladium, out-perform it under very mild conditions. If more vigorous reaction conditions are to be used, however, ruthenium catalysts become useful. In the reduction reaction of 2-furaldehyde a 5 % ruthenium-on-carbon catalyst operating at room temperature and 1400 psi g pressure forms furfuryl alcohol in an 83 % yield (36), whereas similar palladium catalysts become deactivated. If the temperature is increased more ring saturation occurs.

1.3.3 α,β-Unsaturated Aldehydes.

The hydrogenation of α,β-unsaturated aldehydes (ie aldehydes which have a carbon to carbon double bond and a carbonyl bond in conjugation with one another), introduces the potential of catalyst selectivity towards either point of unsaturation. If other isolated double bonds exist, then these also have the potential to be hydrogenated and several possible reaction products can be formed.

The term selectivity is usually used loosely to describe the tendency for a reaction to lead to a particular product, which is an intermediate in a chemical reaction in which several products may be formed.

The degree of selectivity is often expressed as the amount of a specific product formed divided by the total amount of hydrogenated product. For example, in the following reaction -

$$A + B \longrightarrow X + Y + Z$$

The selectivity towards product X is given by the following expression -

Eq 1.5

$$S_x = \frac{W_x}{W_x + W_y + W_z}$$

(where W = weight, volume or a molar amount).

Factors such as the type of metal used, the support, the solvent system, reaction conditions and even the nature of the substrate itself all have a critical role to play in determining catalyst selectivity. For this reason, from a practical point of view it is often difficult to compare directly results from different researchers since small changes in experimental variables can result in erroneous conclusions being drawn.

Research has been carried out on α,β-unsaturated systems aimed at designing catalysts that will selectively hydrogenate the conjugated C=O bond and thus form the corresponding unsaturated alcohol. Unfortunately, the C=C functional group has proved to be the more reactive to a variety of platinum group catalysts and in most cases will be preferentially reduced. The preparation of unsaturated alcohols is important from an industrial point of view since such compounds are often used as precursors to important molecules in the perfumery industry. Molecules such as cinnamaldehyde, crotonaldehyde and citral have been extensively studied in an attempt to elucidate the important factors which determine selectivity to particular products and hence move another step forward to producing catalysts which are tailored towards particular reactions.

1. Unsaturated Aromatic Aldehydes.

Cinnamaldehyde is one of the simplest and most studied unsaturated aromatic aldehyde systems (27, 37, 38, 39, 40, 41, 42). Excluding any possible products resulting from ring hydrogenation, there are three main products to be found - hydrocinnamaldehyde, cinnamyl alcohol and phenylpropanol. This system has been studied as far back as 1915, when the reduction of cinnamaldehyde was studied over a colloidal palladium catalyst (43). In this instance almost 100 % hydrocinnamaldehyde was

formed, whereas later workers, whilst attempting to repeat this work, instead of finding the saturated aldehyde, found a mixture of the unsaturated aldehyde, saturated alcohol and phenylpropane (44). In the literature there has been much conflicting data regarding this system and despite the apparent simplicity of the cinnamaldehyde molecule, the reduction has been described as being 'unusually complicated' (23). Table 1.2 illustrates how small changes in experimental parameters can lead to a significant change in product ratios (23).

Table 1.2 [a]

Experimental Variables		Product Ratio
1. Support [b]	Alumina	100 % HCA
	Carbon	50 % HCA, 50 % PP
2. Solvent [c]	Ethanol	50 % HCA, 50 % PP
	Hexane	No reaction
3. Additives [d]	$FeCl_2$	100 % HCA
	HBr	68 % HCA, 32% PP

[a] 200 mg of 5 % Pd/support, 2.0 ml cinnamaldehyde, 50 ml solvent; room temperature, atmospheric pressure. [b] Reaction carried out in ethanol solvent; [c] Carbon support; [d] Carbon support/methanol solvent. CIN = cinnamaldehyde, HCA = hydrocinnamaldehyde and PP= phenylpropanol. The product ratios were determined when the reaction had stopped spontaneously.

Scheme 1.2 below shows the most likely reaction products from the hydrogenation of cinnamaldehyde -

Scheme 1.2

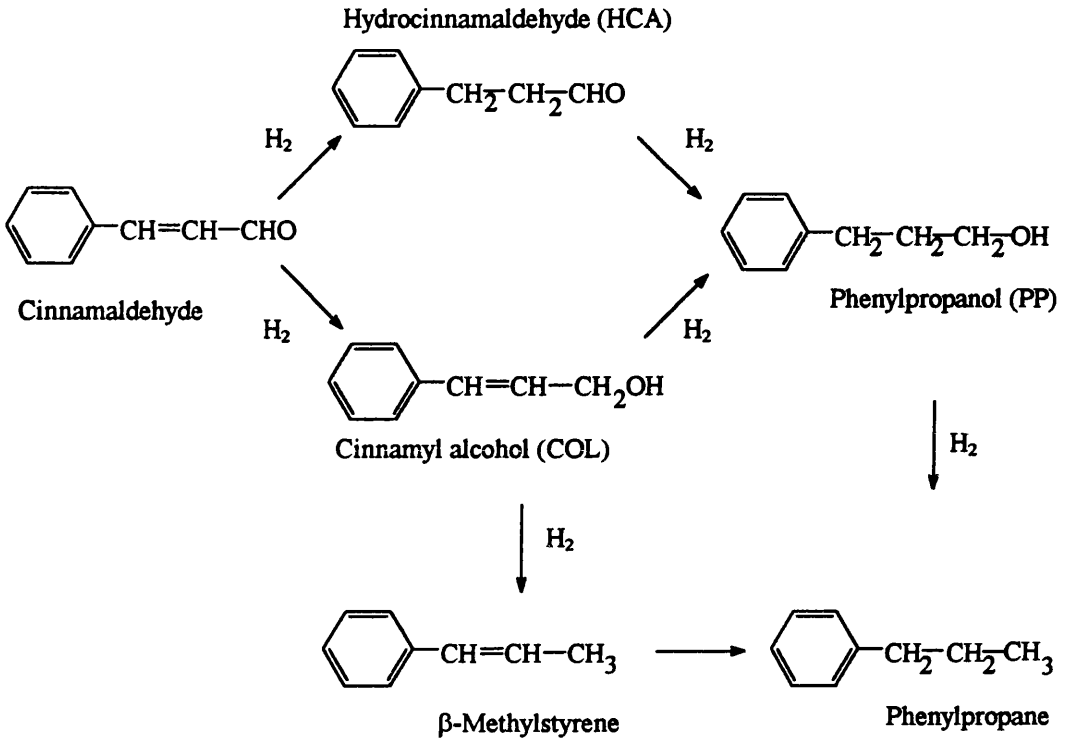

Although formation of β-methylstyrene and phenylpropane have been reported from several catalyst systems, usually they were found in small amounts and in many cases were not produced at all (37). Copper chromite catalysts, however, have been found to produce phenylpropane in reasonable amounts due to the chromite support acting as a site for isomerism and hydro-dehydroxylation reactions (45).

In terms of the production of cinnamyl alcohol, palladium by itself has been found to be unselective. Osmium, iridium and ruthenium catalysts are selective to varying degrees, (as a result of metal-support interactions, and the method of pretreatment) (46, 47), and the selectivity of platinum can be tuned by promotors. Copper-chromite catalysts have also been used with some success, although they are generally a poor choice, however, as the substituted allylic alcohols formed are often strongly bound to the catalyst surface. When used in the hydrogenation of cinnamaldehyde, the major product formed was hydrocinnamaldehyde with cinnamyl alcohol produced as a minor product. Some of the saturated alcohol, phenylpropanol, was also formed before hydrogenation of cinnamaldehyde was complete. As the reaction approached completion, the proportion of phenylpropanol was found to steadily increase.

In addition to the low selectivity of copper-chromite catalysts towards the production of cinnamyl alcohol, the toxicity of the chromium in the chromium oxide support and associated disposal costs weigh heavily against their continuing use on an industrial scale.

Recent work by Gallezot *et al* (46), using tailor-made catalysts, characterised by transmission electron microscopy (TEM) and energy-dispersive X-ray emission analysis (EDX), has helped explain some of these selectivity effects.

Gallezot *et al* examined the following catalysts -

1. Pt/C (3.8 wt % Pt), 2. Ru/C (4.6 wt % Ru), where C = charcoal.
3. Pt / G_{ex} (3.6 wt % Pt), 4. Ru / G_{ex} (3.6 wt % Ru), where G_{ex} = Lonza HSA graphite.

Excluding the results obtained by using shape selective supports such as zeolites, three main factors were identified as being responsible for the selectivity effects observed.

a. Surface Induced Electronic Effects

Higher selectivities were obtained on graphite-supported catalysts, and since particle sizes for both charcoal and graphite supported catalysts were observed to be similar, the increasing selectivity was thought to be due to the support.

Graphite has been shown to act as an electron donating macroligand and is thought to increase the electron density on the metal surface. This in turn reduces the ability of the platinum metal to hydrogenate the olefinic bond of the cinnamaldehyde molecule. By the same reasoning it was concluded that by adding ligands such as phosphine to the reaction medium, the electron density at the metal centres would be increased and the selectivity towards C=C bond hydrogenation reduced. Thus the alteration in selectivity was due to a C=C bond deactivation rather than a C=O bond activation.

b. Metal Particle Morphology.

Differences in the metal particle sizes within groups of the same catalyst caused considerable differences in the selectivity towards cinnamyl alcohol. This was explained in terms of a steric repulsive effect. On particles of diameter greater than 3 nm, the phenyl group of the cinnamaldehyde molecule prevents the molecule adsorbing parallel to the surface and therefore prevents C=C bond hydrogenation. Conversely, no energy barrier was observed for C=O adsorption.

c. Addition of a Second Metal as a Promotor.

When iron chloride ($FeCl_2$) was added to the reaction medium, bimetallic particles of Fe associated with Pt were formed. The Fe^{2+} ions were then reduced to Fe metal by the hydrogen gas. The selectivity towards cinnamyl alcohol was shown to be enhanced. The reasons for this were twofold.

- Fe atoms induce electron transport to the platinum atoms which are more electronegative. This makes the platinum atoms more electron rich and therefore inhibits C=C bond adsorption.

- Fe atoms, being more electropositive, act as Lewis adsorption sites. This facilitates adsorption of the cinnamaldehyde molecule through the lone pair of electrons on the oxygen atom of the carbonyl group. The following reaction is then believed to occur.

Fig 1.3

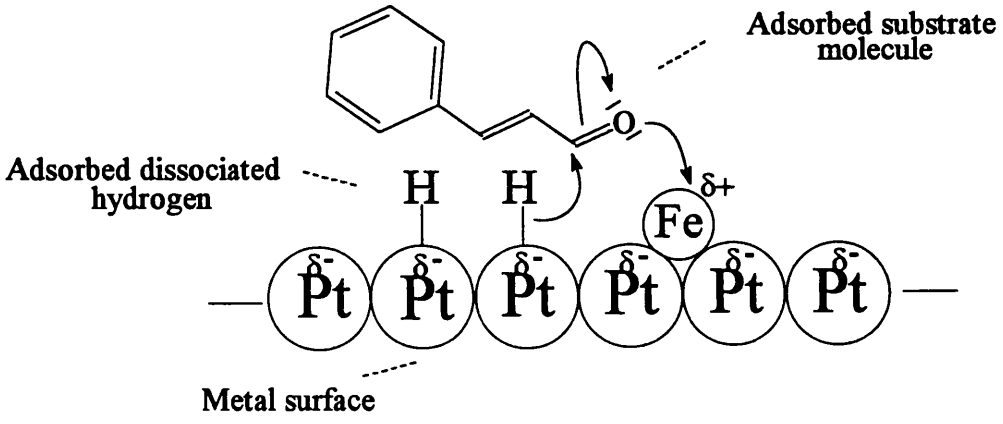

2. Unsaturated Aliphatic Aldehydes

For unsaturated aliphatic aldehydes, hydrogenation of the C=C bond often occurs selectively and where palladium catalysts have been used, the reduction has been shown to stop spontaneously upon formation of the saturated aldehyde. When palladium is used on a variety of supports and in various solvents for the reduction of crotonaldehyde, butyraldehyde was the only product formed. However, for platinum catalysts supported on surfaces such as activated carbon (48) and surfaces which possess excess surface oxygen groups, such as TiO_2 (49), a significant amount of crotyl alcohol was produced. The following scheme shows the possible products of crotonaldehyde hydrogenation.

Scheme 1.3

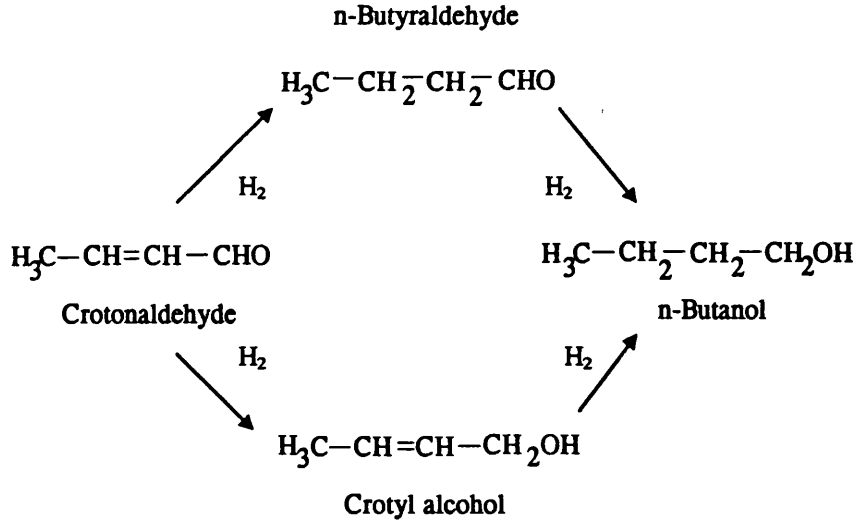

In another instance, Hutchings *et al* discovered that on alumina-supported copper catalysts, selectivity towards crotyl alcohol was achieved by poisoning C=C adsorption sites using sulphur (50). In this instance, the product distribution was shown to shift from the fully saturated alcohol to the unsaturated alcohol.

As the carbon to carbon double bond of the unsaturated aldehyde becomes more substituted, hydrogenation of the carbonyl function becomes the predominant reaction. This is illustrated by the following example in which a 5 % Pd-on-carbon catalyst was shown to selectively reduce the carbonyl function of a 6-formyl group to prepare 6-hydroxymethyl 3-enol ethers derived from cortisone acetate, deoxycorticosterone acetate, and androst-4-ene-3,17-dione in good yield (51).

Eq 1.6.

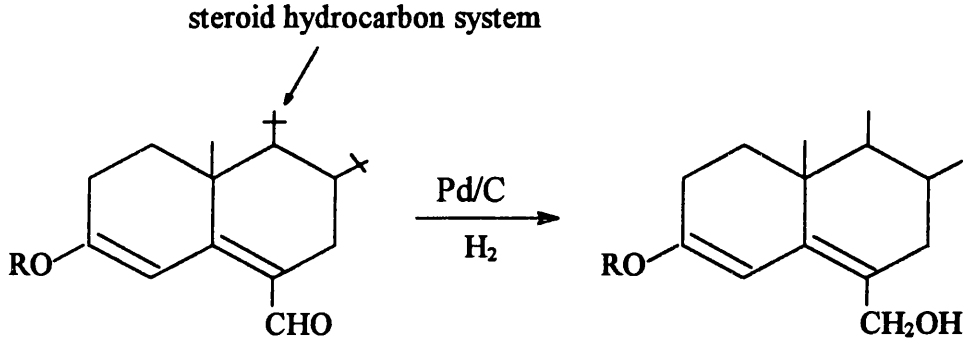

R = $POCl_2$

Citral is another important unsaturated aliphatic aldehyde. As well as possessing an α,β-unsaturated carbonyl system, it also possesses another isolated C=C double bond. In theory several potential extra products may be produced by hydrogenation, although in general the poor reactivity of the isolated double bond means that the conjugated α,β-unsaturated carbonyl system will be hydrogenated first.

Scheme 1.4

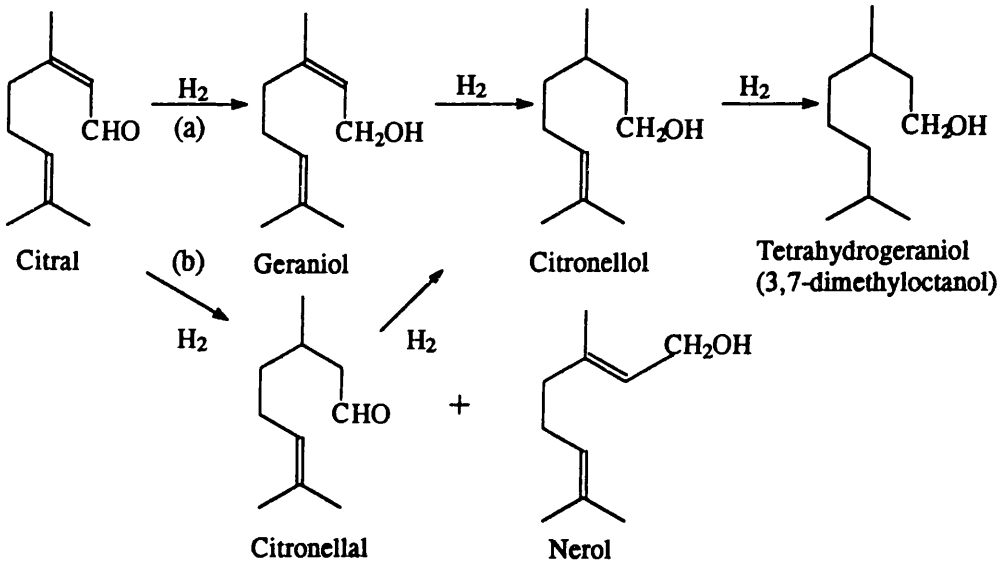

When platinum oxide with an iron promotor (in ethanol solvent) was used as a catalyst, citral was found to be selectively reduced to geraniol (route a). When the reduction was continued, citronellol and finally tetrahydrogeraniol were produced in sequence (23). In contrast, when a copper-chromite catalyst was used, hydrogenation of the unsaturated C=C double bond occurred to give citronellal, and, to a much lesser extent, nerol (route b) (45). In this case, citronellol was formed before the starting substrate had been fully hydrogenated. As the reaction approached

completion, the proportion of citronellol increased steadily. No tetrahydrogeraniol was observed.

The examples illustrated on pages 9 - 25 are by no means a comprehensive review of catalyst mediated aldehyde hydrogenation, but are intended to be a cursory overview of the relevant literature. The purpose of this survey was to illustrate primarily the limitations of many systems, the findings of some of the current work done on aldehyde hydrogenation (in particular, on α,β-unsaturated systems) and some of the problems encountered. In many cases, due to the considerable molecular weight of the molecules discussed and due to hydrogen bond interactions with a variety of different functional groups, the substrate molecules are often liquids or solids. This means that to hydrogenate them, the reaction must take place in the liquid phase or in solution, which leads to the possibility that the rate of reaction may become diffusion limited. The problems of diffusion limitation/mass transport are discussed in section 1.4.

1.4 Physical Limitations to Reaction Rate

1.4.1 Introduction

For a simple bimolecular reaction of the type A + B ⟶ C, there are 5 simple basic requirements for an efficient catalytic process to operate.

Fig 1.4

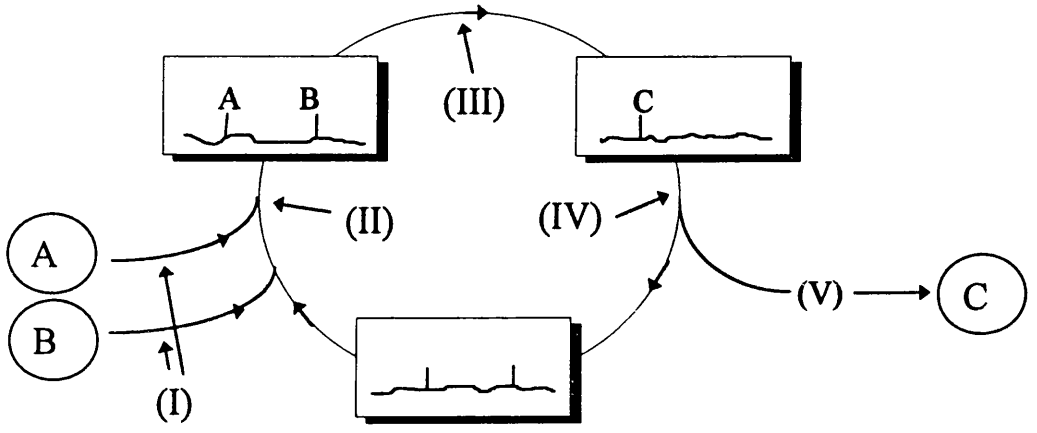

I. Transport of the reactants to the catalyst surface.

II. Chemisorption at an active centre on the catalyst surface.

III. Reaction of chemisorbed reactants to form the product.

IV. Desorption of the product.

V. Transport of the product from the surface.

In many three-phase systems involving hydrogen (gas), the reactant molecule (liquid), and the catalyst (solid), one of the main potential rate limiting steps is the diffusion of hydrogen to the catalyst surface. To ensure

that this does not occur, several considerations must be kept in mind. These are listed below.

1. The solubility of the hydrogen gas in the chosen solvent.

2. The working pressure of the system (higher pressure = greater solubility of hydrogen).

3. The temperature of the system (higher temperature = lower solubility).

4. Agitation conditions. In order to ensure there is adequate contact between the three phases, experimental considerations such as stirring rate and the use of a bubbler to increase hydrogen solubility, must be taken into account (Fig 1.5) (52).

Fig 1.5

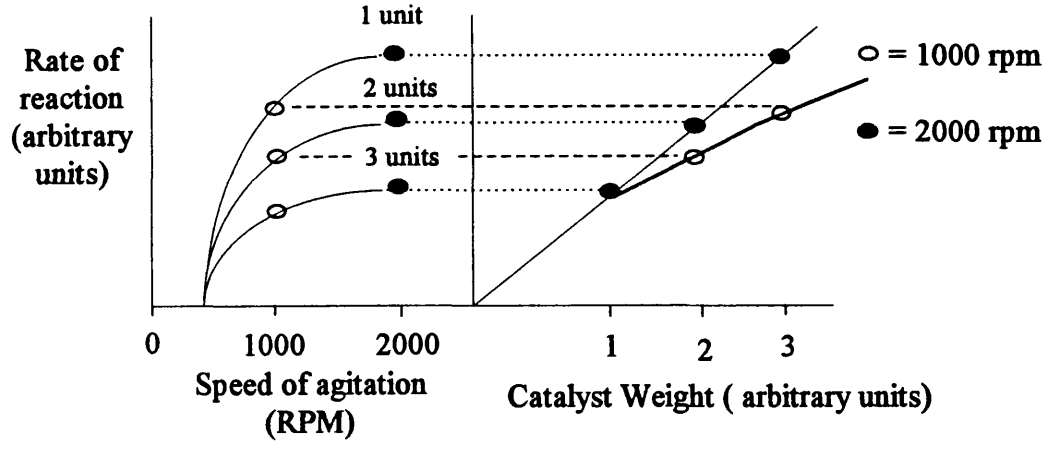

If the reaction rate is not limited by the transport of H_2 to the catalyst surface, the reaction is under chemical control. If it is limited by this factor, however, then it is said to be under external diffusion control (or, mass transport control). Whilst chemical control is desirable, factors such

as the low solubility of H_2 in apolar solvents are more likely to lead to the reaction being diffusion controlled.

Diffusion control in a reaction can be noted by the following factors -

1. A reaction which has an activation energy less than 20 kJ mol^{-1}.

2. A reaction rate which does not increase with the weight of catalyst used.

3. A reaction rate which increases when agitation is improved.

1.4.2 Transport Interactions.

Fig 1.6 illustrates some of the transport interactions which occur in a multi-phase system.

Fig 1.6

$$A\ (gas) + B\ (liquid) \longrightarrow C\ (liquid)$$

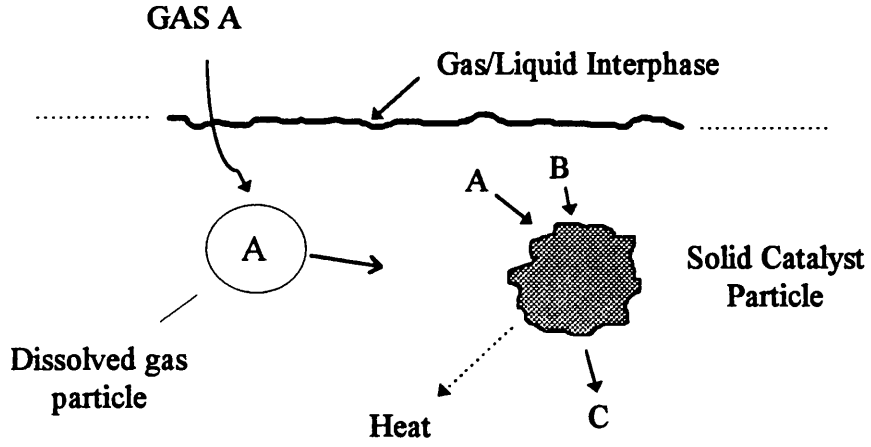

Component A has to be transported across a gas/liquid interface and then once it has been dissolved in the liquid phase, it must then be transported to

the external surface of the solid catalyst particle. As a final step, (A) must then diffuse through the latticework of pores that make up the particle. Once there it reacts with some of the second (liquid phase) reactant (B) to form product (C). The extent to which (A) will diffuse into the particle is random.

For component (B), since it is applied in the liquid phase, no gas/liquid transport is necessary.

For component (C), after it is formed from the reaction of (A) and (B) in the pores of the catalyst particle, it undergoes transport processes which involve diffusion from the interior of the catalyst to the surface, followed by transport into the bulk. Transport out through the catalyst particle is controlled by pore diffusion resistance.

When reactions are exothermic, the heat liberated must find its way out of the catalyst particle. This involves two simple transport steps: the conduction of heat from the interior of the particle to the surface, and, heat transport from the particle surface to the bulk liquid.

As reactants are transferred across gas/liquid, and liquid/solid interfaces, temperature and concentration gradients are set up across the system. It is these heat and mass transport processes that affect the rate of reaction and selectivities of heterogeneous catalyst systems (53).

Table 1.3 overleaf details the major factors concerning mass transport, which relate to reaction rate.

Table 1.3

Controlling Step	Major Factors Influencing Rate
1. Gas/Liquid Mass Transport	Stirring rate
	Reactor design
	Gas phase reactant concentration
2. Liquid/Solid Mass Transport	Amount of catalyst
(gaseous reactant)	Catalyst particle size
	Reactant concentration (gas phase)
3. Liquid/Solid Mass Transport	Amount of catalyst
(liquid reactant)	Catalyst particle size
	Reactant concentration (liq phase)
4. Chemical Reaction	Temperature
(no pore diffusion resistance)	Amount of catalyst
	Reactant concentrations
	Concentration of active component
5. Chemical Reaction	Amount of catalyst
(with pore diffusion resistance)	Reactant concentrations
	Temperature
	Catalyst particle size
	Concentration of active component

1.5 The Support (54)

Inorganic macromolecules such as silica have physical properties which offer considerable advantages as supports for large scale applications of heterogeneous catalysts. The selection of a support is based on it having certain desirable characteristics, namely -

1. Suitable Mechanical Properties

Certain mechanical advantages are gained when a support is used. The most obvious is the conveyance of mechanical strength as a result of the rigid stable structure of support materials. In addition to this, a support functions as a heat sink, conducting away heat localised at reaction sites into the bulk gas/liquid.

2. Favourable Geometrical Features

By using a support material, the surface area can thus be controlled, and areas of up to 1000 m^2g^{-1} achieved. As a result, the metal component can be widely dispersed over the surface, thus maximising activity per unit weight of metal, and reducing costs. In the same way porosity and average particle size can exert an effect. In general it is advisable to have a pore size greater than 50 Å to avoid restricting the entry of fluid into the interior of the particles thereby setting up another unwanted diffusion gradient. The choice of optimum particle size depends on the nature of the system. In general, fine powders are used for slurry type processes whereas fixed bed catalysts are usually in the form of granules, cylinders or spheres with an average particle size ranging from ¼ to $^1/_{32}$ inch.

Another geometrical advantage to using a high surface area support is that it minimises the possibility of catalytic deactivation by sintering or poisoning.

In general, sintering occurs at elevated temperatures. It involves particles aggregating together to reduce the collective surface energy of the system. For a metal catalyst, sintering of the metal particles is hindered by distributing them as widely apart as possible on a high surface area support.

Catalyst poisoning, often by traces of impurities in chemical feedstocks, is extremely undesirable. In certain cases, however, poisoning can be minimised using specific shape selective supports. By using supports with well defined cage structures such as zeolites, the active metal component can react with a suitably sized reactant molecule in the interior of the catalyst, whilst larger catalyst poisons are prevented from entering the cages by size considerations.

3. Chemical stability

Amongst other things, a support is chosen for its stability under a variety of reaction conditions and also for its chemical inactivity towards any undesirable side reactions in the system in which it is being used. Often, interactions between the metal and the support are beneficial, and can lead to increases in catalyst selectivity towards particular reaction products (46, 49).

1.5.1 Properties of Silica as a Support Material

In the course of this study silica was chosen as the support material, as it is mechanically rigid and unaffected by all but the most severe solvent and temperature conditions (55). This section gives an insight into the different types of silica which are commercially available and details some aspects of surface hydroxyl group reactivity.

There are many naturally-occurring silicas, although only diatomite (Kieselguhr) is of practical use as a support material. Its macroporous structure is advantageous in reactions involving large substrate molecules, but with an average surface area of only 30 m^2g^{-1} its use as a catalyst support is limited. Because of this, a large variety of artificial (synthetic) silicas have been produced. Factors such as the surface area, porosity and average particle sizes can be controlled by the choice of preparation conditions and subsequent heat treatments.

The table overleaf illustrates the difference in physical properties of three commercially-available silicas.

Table 1.4.

Properties	Types of Commercially Available Silica		
	HP 220	Gasil 35 M	Gasil WP2
Pore Volume, mlg^{-1}	1.8	1.2	2.0
Average Particle Size, μm	8.6	4.5	2.0
Surface Area BET, m^2g^{-1}	320	320	850
pH (5% aq suspension)	3.5	7	4
% Weight Loss at 105°C (2 hours)	2	1	55

Synthetic silicas can be classified as pyrogenic silicas or silica gels.

Pyrogenic silicas are obtained by burning silicon tetrachloride vapour in a hydrogen/oxygen flame.

Eq 1.7

$$SiCl_4 \xrightarrow[\text{Oxidation or hydrolysis}]{H_2/O_2} SiO_2 \text{ (approx 1 nm in diameter)}$$

Examples of pyrogenic silicas produced in such a way include 'aerosils' and 'cabosils'. These silicas are normally characterised by having surface areas in the 200 - 400 m^2g^{-1} range and a non porous structure.

Silica Gels are obtained by using one of two techniques, polymerisation of silicic acid or floculation of colloidal silica.

Surface area and pore characteristics depend on the pH and the aging conditions. The final product is called a xerogel and is obtained by thermal dehydration of the initial hydrogel. If, however, dehydration is carried out above the critical point of water an 'aerogel' is formed.

Fig 1.7

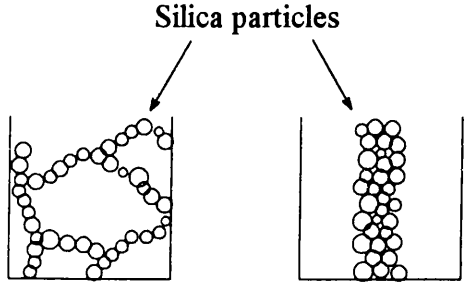

A. Aerogel B. Xerogel

The surface areas of A and B are both in excess of 500 m^2g^{-1} and both have pore diameters in the 2 - 10 nm range.

1.5.1.1 Surface Coverage of Hydroxyl Groups

In 1936, Kiselev (56) proposed that the surface of active silica gel was covered by hydroxyl groups. The surface coverage of hydroxyl groups has been the subject of many papers and reviews. Surface coverage in many ways determines adsorption behaviour and as a result, surface reactivity.

A hydroxylated silica surface contains three possible types of silanol (Si-OH) groups. These are shown overleaf.

1. Vicinal

Fig 1.8

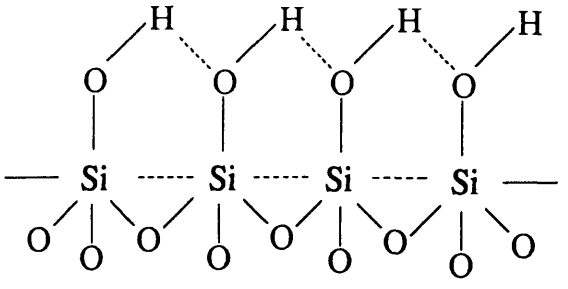

Typical OH - OH distance is sufficiently small (less than the van der Waals contact by *ca.* 0.02 nm) that hydrogen bonding may occur.

This type of bonding can be characterised by infra-red spectroscopy. A broad hydroxyl stretching frequency can be detected at circa 3550 cm^{-1}, although the exact value depends on the OH···O distance and hence on the strength of the hydrogen bond formed (57).

2. Geminal

Fig 1.9

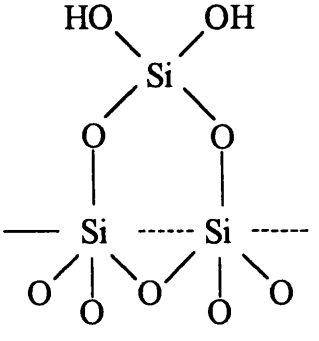

Using solid state ^{31}Si NMR spectroscopy, a single peak can be observed at circa -90 ppm (57), although the low signal intensity of such signals reflects the low frequency of occurence.

3. Isolated hydroxyl group

Fig 1.10

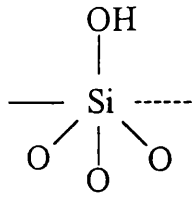

For this type of silanol group, no hydrogen bonding is observed. The minimum OH–H distance between neighbouring silanol groups is greater than 0.33 nm. A narrow IR band can be observed at 3750 cm^{-1} (57).

Solid state ^{31}Si MAS-NMR spectroscopy can be used to detect the different types of silanol groups found on a typical silica surface (57). For example, the spectrum of standard Gasil 35M silica was recorded and is shown below.

Fig 1.11

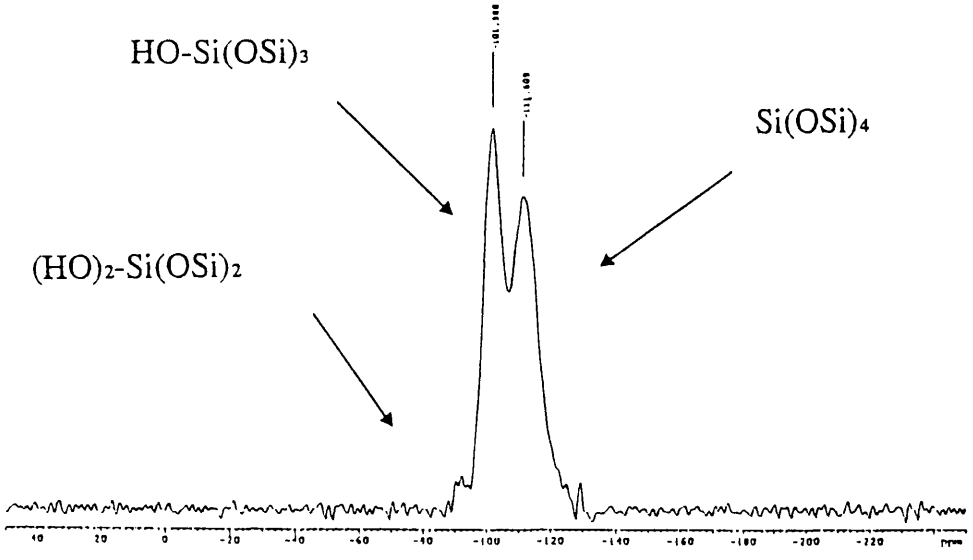

Vacuum heating progressively eliminates hydroxyl groups, forming water in the process as well as Si - O - Si linkages. These linkages are generally very unreactive. However, weak Lewis acid centres are sometimes created due to strain within individual Si - O bonds. Such strain creates asymmetry and hence bond polarity. As a result of this bond polarity, bases such as water can react to form hydrogen bonded silanol pairs. Weak Lewis bases such as CO, form hydrogen-bonded species stable only at 77K, whereas more basic molecules such as ammonia and pyridine lead to hydrogen-bonded species stable at room temperature.

1.6 Interaction of Organometallic Molecules with Oxidic Surfaces (58)

In the course of this study the activities and selectivities of a variety of silica supported palladium phosphine complexes in the liquid phase hydrogenation of cinnamaldehyde have been examined. Although for the complexes used, the absence of a direct metal to carbon bond means that strictly speaking they cannot be classified as organometallic, the reaction of organometallic complexes with oxidic surfaces can be considered as a close analogy. For this reason, the following pages detailing the mode of interaction of organometallic reagents with a variety of oxidic supports have been included.

When ionic oxides such as Al_2O_3 are used, the reactive centres are surface-exposed cations, oxide anions and, often, hydroxyl groups. Exposed or co-ordinately unsaturated metal ions act as Lewis acid sites and thus act as sites at which electron donor ligands can interact, whereas surface anions have Lewis base properties and can effect nucleophilic attack at electrophilic centres. Atomic sites located at defect points on the surface are more co-ordinately unsaturated and hence have higher reactivity.

When covalent oxides such as silica are examined, surface atoms are linked together covalently, and can no longer be thought of as a pattern of alternating charge separated anions and cations. When the surface is fully dehydroxylated incoming molecules with acid or base character can no longer interact with suitable donor/acceptor sites and the interaction is mainly physical in nature. On partially dehydroxylated surfaces however, covalent oxides show weak acidic character and hydrogen bonding can take place with suitable bases.

Research into the interaction of organometallic molecules with oxidic surfaces has centred on three classes of compound (59).

1.6.1 Metal Carbonyls (60, 61)

The interaction of transition metal carbonyl compounds with oxidic surfaces such as silica takes two forms.

1. Ligand Centred Interactions

These comprise of -

a. Hydrogen bonding to OH groups of partially hydroxylated oxides

b. Oxygen bonding to surface Lewis acid sites

c. Weak van der Waals interactions (physical adsorption)

Assuming the oxidic surface is approaching full dehydroxylation, the primary interaction mode is of a donor-acceptor type, between carbon monoxide ligands (CO) and Lewis acid sites on the support surface. This type of interaction forms an oxygen bonded surface adduct. When bridging

CO ligands are present, stronger ligand-bridged surface σ adducts are formed (through the more basic bridging CO ligand), than for terminal CO ligands. As a result there is a significant lowering of the CO stretching frequency, with the frequency of the bridging CO bond being lowered by as much as 400 cm^{-1}. The downward shift of the CO stretching frequency is a consequence of the polarisation induced by the surface Lewis centre in the bonded CO group. It must also be noted that the CO stretching frequency is increased slightly for carbonyls not involved in the CO bridge.

When the surface has not been fully dehydroxylated, the basic oxygen atom of the CO ligand can hydrogen bond to acidic hydroxyl groups (Brønsted acid centres), which leads to a similar qualitative CO frequency shift as described above. The exact extent of the frequency shift depends on the Brønsted acid strength. If the oxidic surface is homopolar, only physical adsorption is possible.

2. Metal Complex Centred Interactions

Interactions involving 'attack' at a metal centre occur when the electron density at the metal carbonyl ligand is altered due to bonding of the carbonyl oxygen atom to the support. This causes a weakening of a M-CO bond (not directly involved in σ bond formation), an increase in the positive character of the CO group carbon atom and an increase in the positive character of the metal. As a result of the electronic imbalance which ensues, several chemical reactions (illustrated overleaf) can take place.

a. CO dissociation and clustering

Fig 1.12

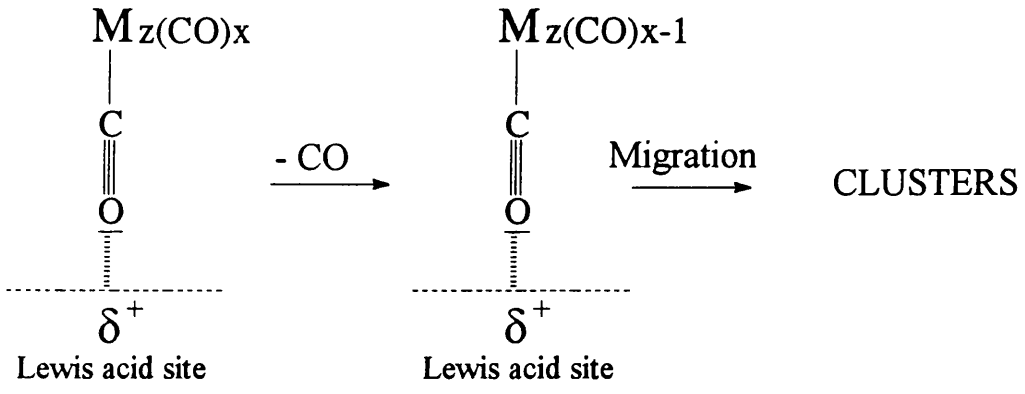

Attempts to free metal co-ordination sites by thermal decarbonylation, often fail because of oxidation of the metal centres by surface hydroxyl groups. If migrating species do meet on the surface after decarbonylation, clustering may occur. These factors often complicate attempts to use supported metal carbonyl compounds as catalysts.

b. Nucleophilic attack by Lewis base sites

Nucleophilic attack at the δ+ve carbon of a σ bonded C=O species can result in the formation of a carbenoid structure, which in turn can result in the production of carbonate-like (adsorbed CO_2) and anionic fragments (Fig 1.13).

Fig 1.13

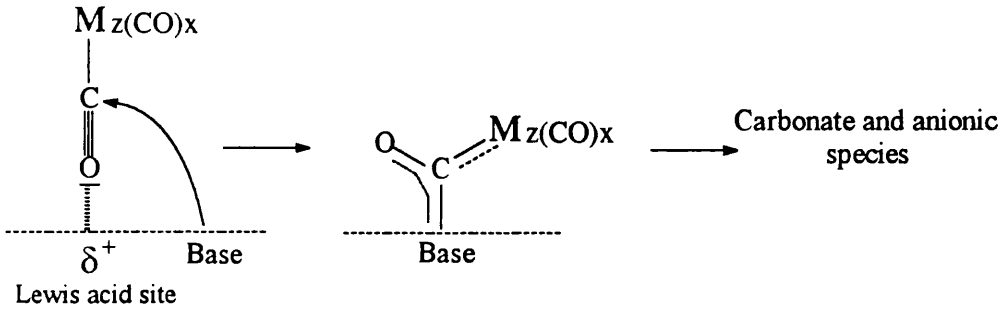

Strong basic sites such as those found on the surface of MgO are required for this type of reaction to take place.

c. Nucleophilic attack by Brønsted base sites

The mechanism of attack for a Brønsted hydroxyl basic site is the same as that for a Lewis basic site, with the exception that bicarbonate and negatively charged carbonyl anions are expected to be major products. Alternatively, bicarbonate and hydrido-carbonyl anions may be formed.

d. Protonation

Acidic hydroxyl groups can donate H^+ ions and thus protonate adsorbed carbonyl groups to yield a hydrido species. Only surface hydroxyls with strong Brønsted character are expected to be able to protonate neutral CO molecules.

Certain supported metal carbonyl compounds have proven to be extremely active and selective hydrogenation catalysts. One example in particular is of interest. Complex cobalt-carbonyl ligand 'cluster of clusters' have been used as well defined molecular precursors for self-supported high surface

area, single metal or bimetallic catalysts. Such catalysts have shown 100 % selectivity in the production of the unsaturated alcohol 2-butenol from the α,β-unsaturated aldehyde 2-butenal (62).

1.6.2 **Metallocenes** (and derivatives)

The metallocene Cp_2Cr (Cp = cyclopentadienyl), supported on silica has proved to be an effective catalyst in the polymerisation of ethene (63).

Polymerisation reactions are carried out annually on the megatonne scale. As a result of their economic importance, there has been extensive research aimed at finding more efficient catalysts and to this end many derivatives of metallocenes have been investigated in an attempt to form stereoregular polymers (64).

On a fully dehydroxylated surface, no chemical reaction between the reactive hydroxyl function and the Cp_2Cr molecule can take place. In this case the only interaction mode is weak physical adsorption and the chromocene molecules tend to aggregate.

If, however, isolated hydroxyl groups are present, the following reaction takes place (Fig 1.14).

Fig 1.14

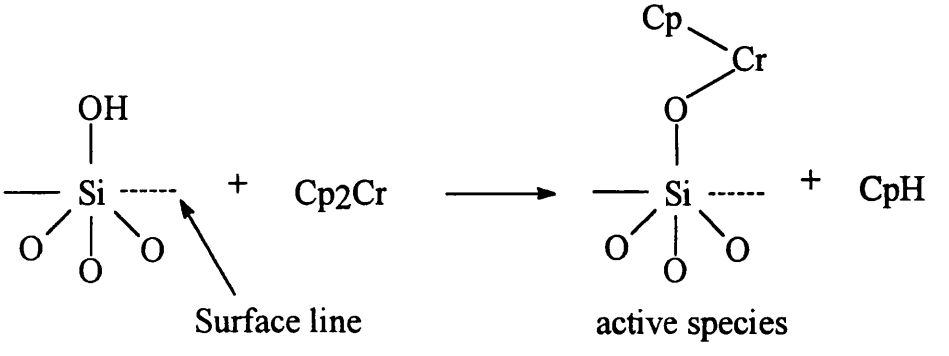

If the surface of the silica is saturated with vicinal hydroxyl groups, the proximity of silanol groups to one another can lead to a dimerisation reaction which leads to catalytically inactive centres (Fig 1.15).

Fig 1.15

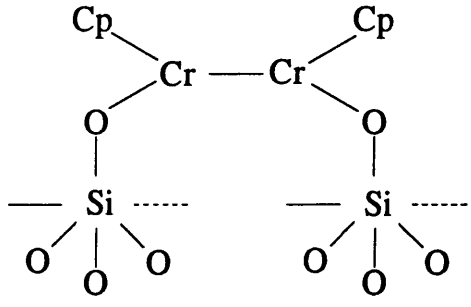

Formation of the above dimer species can be minimised by outgassing the support at temperatures between 700°C and 800°C, therefore maximising catalyst activity.

1.6.3 Metal Alkyl and Allyl Derivatives

Silica-bonded rhodium allyl species have been used as precursors to supported rhodium hydride catalysts in the hydrogenation of olefins (65). The following reaction was found to occur.

Fig 1.16

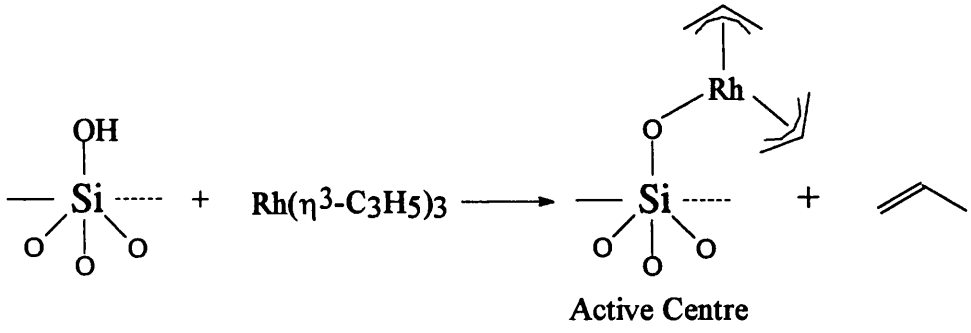

Active Centre

Subsequent treatment of the active centre with hydrogen leads to the formation of a supported rhodium hydride species which readily reacts with a variety of olefins to form the corresponding saturated alkane.

Similar reactions have also been noted with other transition metal allyl compounds such as $Mo_2(\eta^3\text{-}C_3H_5)_4$. In this case the active centre formed functions as an effective oxidation catalyst (66).

Metal alkyl species have also been used to prepare a variety of well defined bimetallic catalysts. Research has centred on the reactions between group 14 organometallic compounds and certain group 8, 9 and 10 metals. When silica supported particles of Rh(0) or Ru(0) were reacted with $Sn(n\text{-}C_4H_9)_4$ in the presence of hydrogen gas, a hydrogenolysis reaction occurs, and the following bimetallic catalysts were formed - $Rh[M'(n\text{-}C_4H_9)_x]_y/\ SiO_2$,(M'= Ge, Sn, Pb), ($x \approx 2$, $y \geq 0.3$). The catalysts thus formed have proven to be extremely active and selective in the hydrogenation of α,β-unsaturated aldehydes such as citral. 96 % selectivity towards the unsaturated alcohols (nerol and geraniol) at 100 % conversion was observed (67, 68).

1.7 Theory of Techniques

In an attempt to gain a further insight into the nature of the species responsible for the selectivity observed on several of the catalysts examined, it was necessary to use the surface-sensitive technique of X-ray photoelectron spectroscopy (XPS) and the elemental analysis technique of neutron activation analysis (NAA). Since XPS and NAA are very different from more routine methods of analysis such as IR and NMR spectroscopy and microanalyses, this section is included to outline the theory behind these techniques, to indicate how spectra and analyses were obtained and to explain why these techniques were used.

1.8 X-ray Photoelectron Spectroscopy (XPS) (69)

1.8.1 XPS Theory

Surface analysis by XPS is carried out by irradiating a sample with mono-energetic soft X-rays and analysing the energy of the ejected electrons. The X-ray photons can only penetrate to the order of 1-10μm into a solid, therefore, only atoms in surface regions of solids are affected, causing electrons to be emitted by the photoelectric effect. Such emitted electrons have measured kinetic energies given by the following equation -

Eq 1.8. $$[\ K.E = h\upsilon - BE - \phi s\ ]$$

($h\upsilon$ = the energy of the photons; BE = binding energy of the orbital where the electron originates, and ϕs is the spectrometer work function).

The binding energy is the energy difference between the initial and final states, after the photoelectron has left the atom. Since there is a variety of possible final states of the ions from each type of atom, there is a corresponding variety of kinetic energy values for the emitted electrons.

The diagram below illustrates the XPS emission process.

Fig 1.17

XPS Emission Process for a Model Atom
An incoming photon causes the ejection of a photoelectron.

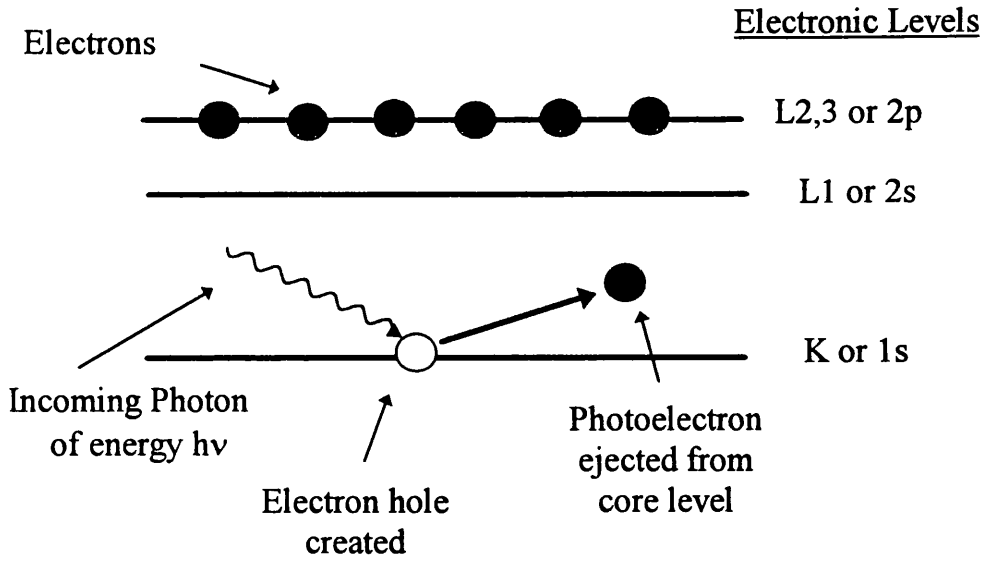

Since each element has a unique set of binding energies, XPS can be used to identify and determine the concentration of elements at a surface. Variations in elemental binding energies (chemical shifts) arise from differences in chemical potential and the polarisability of these compounds.

These chemical shifts are used to identify the chemical state of the material being analysed.

In addition to photoelectrons emitted in the photoelectric process, Auger electrons may be emitted because of relaxation of the excited ions remaining after photoemission. In the Auger process an outer electron falls into the inner orbital vacancy and a second electron is simultaneously excited, carrying away the excess energy. This Auger electron possesses kinetic energy equal to the difference between it and the singly charged species. Therefore, photoionisation is a three electron process that normally leads to two emitted electrons - a photoelectron and an Auger electron.

The diagram below illustrates the Auger process.

Fig 1.18

The relaxation process for a model atom resulting in the emission of a $KL_{23}L_{23}$ electron. The simultaneous 2 electron colombic rearrangement results in a final state with 2 electron vacancies,

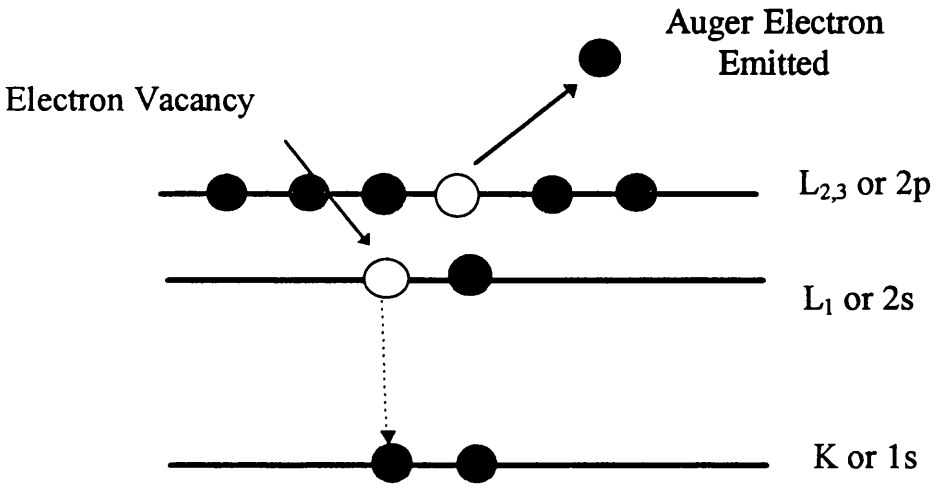

The path length of electrons is only of the order of a few tens of Angstroms (A^{o}), thus, whilst ionisation occurs to a depth of a few micrometers, only those electrons originating within tens of Angstroms below the surface can leave without energy loss. The electrons that leave the surface without energy loss produce the peaks in the spectra.

The electrons leaving the sample are detected by an electron spectrometer according to their kinetic energy. The analyser is operated on an energy window, referred to as the pass energy, accepting only those electrons having an energy within the range of this window. To maintain a constant energy resolution, the path energy is fixed. Incoming electrons are adjusted to the pass energy before entering the energy analyser. Scanning for different energies is accomplished by applying a variable electrostatic field before the analyser. Electrons are detected as discrete events, and the number of electrons for a given detection time and energy is stored and displayed.

Fig 1.19 shown overleaf illustrates the SCIENTA ESCA 300 XPS spectrometer used to record the spectra.

Fig 1.19 - SCIENTA ESCA 300 XPS SPECTROMETER

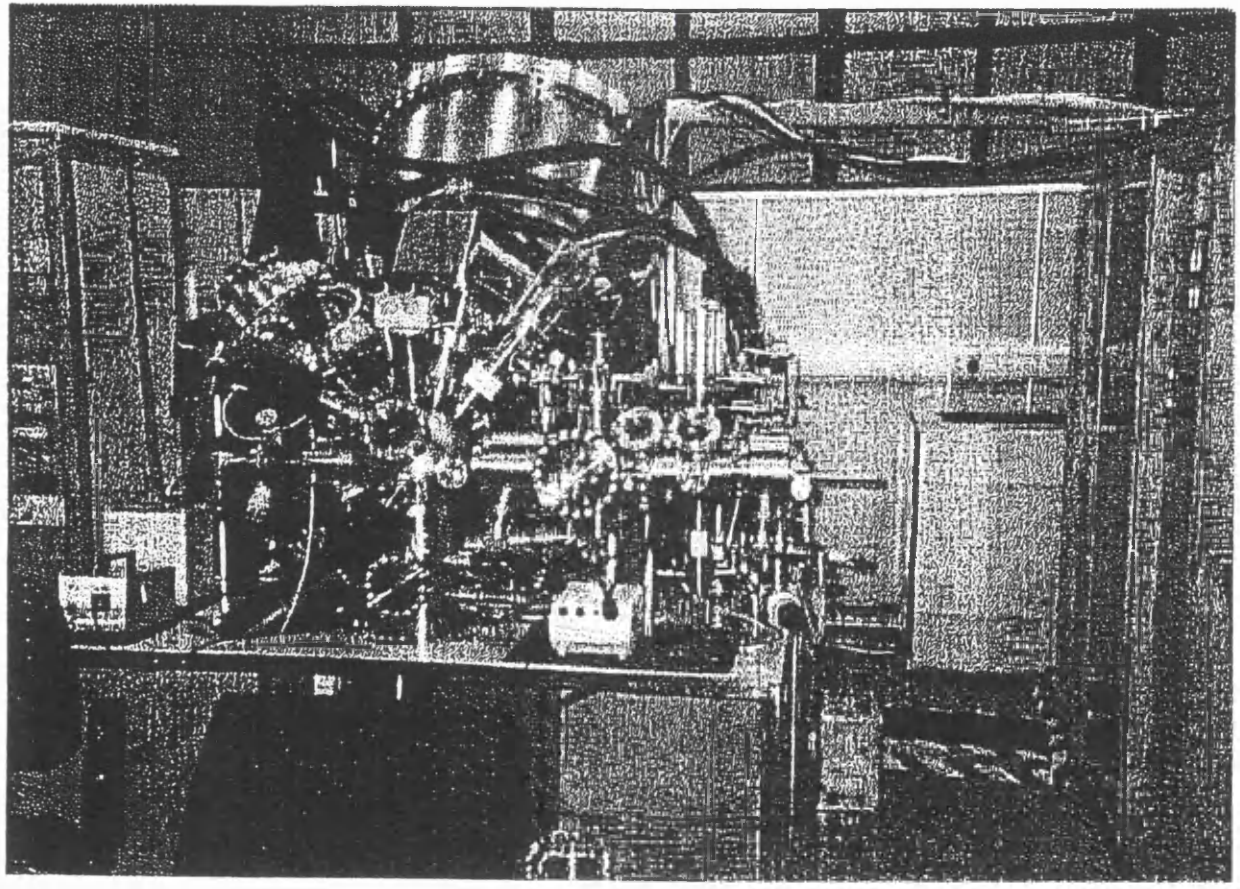

1.8.2 Instrumentation and Sample Handling (70)

Sample handling refers to sample preparation, insertion of the sample into the spectrometer and positioning of the sample inside the spectrometer.

1. Sample preparation

Samples to be analysed were in a powder form. To prevent spilling of the sample as it is transferred through the various vacuum systems, the powder must therefore be immobilised or 'fixed'. The method used was to mount the powder using double sided polymer based adhesive tape. A suspension of hexane and catalyst powder was used to mount the powder onto a thin film of double sided adhesive tape on top of a metal stub. The suspension was added dropwise to the surface of the stub and allowed to dry. A uniform 'fixed' powder surface was then achieved. All the tools used in the fixing process were grease free and gloves were worn to prevent contamination.

2. Sample Insertion

In the process of sample insertion, the sample, which was mounted on a metal stub, was transferred from atmospheric pressure to a fixed analysis chamber within the spectrometer which operates under ultra high vacuum conditions (UHV) ($<1 \times 10^{-8}$ torr). The form of specimen insertion used, was termed as 'the successive transfer method'. The stub was placed on a holder in a small fore-chamber that was sealed to the atmosphere and then using a primary low pressure oil diffusion pump, the pressure was quickly reduced to around 1×10^{-5} torr. Care was taken at this stage as the initial evacuation if carried out too quickly can cause 'explosive' outgassing of the sample.

A valve between the fore-chamber and a second, or preparation chamber was then opened and the carrier was moved into the second chamber on a trolley entirely enclosed within the vacuum. The stub was then transferred manually by means of a sealed bellows fork manipulation device onto another trolley within the preparation chamber. After the first trolley was returned to the fore-chamber, the valve between the two sections was closed. A large diffusion pump then reduced the pressure to approximately 1×10^{-8} torr. At this point, if the sample was found to be a source of gas, it can be pumped down for several hours until a suitable pressure is achieved.

A second valve between the preparation and analysis chambers was then opened and the sample transferred as before. After the sample was sealed in the analysis chamber, UHV conditions are achieved, prior to operation of the X-ray source.

3. Sample Positioning

It is important once a sample has been inserted into the spectrometer and brought into the proximity of the energy analyser, that it can be manipulated in a controlled manner. There are three reasons for this.

a. Shapes and sizes of samples vary, so that the optimum position in terms of sensitivity and energy resolution for one sample may vary for another.

b. It may be desirable to move a sample laterally in a reproducible way to allow different areas to be analysed.

c. It is often desirable to be able to rotate samples in a reproducible way to alter the angle of take-off electrons accepted by the analyser.

To be able to manipulate samples accurately, spectrometers are built with high precision manipulators. Such manipulators have a minimum of four degrees of freedom - X, Y and Z linear motions and an axial rotation motion.

1.8.3 The X-ray source

X-rays are produced when rapidly moving electrons that have been accelerated through a potential difference of the order of 10^3 - 10^6 V strike a metal target. The X-rays produced consist of a broad background called Bremstrahlung superimposed on characteristic narrow lines. Removal of this background is carried out using a monochromator.

The surface specificity of the XPS technique depends on using soft X-rays of characteristic energies - typically a few kiloelectron volts.

1.8.4 The Vacuum System

There are two reasons why electron spectrometers must operate under vacuum -

1. Electrons emitted from a sample should meet as few gas molecules as possible on their way to the analyser so that they are not scattered and lost from the analysis.

2. Most of the electrons analysed originate in the first one or two atom layers. This means that the technique is very sensitive to surface

contamination, such as adsorbed residual gas in the vacuum system. Thus UHV pressures are required to avoid this problem. To achieve such pressures, low pressure oil diffusion pumps are commonly used. Such diffusion pumps are operated with efficient nitrogen traps situated between them and the UHV.

1.8.5 The Electron Energy Analyser.

There are two main energy analysers - the cylindrical mirror analyser (CMA), and the concentric hemispherical analyser (CHA). The CHA is most commonly used, and is discussed here.

A schematic diagram of a concentric hemispherical analyser is shown below -

Fig 1.20

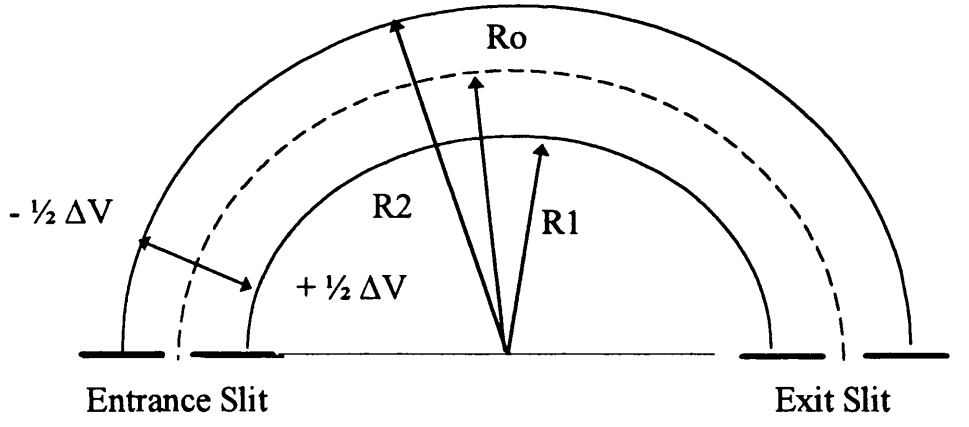

Two hemispherical surfaces are positioned concentrically and a voltage applied (ΔV) between the surfaces, so that the outer sphere is negatively charged with respect to the inner sphere. There is a median equipotential between the hemispheres which ideally has radius *Ro* and is defined by the following equation -

Eq 1.9

$$Ro = \frac{(R1 + R2)}{2}$$

R1, is the radius of the inner sphere and *R2* is the radius of the outer sphere along which electrons must pass in order to travel through the analyser. The entrance and exit slits are both centred on *Ro*. If E is the ideal kinetic energy of an electron travelling in an orbit of radius *Ro*, then the relationship between E and V as given by the expression below -

Eq 1.10

$$e\Delta V = E\left(\frac{R2}{R1} - \frac{R1}{R2}\right)$$

$e\Delta V_o = E_o$ (energy of an electron entering the analyser at an angle α to the slit normal).

Once the electrons exit the CHA, the signal is then amplified and recorded. Therefore, from the above equation, if the voltage is altered, different energy electrons will exit and thus be recorded.

Eq 1.11 $$[\rho = \frac{Ro}{w}]$$

(where w = slit width)

Therefore, the larger the analyser the larger the value of *R*o and as a result, resolving power increases. However, large analysers are very expensive and it is standard practice to retard the kinetic energies of the photo electrons to a chosen analyser energy called the pass energy which increases the resolution of the analyser. This is generally done using planar grids across the entrance slit.

1.8.6 The X-ray Photoelectron Energy Spectrum - Primary Structure.

When recording an XPS spectra of an unknown sample, a broad sweep (0 - 1150 eV), known as a survey scan is carried out. A series of peaks are observed on a background which generally increases to high binding energy and which also show step like increases on the high binding energy side of each significant peak. Photoemission processes are assumed to be elastic, therefore the incident X-rays give rise to a series of photoelectron peaks which are representative of discrete electron binding energies and hence the elements present in a sample. If, however, some of the photoelectrons lose energy before they are analysed (suffer inelastic collision), this results in the step like increases seen at the higher binding energies associated with main peaks.

Peaks can be grouped into two basic bands: those that arise due to photoemission from core and valence levels and those due to X-ray excited Auger emission.

In the samples examined, the peaks resulting from electron transfer from the Pd 3d$\frac{5}{2}$, $\frac{3}{2}$, Cl 2p$\frac{3}{2}$ and the Br 3d $\frac{5}{2}$ core levels were investigated.

1.8.6.1 Core Levels

The core level structure is a direct reflection of the electronic structure of a particular atom. Non s-levels are always observed as doublets in any recorded spectrum. These doublets arise through spin orbit (j-j) coupling. For a particular electron, the total angular momentum is characterised by the quantum number j, (where j is the vector sum of the individual electronic spin and angular momenta). Therefore, since $j = \ell + s$, j can have values of $\frac{1}{2}$, $\frac{3}{2}$, $\frac{5}{2}$ etc. Under the j-j coupling scheme, the nomenclature is based on the principal quantum number n and on the electronic quantum numbers ℓ and j.

For spectroscopic nomenclature, the principal quantum number appears first, then the states with $\ell = 0, 1, 2, 3 =$ s, p, d and f and finally, the j values are given as suffixes as shown in the table overleaf (table 1.5).

Table 1.5.

Quantum Numbers			Spectroscopic Levels
n	ℓ	j	
1	0	½	1s½
2	0	½	2s½
2	1	½	2p½
2	1	³/₂	2p³/₂
3	0	½	3s½
3	1	½	3p½
3	1	³/₂	3p³/₂

Thus, when $\ell > 0$, two possible states arise, with the energy difference (ΔE_j), reflecting the parallel or anti-parallel nature of the spin and orbital angular momentum vectors of the remaining electron.

For Auger transitions, where the final state is doubly ionised, interactions between the two holes in the final state can lead to situations where the j-j description is inadequate and as a result, X-ray notation is used. Historically, in X-ray notation, states with n = 1, 2, 3, 4 are designated as K, L, M, N respectively, whilst states with various combinations of ℓ = 0, 1, 2, 3... and j = ½, ³/₂, ⁵/₂, ⁷/₂ ... are given conventional suffixes, 1, 2, 3, 4 as shown in the table 1.6, overleaf.

Table 1.6.

X-Ray Suffix	X-ray Level	Spectroscopic level
1	K	$1s_{1/2}$
1	L_1	$2s_{1/2}$
2	L_2	$2p_{1/2}$
3	L_3	$2p_{3/2}$
1	M_1	$3s_{1/2}$
2	M_2	$3p_{1/2}$
3	M_3	$3p_{3/2}$
4	M_4	$3d_{3/2}$
5	M_5	$3d^5/_2$

In j-j coupling, there are therefore six possible KLL transitions i.e. KL_1L_1, KL_1L_2, KL_1L_3, KL_2L_2, KL_2L_3 and KL_3L_3. This is the most universally used nomenclature in AES.

1.8.6.2 Information from Primary Structure - Core Level Chemical Shifts

Non-equivalent atoms of the same element in a solid give rise to core level peaks with measurably different binding energies. This binding energy difference is known as the chemical shift. Non equivalence in atoms can arise due to a difference in oxidation state and also due to differences in the chemical environment. In general, binding energy values for a particular core level electronic emission, increase with an increase in the formal oxidation number at a particular atom. The general rule is that the core level binding energy of the central atom increases as the electronegativity of attached groups or atoms increases. This is demonstrated by the N1s spectrum of $[Co(NH_2CH_2CH_2NH_2)_2(NO_2)_2]NO_3$.

Fig 1.22 - The N1s spectrum of $[Co(NH_2CH_2CH_2NH_2)_2(NO_2)_2]NO_3$.

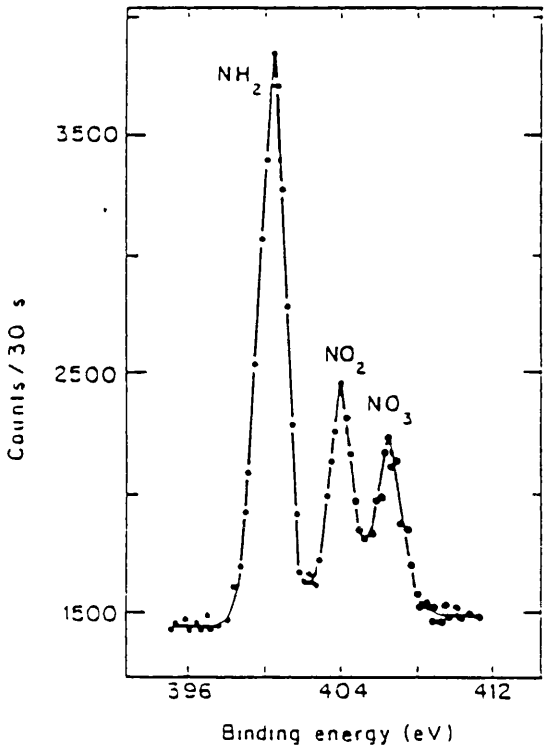

1.8.7 Static Charge Referencing

On insulating samples, the loss of photoelectrons is not balanced by replacement within the specimen and so there is a build up of positive charge which produces a retarding field in front of the specimen. As a result the kinetic energy of photoelectrons have a lower energy than predicted -

Eq 1.11 $[E_k = h\nu - E_B - C]$

($h\nu$ = the energy of x-ray photons, E_B = binding energy of core level and C = steady state charge value).

To determine the value for C a low energy electron flood gun is used. The flood gun fires low energy electrons at the surface of the sample to maximise the neutralisation effect and reduce the number of electron bombardment induced reactions.

In almost all cases the surfaces of all specimens suffer from contamination due to adsorption of gases (especially in instruments using oil diffusion pumps). Carbon is the element most commonly detected in contamination layers and photoelectrons from the C1s atomic energy level are those most commonly used for referencing purposes. A binding energy value of 285.0 ± 0.2 eV is often used for this C1s level and the difference between the C1s value of the measured spectrum and the value above gives the charging value C. Experimentally, for each flood gun setting the C1s spectrum is measured. The flood gun setting with the best line shape and intensity is noted along with the relative C1s value. By deducting this value from the constant C1s = 285.0 eV, the C value is obtained and this value can be applied to any recorded peak binding energy values.

1.9 Neutron Activation Analysis (NAA) (71, 72)

Neutron Activation Analysis is an extremely powerful trace elemental technique in which a sample is bombarded with thermal neutrons for appropriately chosen lengths of time. The chemical elements are identified and assayed after irradiation by measurement of characteristic radiation emitted from nuclides formed during the (n,γ) reaction. Chemical separation of individual components is not required due to the excellent energy resolution of lithium-doped germanium detectors. Standardisation is provided by irradiation of a sample containing a known amount of the element to be analysed as well as the unknown sample. In the course of this

study NAA was used to determine the palladium content of several samples since the standard technique of determining metal loadings in catalysts, atomic absorption (AA), proved to be ineffective.

1.9.1 NAA Theory

For x target atoms of capture cross section σ, irradiated in a constant neutron flux ϕ -

Eq 1.13 $$\left[\frac{dN}{dt} = x\sigma\phi - N\lambda\right]$$

$\frac{dN}{dt}$ = Change in number of radioactive atoms

$x\sigma\phi$ = Rate of formation

$N\lambda$ = Rate of decay

$x\sigma\phi$ is constant for a constant neutron flux (independent of N). In the early stages of irradiation, the rate of formation far exceeds the rate of decay, so N increases with time. Eventually N increases to the point where the rate of formation equals the rate of decay. At this point, N is said to be at saturation point, N_{sat}.

Eq 1.14 $$x\sigma\phi = N_{sat}\lambda$$

Therefore, substituting this into, $\frac{dN}{dt} = x\sigma\phi - N\lambda$, gives the following-

$$\frac{dN}{dt} = N_{sat}\lambda - N\lambda = (N_{sat} - N)\lambda \text{ and hence } \frac{dN}{(N_{sat} - N)} = \lambda dt$$

Thus, integrating by change of variable: Let $U = N_{sat} - N$, therefore, $dU = -dN$, since N_{sat} is a constant. $\frac{dU}{U} = -\lambda dt$. Integrating, $\ln U = -\lambda t + C$

When $t = 0$, $N = 0$ so $C = \ln N_{sat}$. $\ln (N_{sat} - N) = \ln N_{sat} - \lambda t$.

$(N_{sat} - N) = N_{sat} e^{-\lambda t}$ so $N = N_{sat} (1 - e^{-\lambda t})$, therefore -

Eq 1.15 $$N = \frac{x\sigma\phi(1-e^{-\lambda t})}{\lambda}$$

In terms of activity, since $A = N\lambda$, the following equation gives the activity of a sample immediately after irradiation -

Eq 1.16 $$A_{t=0} = x\sigma\phi(1-e^{-\lambda t})$$

Therefore, since $A = A_o e^{-\lambda t}$, $A = x\sigma\phi(1-e^{-\lambda t(\text{irradiation})})(e^{-\lambda t(\text{cool})})$

(where t(cool) = the time elapsed immediately following irradiation).

From this equation it is possible to calculate the number of target atoms directly. However, due to significant uncertainties in literature nuclear parameters and variances in flux density figures, a comparator method is used (Eq 1.17 shown overleaf). This method involves using a standard of known mass and composition along with the unknown sample. In this way,

neutron flux, cross sections, irradiation times and all other variables associated with counting are constant for both the standard and the sample.

Eq 1.17

Comparator equation - $$\frac{R_{std} = w_{std}(e^{-\lambda T})_{std}}{R_{sam} = w_{sam}(e^{-\lambda T})_{sam}}$$

R = counting rate (counts per second)

w = weight of element being analysed (μg)

T = decay time (mins)

The sensitivity of this technique depends in the main on the strength of the neutron flux. In a typical research nuclear reactor, a flux of 10^{12} - 10^{15} $ncm^{-2}s^{-1}$ is possible. With this flux rate, elements such as palladium have a detectable limit of 4 - 9 x 10^{-4} μg.

To investigate the Palladium content of samples -

$^{108}_{46}Pd$ is 26.7 % abundant and has a cross section σ of 11 Barns.

Scheme 1.5

$$^{108}_{46}Pd + {}^{1}_{0}n \longrightarrow {}^{109}_{46}Pd \longrightarrow {}^{109}_{47}Ag + {}^{0}_{-1}e + \gamma$$

Since only ^{109}Pd is active, the isotopic abundance of ^{108}Pd must be taken into account in calculations. The half life for ^{109}Pd is 13.43 hours.

The relevant γ energies for ^{109}Pd are 88.0 and 311.5 KeV, but the intensity of the 311.5 KeV γ ray peak is only 10 % that for the 88.0 KeV peak. As a consequence, the 88.0 KeV signal was therefore used.

Since all the samples and standards to be analysed are comprised of 5 % complex and 95 % silica, the following reaction may cause interference -

Eq 1.18

$$^{30}_{14}\mathrm{Si} + ^{1}_{0}\mathrm{n} \longrightarrow ^{31}_{14}\mathrm{Si}$$

$^{31}_{14}$Si has a half life 2.62 hours and decays with a γ energy of 1266.2 KeV). Since the respective t ½ values for ^{109}Pd and ^{31}Si are 13.43 h and 2.62 h respectively, the sample would benefit from leaving overnight after irradiation. This would ensure that most of the ^{31}Si had decayed before counting was carried out. The samples were irradiated in the reactor at a flux of 3 x 10^{12} $ncm^{-2}s^{-1}$ for exactly 5 minutes and counting of the samples was done approximately 24 hours later. This gave a decay corrected activity of around 1 x 10^{6} Bq.

1.9.2 Experimental Procedure

1. Sample Preparation

Approximately 0.25 g of catalyst sample was accurately weighed (4dp), and transferred into a polypropylene container called an epindorph. Once transferred, the epindorph was then sealed to avoid spillage during the

irradiation stage. The same procedure was carried out when preparing the standards.

Standards containing 5 % and 1 % palladium were made up. Approximately 12.5 mg and 2.5 mg of palladium were accurately weighed out and made up to 0.25 g using Gasil 35M silica. The metallic palladium and silica were intimately mixed using a shaker for a period of one hour. Once the samples were sealed, mixed and labelled, they were then transferred into a larger container called a 'rabbit'. The rabbit was used to transfer simultaneously all the samples into and out of the reactor for irradiation purposes.

The correct stacking of the samples was extremely important. Several samples of unknown composition were loaded on the same level as two standards (each rabbit contains at least 2 or 3 such levels). In this way the standard samples get the same neutron flux as the unknown samples on the same level and comparison of count rates was then possible.

Pneumatic air was used to transfer the rabbit between the laboratory and the reactor through a series of transfer tubes. After irradiation and removal, the samples were allowed to decay to remove short lived radioactive nuclides and lower the overall activities of the samples. After opening the rabbit, the individual epindorphs were then wiped clean to avoid surface contamination and counted. Counting was done in a low background area located outside the reactor compartment.

Chapter 2

OBJECTIVES

2.0 OBJECTIVES

The main focus of this work was to investigate the activities and selectivities of a series of silica-supported palladium phosphine complexes, $[PdX_2(PR_3)_2]$ (X=Cl, Br or I; R =Me), and $[Pd_2X_4(PR_3)_2]$ (X=Cl, Br or I; R=Me, Et, Pr^i or Bu) in the liquid phase hydrogenation of cinnamaldehyde and to compare the results with the performance of a 5 % $[Pd/SiO_2]$ catalyst prepared from $Pd(NO_3)_2$.

To this end, a list of the primary objectives is included below.

1. To prepare the complexes detailed above and to ensure purity by the use of $^1H/^{31}P$ NMR and microanalysis; to prepare high surface area heterogeneous catalysts by supporting them on Gasil 35M silica.

2. To investigate the product ratios formed when the supported complexes are used in the hydrogenation of cinnamaldehyde and to correlate the results with the nature of the halogen and phosphine constituents.

3. To gain mechanistic information on the mode of catalyst activity by investigating the hydrogenation of reaction intermediates such as hydrocinnamaldehyde and cinnamyl alcohol.

4. To compare and contrast the activities of the unsupported complexes with the silica supported analogues.

The next stage of the work described in this thesis involved the characterisation of the catalysts examined, both prior to use and after extraction at various time periods from the reaction mixture, in an attempt

to throw light upon the nature of the 'active sites' formed. The techniques used in this investigation include -

1. X-ray photoelectron spectroscopy (XPS), to investigate changes in the oxidation state of the palladium component.

2. Solid state ^{31}P magic angle spinning NMR (MAS-NMR), to investigate changes in the chemical nature of the complex during reaction.

3. Microanalyses (M/A), to investigate how the chemical composition of the catalyst varied with reaction time.

4. Thermogravimetric Analysis (TGA), to investigate possible trends in weight loss measurements amongst the catalysts examined.

5. Neutron Activation Analysis (NAA), to investigate the possibility of metal leeching, and to check the palladium loading in the catalyst precursors.

It was hoped that correlation of the catalyst characterisation data with catalytic activities and selectivities would enable the observed catalytic behaviour to be understood.

Chapter 3

EXPERIMENTAL

3.1 INTRODUCTION

A series of mononuclear palladium phosphine complexes, trans-$[PdX_2(PR_3)_2]$ and the binuclear analogues, trans-$[Pd_2X_4(PR_3)_2]$ (X= Cl, Br or I; R= Me, Et, Pr^i or Bu) were prepared. Characterisation was carried out using ^1H and ^{31}P NMR spectroscopy and microanalysis.

These complexes were supported on silica by a wet impregnation technique. The catalyst precursors thus formed were tested for their activities and selectivities in the liquid phase hydrogenation of cinnamaldehyde using a glass reactor operating at atmospheric pressure. Analysis of the reaction products was carried out by Gas Chromatography (GC). A small number of catalysts were also tested for their activities and selectivities in the liquid phase hydrogenation of 2-cyclohexene-1-one and the reaction products were again analysed by gas chromatography.

Characterisation of the catalysts and precursors was accomplished using a variety of chemical techniques. X-ray photoelectron spectra (XPS) were recorded at the Daresbury Laboratories, Daresbury England. Neutron activation analysis (NAA), at the Reactor Centre, East Kilbride and solid state ^{31}P magic angle spinning nuclear magnetic resonance spectra (MAS-NMR), at UMIST Chemistry Department. Thermogravimetric analysis (TGA), transmission electron microscopy (TEM) and microanalysis (M/A) were all carried out at the University of Glasgow Chemistry Department.

3.2 Complex Preparation and Analysis

Preparation of Mononuclear Palladium(II) Bis (tertiary phosphine) Complexes - trans-$[PdX_2(PR_3)_2]$ (X= Cl, Br, I and R= Me, Et).

All complexes unless otherwise stated were prepared in a nitrogen atmosphere. NMR spectra were recorded on a Bruker AM 200 spectrometer operating in the Fourier-transform mode.

Dichloromethane, chloroform and diethyl ether solvents were dried and deoxygenated by distillation under oxygen-free nitrogen. Analar grade ethanol (99.7 %+), pentane (98 %) and chlorobenzene (99 %) were supplied by the Aldrich Chemical Company. Potassium tetrabromopalladate(II) (99 %+), lithium bromide (99 %+), lithium iodide (99 %), tri-n-butyl phosphine (97 %) and triisopropylphosphine (90 %) were also obtained from Aldrich. Sodium tetrachloropalladate(II) (99 %) was obtained from Johnson Matthey PLC, palladium(II) chloride anhydrous (99 %), from Fluka, trimethylphosphine (97 %+) and triethyl phosphine (95 %), from Strem Chemicals and celite 30-80 mesh from BDH.

3.2.1 Preparation of trans-[$PdCl_2(PMe_3)_2$] (73, 74, 75, 76, 83)

Sodium tetrachloropalladate(II) (Na_2PdCl_4) (5.00 g, 17 mmol) was dissolved in degassed ethanol (100 ml), to give a wine coloured solution. After 15 minutes, trimethylphosphine (PMe_3), (2.58 g, 34 mmol) was injected into the solution. The solution turned yellow and a large amount of sodium chloride (as precipitate) was formed. The mixture was stirred for 3 hours and then refluxed for 30 minutes to convert any $[Pd(PMe_3)_4]^{2+}[PdCl_4]^{2-}$ formed to trans-[$PdCl_2(PMe_3)_2$]. The sodium chloride precipitate was removed by filtration and washed with 50 ml dichloromethane. The remaining filtrate was rotary evaporated to dryness to give 4.25 g of crude trans-[$PdCl_2(PMe_3)_2$]. Yield = 53.2 %. Recrystallisation from methanol then gave 2.98 g of pure trans-[$PdCl_2(PMe_3)_2$] as a yellow microcrystalline powder. (Found: C, 21.9; H, 5.7. Calc. for $C_6H_{18}Cl_2P_2Pd$: C, 21.9; H, 5.5 %). NMR ($CDCl_3$): ^1H, δ 1.42 (t, 18 H, CH_3); ^{31}P, (s), δ -11.90. M.Pt 279 - 281°C (with decomp).

3.2.2 Preparation of trans-[$PdBr_2(PMe_3)_2$] (73, 74, 75, 76, 83)

Trans-[$PdCl_2(PMe_3)_2$] (0.30 g, 0.91 mmol) was dissolved in 20 ml of hot ethanol and stirred. A large excess of LiBr, (0.63 g, 1.82 mmol) was added. The mixture was refluxed for 2 hours and was then filtered. Upon cooling overnight at a temperature of -15°C, yellow crystals of trans-[$PdBr_2(PMe_3)_2$] were formed. These were filtered off and washed with 20 ml of water to remove any LiCl or unreacted LiBr. 0.225 g of trans-[$PdBr_2(PMe_3)_2$] microcrystals were obtained. Yield = 59.1 %. (Found: C, 17.6; H, 4.4. Calc. for $C_6H_{18}Br_2P_2Pd$: C, 17.2; H, 4.3 %). NMR ($CDCl_3$): ^1H, δ 1.57 (s, 18 H, CH_3); ^{31}P, (s), δ -15.96.

3.2.3 Preparation of trans-[$PdI_2(PMe_3)_2$] (73, 74, 75, 76, 83)

Trans-[$PdCl_2(PMe_3)_2$] (0.40 g, 1.21 mmol) was dissolved in 25 ml of hot ethanol and the mixture stirred. Excess lithium iodide, (1.30 g, 9.7 mmol) was then added and an immediate colour change (from yellow to wine) was observed. The mixture was refluxed for three hours, filtered and then cooled at a temperature of -15°C overnight. Orange needle crystals of trans-[$PdI_2(PMe_3)_2$] were formed. These were washed with 20 ml of water to remove any LiCl or excess LiI present. 0.328g of trans-[$PdI_2(PMe_3)_2$] crystals were obtained. Yield = 53.0 %. (Found: C, 14.2; H, 3.5. Calc. for $C_6H_{18}I_2P_2Pd$: C, 14.1; H, 3.4 %). NMR ($CDCl_3$): ^1H, δ 1.83 (t, 18 H, CH_3); ^{31}P, (s), δ -27.2.

3.2.4 Preparation of trans-[$PdCl_2(PEt_3)_2$] (77 ,78, 79, 82, 83)

Na_2PdCl_4 (2.0 g, 6.8 mmol) was dissolved in 50 ml ethanol. Triethyl phosphine (PEt_3), (0.12 g, 0.6 mmol) was then added using a syringe and the mixture stirred for 2 hours, followed by a ½ hour reflux (to convert any [$Pd(PEt_3)_4^{2+}$][$PdCl_4^{2-}$] into trans-[$PdCl_2(PEt_3)_2$]. After filtering, a clear yellow filtrate was observed. Upon cooling overnight at -15°C, no crystals were formed. The solution was then rotary evaporated and vacuum dried to give a yellow powder identified as trans-[$PdCl_2(PEt_3)_2$]. 1.65 g in total were produced. Yield = 58.7 %. (Found: C, 35.0; H, 7.4. Calc. for $C_{12}H_{30}Cl_2P_2Pd$: C, 34.8; H, 7.3 %). NMR ($CDCl_3$): ^1H, δ 1.12 (quintet, 18 H, CH_3), 1.80 (m, 12 H, CH_2); ^{31}P, (s), δ -17.8.

3.2.5 Preparation of trans $[PdI_2(PEt_3)_2]$ (78, 79, 83)

Na_2PdCl_4, (0.5 g, 1.7 mmol) was dissolved in 50 ml of hot ethanol and LiI, (3.64 g, 27.2 mmol) was added. PEt_3, (0.70 g, 3.4 mmol), was then injected into the reaction vessel. This was then stirred for 2 hours and then finally refluxed for a final 30 minutes. After filtering the mixture, orange crystals of trans-$[PdI_2(PEt_3)_2]$ were formed. The solution was then left overnight to facilitate crystal growth, after which the trans-$[PdI_2(PEt_3)_2]$ was removed and washed with 20 ml of distilled water. Overall, 0.269 g of the monomer product was obtained. Yield = 49.0 %. (Found: C, 24.3; H, 5.2. Calc. for $C_{12}H_{30}I_2P_2Pd$: C, 24.1; H, 5.0 %). NMR ($CDCl_3$): ^1H, δ 1.09 (quintet, 18 H, CH_3), 2.27 (m, 12 H, CH_2); ^{31}P, (s), δ -17.8.

Preparation of Binuclear Palladium(II) Bis (tertiary phosphine) Complexes - trans-$[Pd_2X_4(PR_3)_2]$ (X= Cl, Br, I and R= Me, Et, Pr^i or Bu).

3.2.6 Preparation of trans-$[Pd_2Cl_4(PMe_3)_2]$ (75, 76, 80, 83)

Trans-$[PdCl_2(PMe_3)_2]$ (4.0 g, 12.1 mmol) was dissolved in 150 ml of hot ethanol and stirred. Na_2PdCl_4, (3.56 g, 12.1 mmol) was then added. A white precipitate of NaCl was formed. After refluxing for 2 hours, the mixture was filtered and an orange precipitate of trans-$[Pd_2Cl_4(PMe_3)_2]$ formed. The solution was left overnight at a temperature of -15°C after which the precipitate was filtered off. 3.70g of pure trans-$[Pd_2Cl_4(PMe_3)_2]$ was obtained. Yield = 61.0 %. The yield may be improved by extracting additional product from the NaCl side product by refluxing in $CHCl_3$, filtering, rotary evaporating the filtrate to dryness and then recrystallising from hot ethanol. (Found: C, 14.5; H, 3.8. Calc. for $C_6H_{18}Cl_4P_2Pd_2$: C,

14.2; H, 3.6 %). NMR ($CDCl_3$): ^1H, δ 1.59 (d, 18 H, CH_3); ^{31}P, (s), δ 14.8.

3.2.7 Preparation of trans-[$Pd_2Br_4(PMe_3)_2$] (74, 75, 76, 83)

Trans-[$Pd_2Cl_4(PMe_3)_2$] (0.24 g, 0.47 mmol) was dissolved in 25 ml of hot ethanol and the mixture stirred. Excess LiBr, (0.66 g, 7.6 mmol), was then added and the mixture refluxed for 2 hours. Upon filtering, an orange precipitate of trans-[$Pd_2Br_4(PMe_3)_2$] was produced. This was left overnight at -15°C, after which the precipitate was filtered off. 0.17g of trans-[$Pd_2Br_4(PMe_3)_2$] in total were obtained. Yield = 53.0 %. (Found: C, 10.5; H, 2.8. Calc. for $C_6H_{18}Br_4P_2Pd_2$: C, 10.5; H, 2.6 %). NMR ($CDCl_3$): ^1H, δ 1.72 (d, 18 H, CH_3); ^{31}P, (s), δ 12.3.

3.2.8 Preparation of trans-[$Pd_2I_4(PMe_3)_2$] (74, 75, 76, 83)

Trans-[$PdCl_2(PMe_3)_2$] (0.25 g, 0.76 mmol) was dissolved in 50 ml of hot acetone. To this Na_2PdCl_4, (0.25 g, 0.76 mmol) and an excess of LiI (1.63 g, 12.2 mmol) were added. The mixture was then refluxed for 2 hours and diethyl ether (25mls) added, to precipitate out the trans-[$Pd_2I_4(PMe_3)_2$] complex. After filtering, the complex was then washed with 20 ml of water to remove any NaCl, LiCl or unreacted LiI present. 0.29 g of trans-[$Pd_2I_4(PMe_3)_2$] were obtained. Yield = 44.0 %. (Found: C, 8.6; H, 2.2. Calc. for $C_6H_{18}I_4P_2Pd_2$: C, 8.3; H, 2.1 %). NMR ($CDCl_3$): ^1H, δ 1.92 (d, 18 H, CH_3); ^{31}P, (s), δ 4.9.

3.2.9 Preparation of trans-[$Pd_2Cl_4(PBu_3)_2$] (81, 82)

Palladium dichloride ($PdCl_2$), (0.5 g, 5.6 mmol) along with tributylphosphine, (1.13 g, 5.6 mmol) were added to 15 ml of chlorobenzene and refluxed for 1.5 hours. The colour of the solution was observed to change from brown to yellow/orange. Another equivalent of $PdCl_2$, (0.5 g, 5.6 mmol) was then added and the mixture refluxed for a further 1.5 hours, before being filtered through celite (pre-washed with chlorobenzene). A clear orange filtrate was observed. After vacuum drying the solution an orange solid was formed. Recrystallisation from a chloroform/pentane mixture proved unsuccessful. After reducing the volume of the chloroform/pentane solution to half, a precipitate formed and filtering gave a wet solid. This was then air dried to give crystals of trans-[$Pd_2Cl_4(PBu_3)_2$], which were washed with 10 ml of pentane. 0.58 g of trans-[$Pd_2Cl_4(PBu_3)_2$] were obtained. Yield = 27.2 %. (Found: C, 38.0; H, 7.3. Calc. for $C_{24}H_{54}Cl_4P_2Pd_2$: C, 37.9; H, 7.1 %). NMR ($CDCl_3$): ^1H, δ 0.95 (t, 18 H, CH_3), 1.65 (m, 36 H); ^{31}P, (s), δ 39.97.

3.2.10 Preparation of trans-[$Pd_2Br_4(PBu_3)_2$]

Trans-[$Pd_2Cl_4(PBu_3)_2$] (0.5 g, 0.66 mmol) was dissolved in 50 ml of hot ethanol and refluxed with LiBr (0.92 g, 10.6 mmol) for 2 hours. The clear orange solution was filtered hot and as it cooled a large amount of orange precipitate formed. After drying 0.26 g of trans-[$Pd_2Br_4(PBu_3)_2$] was obtained. Yield = 41.7 %. (Found: C, 30.4; H, 5.8. Calc. for $C_{24}H_{54}Br_4P_2Pd_2$: C, 30.8; H, 5.8 %). NMR ($CDCl_3$): ^1H, δ 0.95 (t, 18 H, CH_3), 1.51 (m, 24 H), 1.95 (m, 12 H); ^{31}P, (s), δ 39.51.

3.2.11 Preparation of trans-[$Pd_2Br_4(PPr^i_3)_2$]

$PdCl_2$ (0.5 g, 2.8 mmol) was added to 20 ml of chlorobenzene. Triisopropylphospine (PPr^i_3), (4.81 g, 5.64 mmol) was then added using a syringe and the mixture refluxed for two hours. Another equivalent of $PdCl_2$, (0.5 g, 2.8 mmol) was added and the mixture refluxed for a further 2 hours, after which it was filtered. $PdCl_2$ (0.52 g, 2.94 mmol) was recovered unreacted. As the filtrate cooled, orange crystals of trans-[$Pd_2Cl_4(PPr^i_3)_2$] formed. After filtering, the crystals were then washed with a 20 ml portion of water. 0.460g of trans-[$Pd_2Cl_4(PPr^i_3)_2$] were obtained. Yield = 48.4 %. A halogen substitution was then performed on the trans-[$Pd_2Cl_4(PPr^i_3)_2$]. Trans-[$Pd_2Cl_4(PPr^i_3)_2$], (0.25 g, 0.37 mmol) was dissolved in 20 ml of hot ethanol and LiBr, (0.51 g, 5.92 mmol) added. The mixture was then refluxed for 2 hours and filtered hot. As the ethanolic solution cooled, a microcrystalline precipitate of trans-[$Pd_2Br_4(PPr^i_3)_2$] formed. After filtering and washing with 20 ml of water, 0.21g were obtained. Yield = 66.0 %. (Found: C, 25.7; H, 5.0. Calc. for $C_{18}H_{42}Br_4P_2Pd_2$: C, 25.3; H, 4.9 %). NMR ($CDCl_3$): ^1H, δ 1.44 (dd, 36 H), 2.56 (d septets, 6 H); ^{31}P, (s), δ 69.9.

3.2.12 Preparation of trans-[$Pd_2Cl_4(PEt_3)_2$] (79, 81, 82, 83)

Trans-[$PdCl_2(PEt_3)_2$] (0.5 g, 1.2 mmol) was dissolved in 50 ml of hot ethanol, and Na_2PdCl_4, (0.35 g, 1.2 mmol) added. The mixture was refluxed for 2 hours and then filtered hot to leave a clear yellow solution. As the solution cooled needle crystals of trans-[$Pd_2Cl_4(PEt_3)_2$] formed. Total weight obtained = 0.363 g. Yield = 50.8 %. (Found: C, 24.5; H, 5.1. Calc. for $C_{12}H_{30}Cl_4P_2Pd_2$: C, 24.4; H, 5.1 %). NMR ($CDCl_3$): ^1H, δ 1.28 (dt, 18 H, CH_3), 1.88 (dq, 12 H, CH_2); ^{31}P, (s), δ 48.2.

3.2.13 Preparation of trans-[$Pd_2Br_4(PEt_3)_2$] (79)

Trans-[$PdBr_2(PEt_3)_2$] (1.0 g, 2.0 mmol) was dissolved in 50 ml of hot ethanol, and potassium tetrachloropalladate (K_2PdBr_4), (1.0 g, 2.0 mmol) added to 30 ml of distilled water. The mixture was then refluxed for 2 hours and filtered hot. As it cooled, cubic red crystals of trans-[$Pd_2Br_4(PEt_3)_2$] were formed. These were left to grow overnight prior to being filtered off and washed with 20 ml of water. The total weight of crystals formed was 1.09 g. Yield = 70.7 %. (Found: C, 18.9; H, 3.8. Calc. for $C_{12}H_{30}Br_4P_2Pd_2$: C, 18.7; H, 3.9 %). NMR ($CDCl_3$): ^1H, δ 1.28 (dt, 18 H, CH_3), 2.10 (dq, 12 H, CH_2); ^{31}P, (s), δ 47.8.

3.2.14 Preparation of trans-[$Pd_2I_4(PEt_3)_2$] (79)

Na_2PdCl_4 (0.15 g, 0.50 mmol) was dissolved in 40 ml of hot ethanol, and LiI, (1.08 g, 8.05 mmol) added. This was then refluxed for 2 hours and trans-[$PdI_2(PEt_3)_2$], (0.33 g, 5.0 mmol) added. After being refluxed for another 2 hours, the mixture was then filtered hot. Upon cooling, dark (almost black) crystals of trans-[$Pd_2I_4(PEt_3)_2$] were formed from the filtrate. This was then left overnight at room temperature after which the crystals were filtered off, and washed with 20 ml of distilled water. 0.27 g of trans-[$Pd_2I_4(PEt_3)_2$] crystals were obtained. Yield = 55.9 %. (Found: C, 15.4; H, 3.3. Calc. for $C_{12}H_{30}I_4P_2Pd_2$: C, 15.1; H, 3.1 %). NMR ($CDCl_3$): ^1H, δ 1.09 (dt, 18 H, CH_3), 2.27 (dq, 12 H, CH_2); ^{31}P, (s), δ 43.1.

3.2.15 Preparation of the Phosphonium salt [PMe_3H]Br

Acetyl bromide (CH_3COBr), (1.0 g, 9.0 mmol) was added to a solution of methanol (2.0 ml, 49.2 mmol). Upon addition, a vigorous reaction occurred, and white fumes of HBr were observed. The mixture was then stirred for 30 minutes after which trimethyl phosphine (0.69 g, 9.0 mmol) was added. After a further 30 minutes, 5 ml of diethyl ether were used to precipitate out the [PMe_3H]Br as a white solid. This was then vacuum dried, and stored in a desiccator. 0.475 g were obtained. Yield = 33.8 %. NMR (D_2O): ^1H, δ 1.72 (d, 9 H, CH_3), 4.63 (s, 1 H, HOD); ^{31}P, (1:1:1 t, P-D), δ -5.42.

3.3 PREPARATION OF CATALYSTS

Gasil 35M silica was supplied by Crosfield. It has a BET surface area of 320 m^2g^{-1}, an average particle size of 2.3 - 4.5 nm and a pore volume of 1.2 mlg^{-1}. For a 5 % aqueous suspension, pH = 7.0.

Palladium(II) nitrate hydrate $(Pd(NO_3)_2).xH_2O$ and tetrabutylammonium bromide, $[Bu_4N]Br$ (98 %), were obtained from Aldrich. Palladium(II) chloride ($PdCl_2$) (99 %) was obtained from Fluka. Dichloromethane and chloroform solvents were dried and deoxygenated by distillation under an atmosphere of oxygen-free nitrogen. Analar grade ethanol (99.7 %+) was also supplied by Aldrich and acetone (99%+) was supplied by Fisher Scientific.

3.3.1.1 Preparation of a 5 % [Pd/SiO_2] Catalyst

A catalyst with a 5 % (w/w) palladium loading on Gasil 35M silica was prepared using palladium(II) nitrate and used as a reference. The palladium(II) nitrate was supported on the silica using a wet impregnation technique. $Pd(NO_3)_2$ (0.55 g, 2.39 mmol) was added to 50 ml of distilled water and several drops of concentrated nitric acid were added to aid solvation. The mixture was then stirred and heated for 2 hours until all of the $Pd(NO_3)_2$ had gone into solution. Before use the silica was heated in an oven overnight at 100°C. The resulting silica was referred to as pre-dried silica and this procedure was followed in subsequent catalyst preparations. Pre-dried silica (4.4 g, 73.2 mmol) was added to the solution and the impregnated silica was left in the mother liquor overnight. After this, the slurry was dried by rotary evaporation and vacuum. Finally, the impregnated material was heated in an oven at a temperature of 100°C for

one hour. Total weight of the [$Pd(NO_3)_2/SiO_2$] catalyst precursor obtained = 4.77 g.

3.3.1.2 Calcination

Calcination of the [$Pd(NO_3)_2/SiO_2$] catalyst precursor was carried out using the system shown below. An air flow rate of 60 $cm^3 min^{-1}$ through the catalyst precursor was used and a temperature programmer raised the furnace temperature at a rate of 5°C min^{-1} from room temperature to 250°C. After reaching 250°C, the furnace temperature was held constant for a further 3 hours, before cooling back down to room temperature.

The diagram below shows the basic layout of the calcination apparatus -

Fig 3.1.

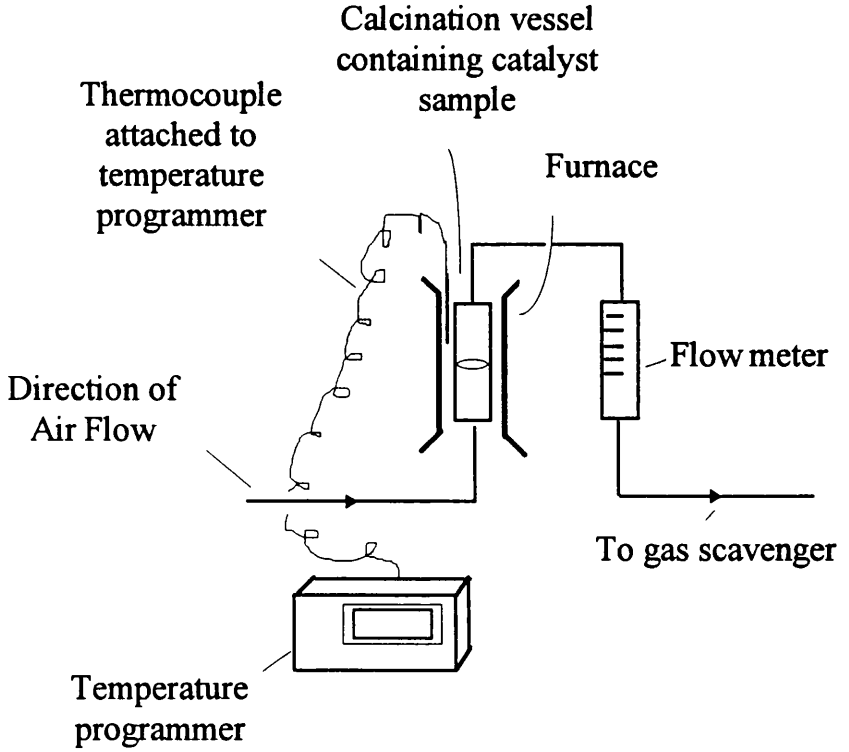

3.3.1.3 Reduction

After the catalyst precursor [$Pd(NO_3)_2/SiO_2$] had been calcined to palladium oxide (PdO) supported on silica, it was then reduced under a flow of hydrogen gas (H_2), to palladium-on-silica. Reduction was carried out using the system detailed below (Fig 3.2). After being placed in the reduction apparatus, the system was sealed and purged of air using a high flow rate of helium gas (> 100 ml min^{-1}) for 30 minutes. When all the air was displaced, the helium gas flow was replaced by hydrogen and the flow adjusted to 60 cm^3 min^{-1}. The temperature at the catalyst precursor was then raised to 200°C by means of a variable voltage supply unit attached to a furnace. Reduction was allowed to continue overnight (18 hours). This reduction treatment converted the calcined catalyst precursor into a 5 % [Pd/SiO_2] catalyst as required.

The diagram below shows the basic layout of the reduction apparatus -

Fig 3.2

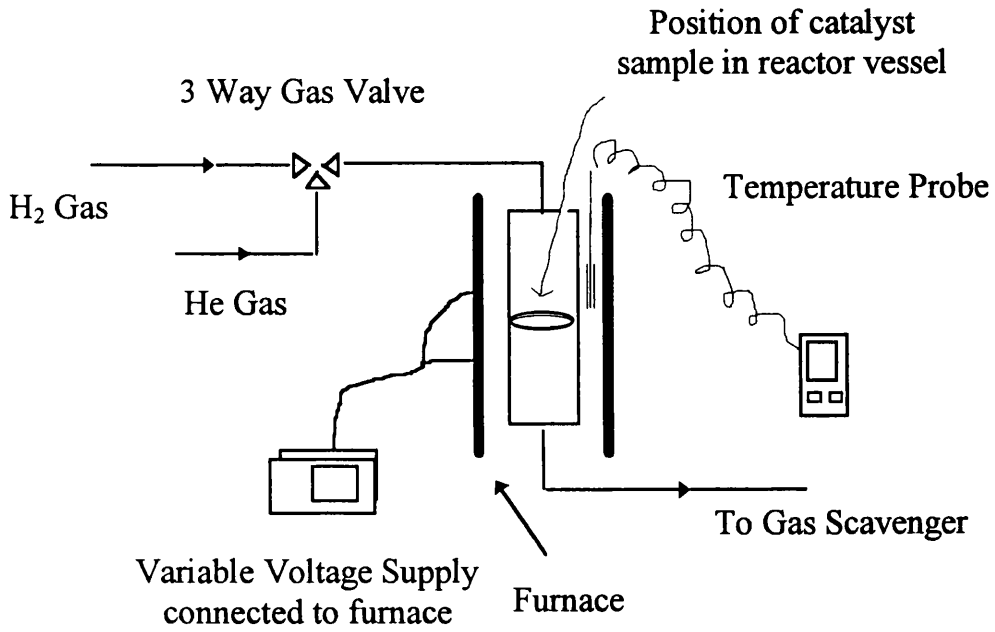

3.3.2 Preparation of [$PdCl_2(PMe_3)_2/SiO_2$] to give a 5 % Pd loading

Trans-[$PdCl_2(PMe_3)_2$] (0.31 g, 0.94 mmol) was dissolved in 30 ml of a 1:1 mixture of dichloromethane: ethanol. Pre-dried silica (1.69 g, 28.1 mmol) was then added and the silica was left in the mother liquor overnight. The solvent was then removed by rotary evaporation and vacuum drying and the dried catalyst precursor was then placed in an oven at a temperature of 100°C for a period of 1 hour. Total weight of [$PdCl_2(PMe_3)_2/SiO_2$] obtained = 1.89 g.

3.3.3 Preparation of [$PdBr_2(PMe_3)_2/SiO_2$] to give a 5 % Pd loading

Trans-[$PdBr_2(PMe_3)_2$] (0.39 g, 0.93 mmol) was dissolved in 30 ml of a 1:1 mixture of dichloromethane: ethanol. Pre-dried silica (1.60 g, 26.6 mmol) was added and the silica was left in the mother liquor overnight (18 hours). The solvent was then removed by rotary evaporation and vacuum drying and the dried catalyst precursor placed in an oven at a temperature of 100°C for a period of one hour. Total weight of [$PdBr_2(PMe_3)_2/SiO_2$] obtained = 1.78 g.

3.3.4 Preparation of [$PdI_2(PMe_3)_2/SiO_2$] to give a 5 % Pd loading

Trans-[$PdI_2(PMe_3)_2$] (0.24 g, 0.47 mmol) was dissolved in 20 ml of a 1:1 solution of dichloromethane: ethanol. Pre-dried silica, (0.77 g, 12.8 mmol) was then added and the silica was left in the mother liquor overnight (18 hours). The solvents were then removed from the slurry mixture by rotary evaporation and vacuum drying and the dried catalyst precursor was then placed in an oven at a temperature of 100°C for a period of one hour. Total weight of [$PdI_2(PMe_3)_2/SiO_2$] obtained = 0.92 g.

3.3.5 Preparation of $[Pd_2Cl_4(PMe_3)_2/SiO_2]$ to give a 5 % Pd loading

Trans-$[Pd_2Cl_4(PMe_3)_2]$ (0.36 g, 0.71 mmol) was dissolved in a 40 ml of a 1:1 ethanol: chloroform mixture. Pre-dried silica (2.64 g, 43.9 mmol) was added and the silica left in the mother liquor overnight (18 hours). The solvents were removed by rotary evaporation and vacuum drying and the dried catalyst precursor was heated in an oven at a temperature of 100°C for one hour. Total weight of $[Pd_2Cl_4(PMe_3)_2/SiO_2]$ obtained = 2.57 g.

3.3.6 Preparation of $[Pd_2Br_4(PMe_3)_2/SiO_2]$ to give a 5 % Pd loading

Trans-$[Pd_2Br_4(PMe_3)_2]$ (0.16 g, 0.23 mmol) was dissolved in 25 ml of a 1:4 solution of dichloromethane: ethanol. Pre-dried silica, (0.85 g, 14.1 mmol) was added and the silica left in the mother liquor overnight (18 hours). The solvents were then removed from the slurry mixture by rotary evaporation and vacuum drying and the dried catalyst precursor placed in an oven at a temperature of 100°C for a period of one hour. Total weight of $[Pd_2Br_4(PMe_3)_2/SiO_2]$ obtained = 0.95 g.

3.3.7 Preparation of $[Pd_2I_4(PMe_3)_2/SiO_2]$ to give a 5 % Pd loading

Trans-$[Pd_2I_4(PMe_3)_2]$ (0.307 g, 0.35 mmol) was dissolved in 30 ml of acetone. Pre-dried silica (1.19 g, 19.8 mmol) was added and the silica left in the mother liquor overnight (18 hours). The solvent was then removed from the slurry mixture by rotary evaporation and vacuum drying and the dried catalyst precursor was placed in an oven at a temperature of 100°C for a period of one hour. Total weight of $[Pd_2I_4(PMe_3)_2/SiO_2]$ obtained = 1.43 g.

3.3.8 Preparation of $[Pd_2Cl_4(PEt_3)_2/SiO_2]$ to give a 5 % Pd loading

Trans-$[Pd_2Cl_4(PEt_3)_2]$ (0.35 g, 0.59 mmol) was dissolved in 40 ml of a 1:1 solution of ethanol: dichloromethane. Pre-dried silica (2.15 g, 35.8 mmol) was added and the silica left in the mother liquor overnight (18 hours). The solvents were then removed from the slurry mixture by rotary evaporation and vacuum drying and the dried catalyst precursor was placed in an oven at a temperature of 100°C for a period of one hour. Total weight of $[Pd_2Cl_4(PEt_3)_2/SiO_2]$ obtained = 2.16 g.

3.3.9 Preparation of $[Pd_2Br_4(PEt_3)_2/SiO_2]$ to give a 5 % Pd loading

Trans-$[Pd_2Br_4(PEt_3)_2]$ (0.24 g, 0.31 mmol) was dissolved in 40 ml of a 1:1 ethanol: dichloromethane solution. Pre-dried silica (1.05 g, 17.5 mmol) was added and the silica left in the mother liquor overnight (18 hours). The solvents were then removed from the slurry mixture by rotary evaporation and vacuum drying and the dried catalyst precursor was placed in an oven at a temperature of 100°C for a period of one hour. Total weight of $[Pd_2Br_4(PEt_3)_2/SiO_2]$ obtained = 1.22 g.

3.3.10 Preparation of $[Pd_2Br_4(PBu_3)_2/SiO_2]$ to give a 5 % Pd loading

Trans-$[Pd_2Br_4(PBu_3)_2]$ (0.22 g, 0.23 mmol) was dissolved in 50 ml of a 1:1 ethanol: dichloromethane solution. Pre-dried silica (0.78 g, 13.1 mmol) was added and the silica left in the mother liquor overnight (18 hours). The solvents were then removed from the slurry mixture by rotary evaporation and vacuum drying and the dried catalyst precursor was placed in an oven at a temperature of 100°C for a period of one hour. Total weight of $[Pd_2Br_4(PBu_3)_2/SiO_2]$ obtained = 0.82 g.

3.3.11 Preparation of $[Pd_2Br_4(PPr^i_3)_2/SiO_2]$ to give a 5 % Pd loading

Trans-$[Pd_2Br_4(PPr^i_3)_2]$ (0.20 g, 0.23 mmol) was dissolved in 40 ml of a 1:1 ethanol: dichloromethane solution. Pre-dried silica, (0.80 g, 13.3 mmol) was added and the silica left in the mother liquor overnight (18 hours). The solvents were removed from the slurry mixture by rotary evaporation and vacuum drying and the dried catalyst precursor was placed in an oven at a temperature of 100°C for a period of one hour. Total weight of $[Pd_2Br_4(PPr^i_3)_2/SiO_2]$ obtained = 0.91 g.

3.3.12 Preparation of $[Pd_2I_4(PEt_3)_2/SiO_2]$ to give a 5 % Pd loading

Trans-$[Pd_2I_4(PEt_3)_2]$, (0.223 g, 0.23 mmol) was dissolved in 40 ml of chloroform. Pre-dried silica, (0.78 g, 13.0 mmol) was added and the silica left in the mother liquor overnight (18 hours). The solvent was then removed from the slurry mixture by rotary evaporation and vacuum drying and the dried catalyst precursor was placed in an oven at a temperature of 100°C for a period of one hour. Total weight of $[Pd_2I_4(PEt_3)_2/SiO_2]$ obtained = 0.87 g.

In addition to the precursors prepared as described in sections 3.3.1 to 3.3.12, several other catalyst precursors were prepared and tested.

3.3.13 Preparation of a mechanical mixture of $[PdCl_2/SiO_2]$ to give a 5 % Pd loading

$PdCl_2$ (0.17 g, 0.96 mmol) was mechanically mixed with pre-dried silica (1.83 g, 30.5 mmol). This was achieved by grinding the two components together using a mortar and pestle for a period of approximately 15 minutes. Total weight of $[PdCl_2/SiO_2]$ obtained = 1.94 g.

3.3.14 Preparation of a mechanical mixture of [$PdBr_2/SiO_2$] to give a 5 % Pd loading

$PdBr_2$ (0.25 g, 0.9 mmol) was mechanically mixed with pre-dried silica (1.75 g, 29.1 mmol). This was achieved by grinding the two components together using a mortar and pestle for a period of approximately 15 minutes. Total weight of [$PdBr_2/SiO_2$] obtained = 1.92 g.

3.3.15 Preparation of a 5 % [Pd/SiO_2] catalyst modified by [Bu_4N]Br

0.5 g of a 5 % [Pd/SiO_2] catalyst was prepared using the procedures detailed in section 3.3.1.1 to 3.3.1.3. [Bu_4N]Br (0.151 g, 0.47 mmol) was dissolved in 20 ml of ethanol and the solution injected into the reaction vessel containing the reduced catalyst. An atmosphere of helium was maintained during the modification procedure. The palladium catalyst and modifier solution was left overnight, after which the solution was removed using a water pump. The modified catalyst was then washed with a further 20 ml of ethanol prior to use.

3.3.16 Preparation of [PMe_3H]Br/SiO_2

[PMe_3H]Br (0.225 g, 1.4 mmol) was dissolved in 10 ml of distilled H_2O. Pre-dried silica (2.78 g, 35.9 mmol) was added and the silica left in the solution overnight (18 hours). The water was removed from the slurry mixture by rotary evaporation and vacuum drying and the supported trimethylphosphonium bromide was then placed in an oven at a temperature of 100°C for a period of one hour. Total weight of [PMe_3H]Br/SiO_2 obtained = 2.94 g.

3.4 CHARACTERISATION OF CATALYSTS

3.4.1 Thermogravimetric Analysis (TGA)

Analyses were carried out using a Dupont 951 Thermogravimetric Analyser connected to a modular 990 Thermal Analyser.

In the technique of TGA, the weight and rate of weight change of a material is continuously measured as a function of temperature. A sample weight of approximately 10 mg was used. In general the following experimental settings were observed - 50 % suppression, programmed heating rate of 5°C min^{-1}, atmosphere of 6 % H_2/: 94 % N_2 and a gas flow rate of 50 ml min^{-1}. The temperature was increased from 25°C to 400°C. The catalysts and precursors examined are detailed in section 4.2

3.4.2 Transmission Electron Microscopy (TEM)

Selected catalysts and precursors were examined using a Jeol 1200 EX transmission electron microscope.

Samples to be examined were mounted onto carbon coated copper grids. A volume of water was added to a small sample of catalyst and dispersion was aided using a sonic bath. The dispersed sample was then added dropwise to a copper grid and allowed to dry, prior to insertion into and analysis under the microscope. The catalysts examined are detailed in section 4.3.

3.4.3 Solid State ^{31}P Magic Angle Spinning NMR (MAS-NMR)

Solid state NMR spectra were recorded using the EPSRC Solid - State NMR service at UMIST, Manchester. Cross polarisation (CPMAS) and single pulse (SPMAS) experiments were performed. Solid state ^{31}P spectra were recorded with respect to an external standard comprising of 80 % H_3PO_4. The catalysts and precursors examined are detailed in section 4.4.

3.4.4 Microanalyses

Carbon, hydrogen, halogen and phosphorus microanalyses were carried out using the University of Glasgow microanalysis service. Standard combustion and volumetric titration methods were employed. The catalysts and precursors examined are detailed in section 4.5.

3.4.5 Neutron Activation Analysis (NAA)

Neutron activation analysis was carried out on a selection of catalysts and precursors. Samples were irradiated for exactly 5.00 minutes at a flux of 3 x 10^{12} $ncm^{-2}s^{-1}$ and counting of the samples was carried out approximately 24 hours later. The catalysts and precursors examined are detailed in section 4.6.

3.4.6 X-Ray Photoelectron Spectroscopy (XPS)

X-ray photoelectron spectra were recorded for a selection of catalysts and precursors using a SCIENTA ESCA X-ray photoelectron spectrometer. AlKα ($h\upsilon$ = 1486.6 eV) incident monochromatised radiation was used. All spectra were recorded at room temperature and a low energy electron flood gun used to correct for differential charging. Results

were referenced to C1s with a binding energy of 285.0 ± 0.2 eV. The catalysts and precursors examined are detailed in section 4.7.

3.5 The Hydrogenation Reaction

The reaction being investigated primarily was the liquid phase hydrogenation of cinnamaldehyde, although experiments involving the use of hydrocinnamaldehyde, cinnamyl alcohol as well as 2-cyclohexene-1-one were also investigated. The solvents used for these reactions were decahydronapthalene (decalin) and heptane. The results of all the hydrogenation reactions are presented in section 4.1.

3.5.1 Materials / Reagents Used

Trans-cinnamaldehyde (99 %), phenylpropanol (98 %), trans-cinnamyl alcohol (98 %), (hydrocinnamaldehyde) (95 %), decahydronapthalene anhydrous (99 %+ mix of cis and trans isomers) and heptane (99 %+) (HPLC grade) were all obtained from the Aldrich Chemical Company. Cyclohexanol (99 %), cyclohexanone (99 %+), 2-cyclohexene-1-ol (95 %) and 2-cyclohexene-1-one (95 %+) were also obtained from the Aldrich Chemical Company.

3.5.2 Apparatus/Conditions

In the hydrogenation reactions involving cinnamaldehyde, hydrocinnamaldehyde, cinnamyl alcohol and 2-cyclohexene-1-one the following glass reactor vessel was used -

Fig 3.3.

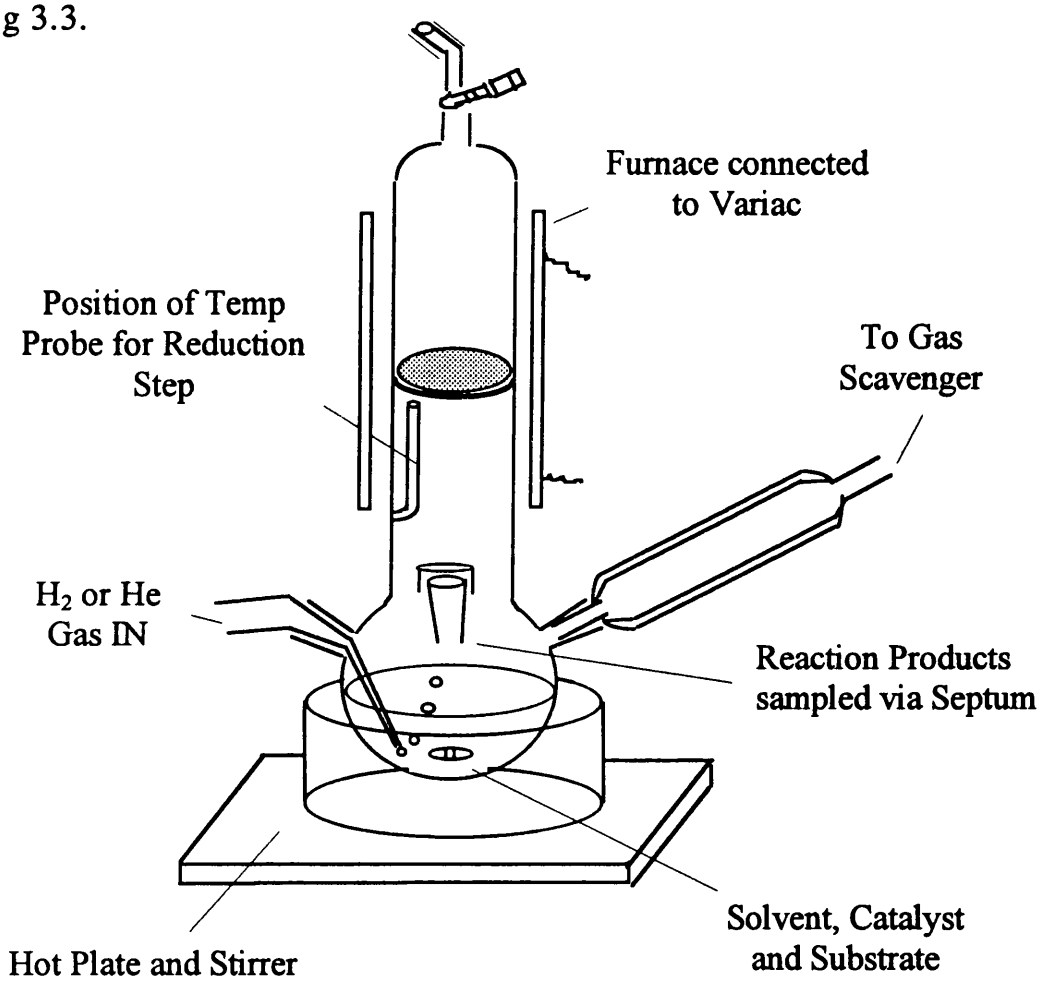

0.5 g of catalyst precursor were added to the round bottomed section of the reactor vessel along with a magnetic stirrer bar. The system was then sealed to the atmosphere and a fast flow of helium (>100 ml min^{-1} for 15 minutes) was used to purge the air from the vessel. 25 ml of the appropriate degassed solvent was then added through the sampling septum.

The system was left for a further 15 minutes to ensure complete removal of any air still present. The desired temperature of the catalyst/solvent suspension was then achieved using an oil bath. At this point 0.25 ml of sample was then added by injection and the gas flow changed from > 100 ml He min^{-1} to 60 ml H_2 min^{-1}. A stopwatch was activated to record the reaction time.

3.5.3 Gas Chromatographic Analysis (GC)

Samples to be analysed were first filtered and then diluted to the correct concentration. A 1$\mu\ell$ aliquot was then injected onto the column of the G.C through the injection port. By comparing the signal obtained from a sample with those from standards with known retention times, the nature and amount of each individual component was obtained.

3.5.4 Instrument Settings

All samples were analysed using a Phillips PU4500 Gas Chromatograph with Flame Ionisation Detector (FID), attached to an electronic integrator.

Samples were injected onto a 2 meter glass column (internal diameter 4mm) using a 5$\mu\ell$ syringe. Samples were injected onto the column through the injection port (held at a temperature of 220°C). The column itself was packed with carbowax 20M on chromosorb W.AW 80-100 and a 40 ml min^{-1} flow rate of N_2 as the carrier gas was used.

For the cinnamaldehyde system, decalin or heptane was used as the solvent. For each solvent the G.C settings were the same.

1µl of filtered reaction mixture was injected onto the column (injection port temperature = 220°C). Column temperature was held at 130°C isothermally for 10 minutes and was then increased to 160°C at a rate of 1°C/min^{-1}. Upon reaching a temperature of 160°C the oven was then programmed to slowly cool back down to the starting temperature in preparation for the next analysis. The total run time was 45 minutes per sample. The detector temperature was set at 260°C and a small hydrogen/air flame was used.

Elution of reaction components occurred in the following order: approximate retention times of each component are shown in the brackets.

Decalin < Hydrocinnamaldehyde (5-6 min) < Cinnamaldehyde (15-16 min) < Phenylpropanol (16-17 min) <Cinnamyl alcohol (30-32 min)

The G.C trace below illustrates the analysis of a standard sample containing all the components of the cinnamaldehyde system -

Fig 3.4

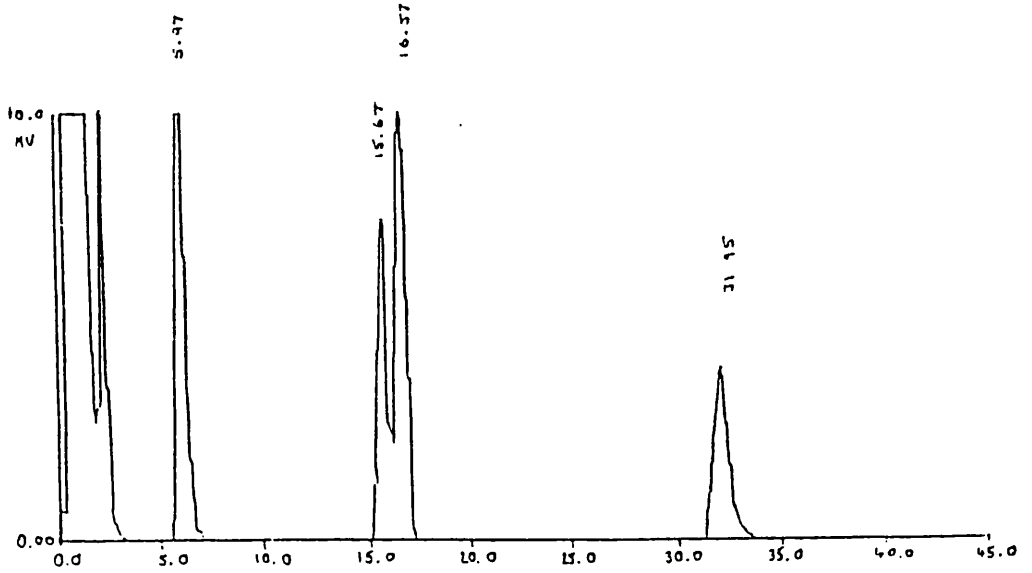

For the 2-cyclohexene-1-one system only heptane was used as the solvent. The injection volume, injector port temperature as well as the detector temperature were the same as for the cinnamaldehyde system. The column temperature was held isothermally at 80°C for 10 minutes during which time all the individual components in the system were separated.

Elution of reaction components occurred in the following order: approximate retention times of each component are shown in the brackets.

Heptane < Cyclohexanone (3.5-4.0 mins) < Cyclohexanol (6.2-6.8 mins) < 2-Cyclohexene-1-one (7.5-8.0 mins) < 2-Cyclohexene-1-ol (9.0 - 10.0 mins)

The G.C trace below illustrates the analysis of a standard sample containing all the components of the 2-cyclohexene-1-one system -

Fig 3.5

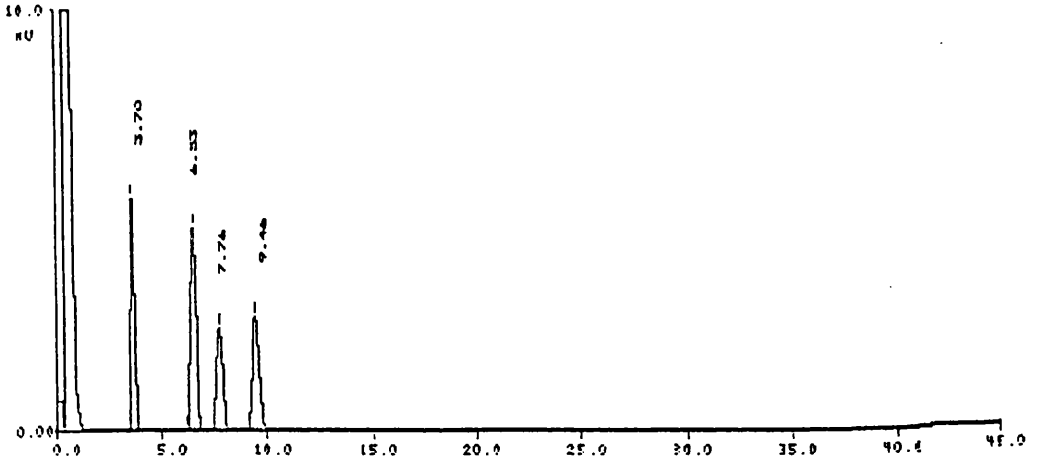

3.5.5 Standardisation of results

In order to accurately correlate the area unit values for individual components directly to the number of moles present, a series of standards of known concentration were made up. Standard graphs of area units against moles of component were plotted and from these the mole fractions of each component present in a reaction mixture were calculated.

For cinnamaldehyde, hydrocinnamaldehyde, phenylpropanol and cinnamyl alcohol, a series of standards of various concentrations were made up by diluting samples of the pure component with ethyl acetate. By varying the amount of component added and the volume of ethyl acetate for each 1 μl injection, a different (but known) number of moles of component was delivered onto the G.C column. Each concentration corresponded to a particular area unit value. Linear calibration graphs of area units versus moles of component were then drawn. These are illustrated in graphs 3.1 - 3.4.

The same procedure was adopted for the 2-cyclohexene-1-one system as illustrated in graphs 3.5 - 3.8.

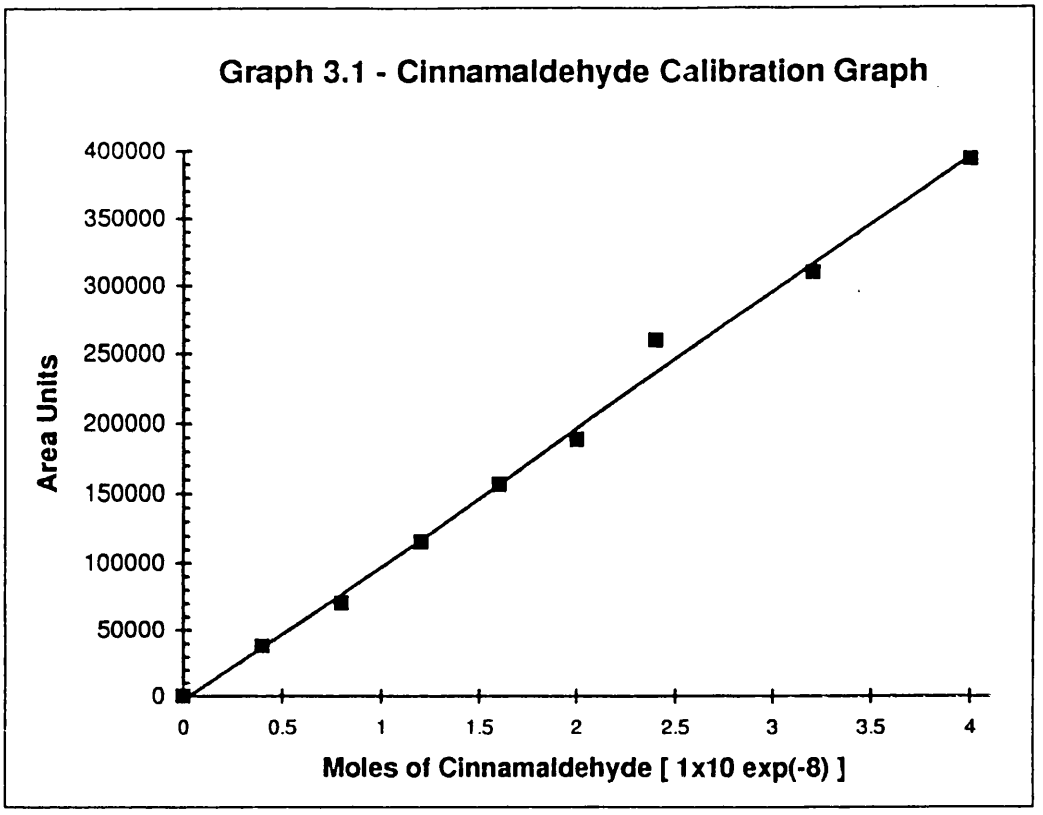
Graph 3.1 - Cinnamaldehyde Calibration Graph
Area Units
400000
350000
300000
250000
200000
150000
100000
50000
0
0
0.5
1
1.5
2
2.5
3
3.5
4
Moles of Cinnamaldehyde [1x10 exp(-8)]

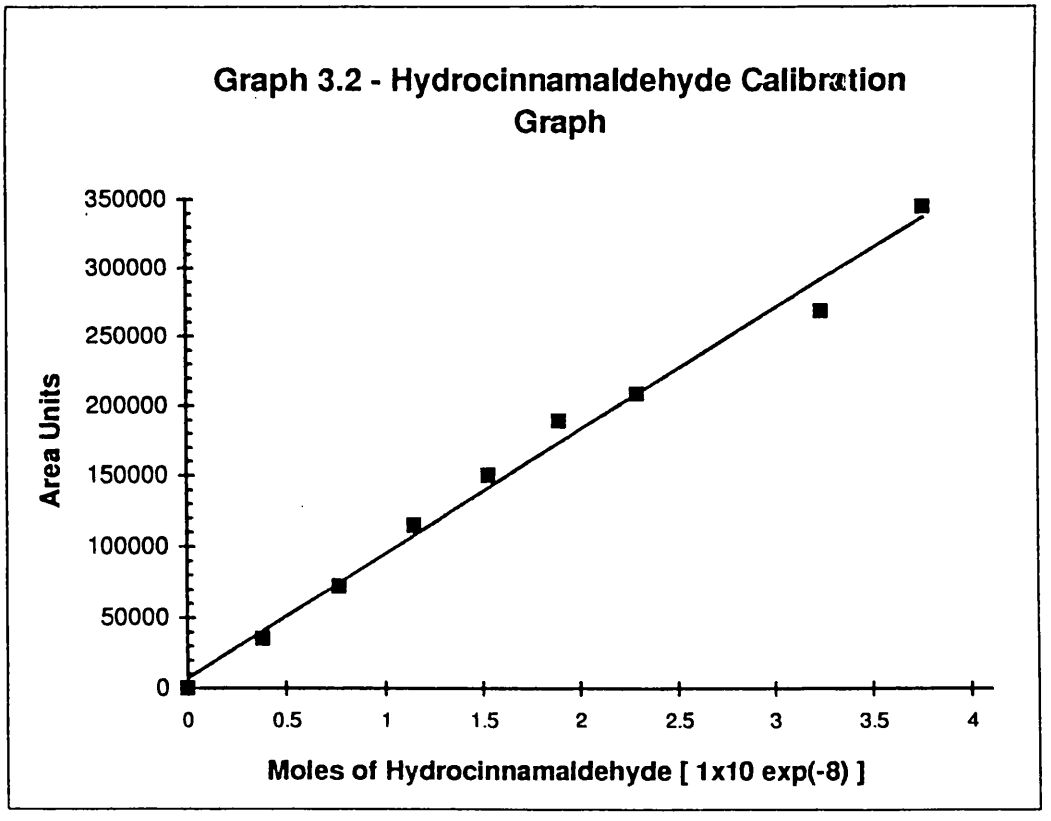
Graph 3.2 - Hydrocinnamaldehyde Calibration Graph
Area Units
350000
300000
250000
200000
150000
100000
50000
0
0
0.5
1
1.5
2
2.5
3
3.5
4
Moles of Hydrocinnamaldehyde [1x10 exp(-8)]

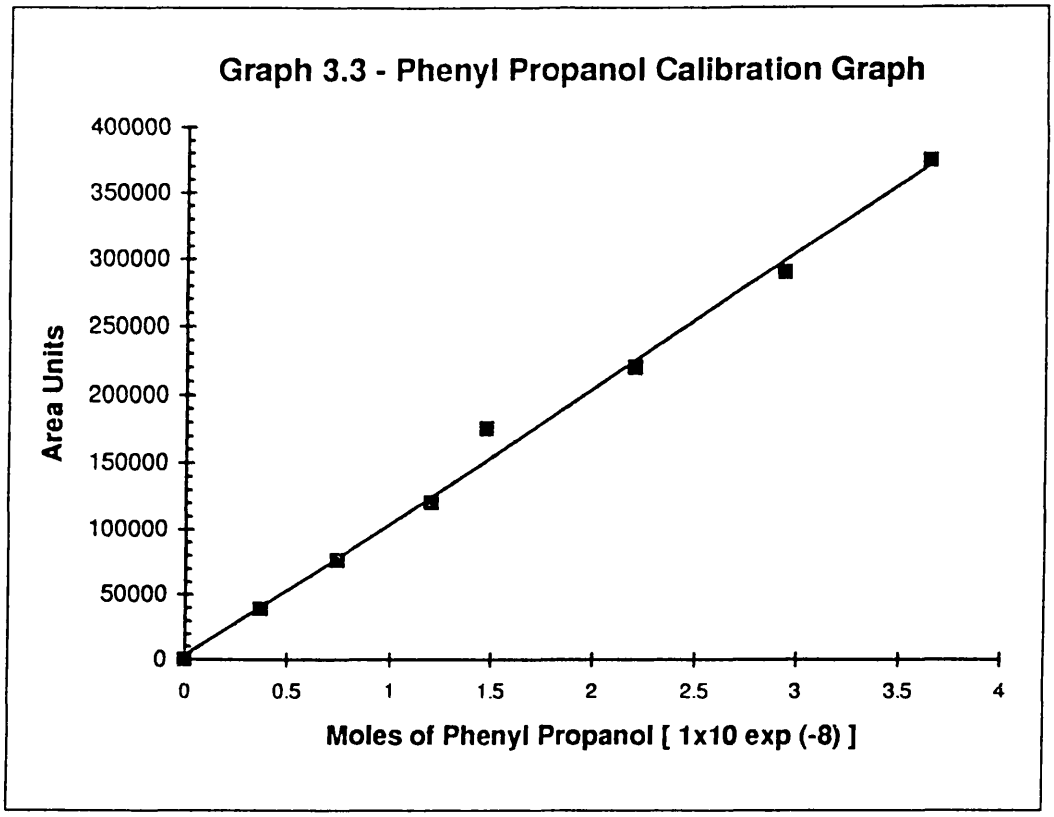
Graph 3.3 - Phenyl Propanol Calibration Graph
Area Units
400000
350000
300000
250000
200000
150000
100000
50000
0
0
0.5
1
1.5
2
2.5
3
3.5
4
Moles of Phenyl Propanol [1x10 exp (-8)]

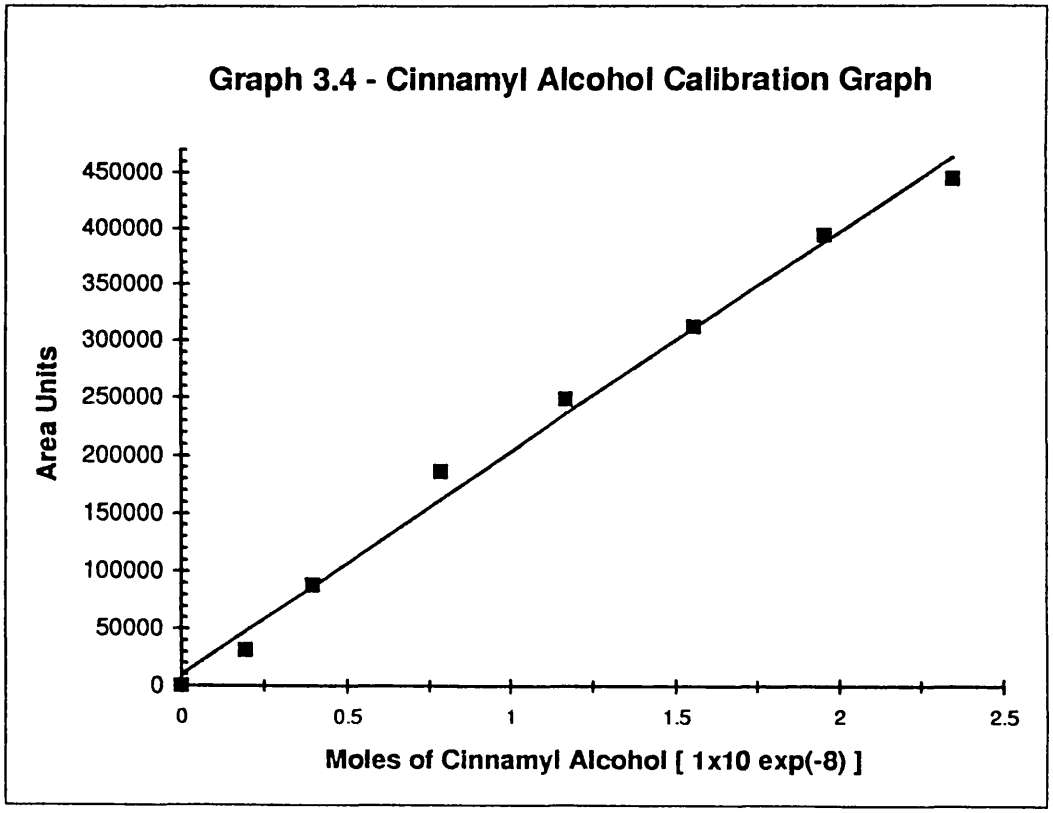
Graph 3.4 - Cinnamyl Alcohol Calibration Graph
Area Units
450000
400000
350000
300000
250000
200000
150000
100000
50000
0
0
0.5
1
1.5
2
2.5
Moles of Cinnamyl Alcohol [1x10 exp(-8)]

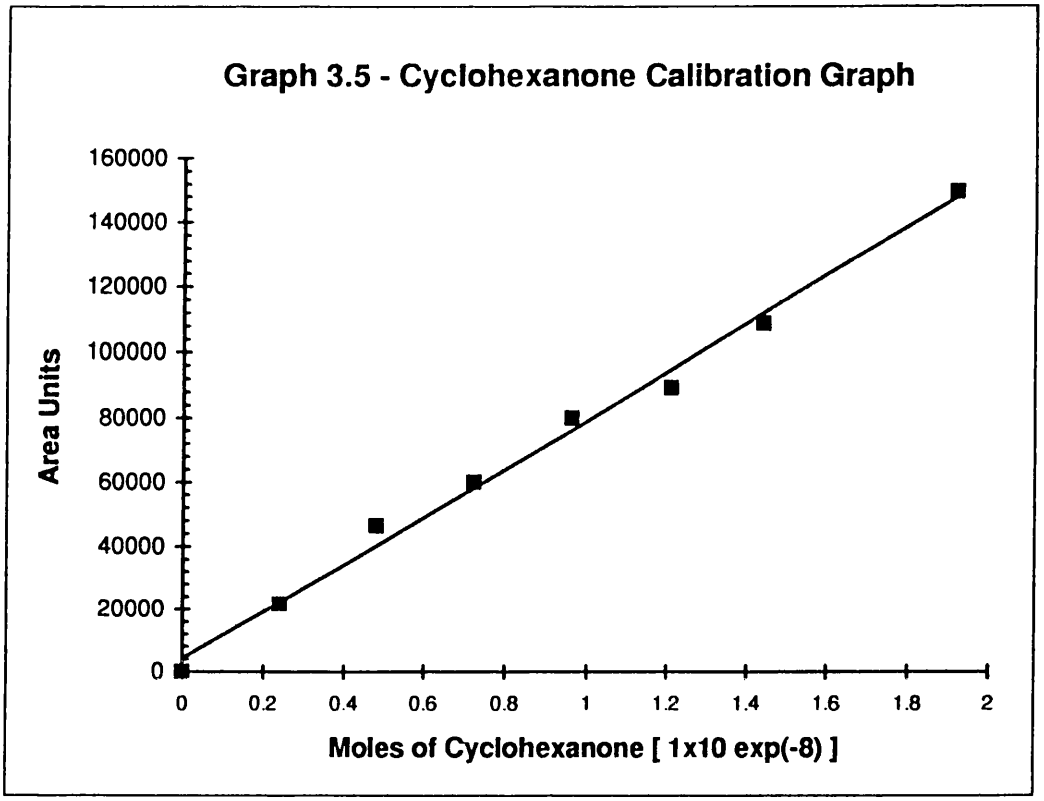
Graph 3.5 - Cyclohexanone Calibration Graph
160000
140000
120000
100000
80000
60000
40000
20000
0
Area Units
0
0.2
0.4
0.6
0.8
1
1.2
1.4
1.6
1.8
2
Moles of Cyclohexanone [1x10 exp(-8)]

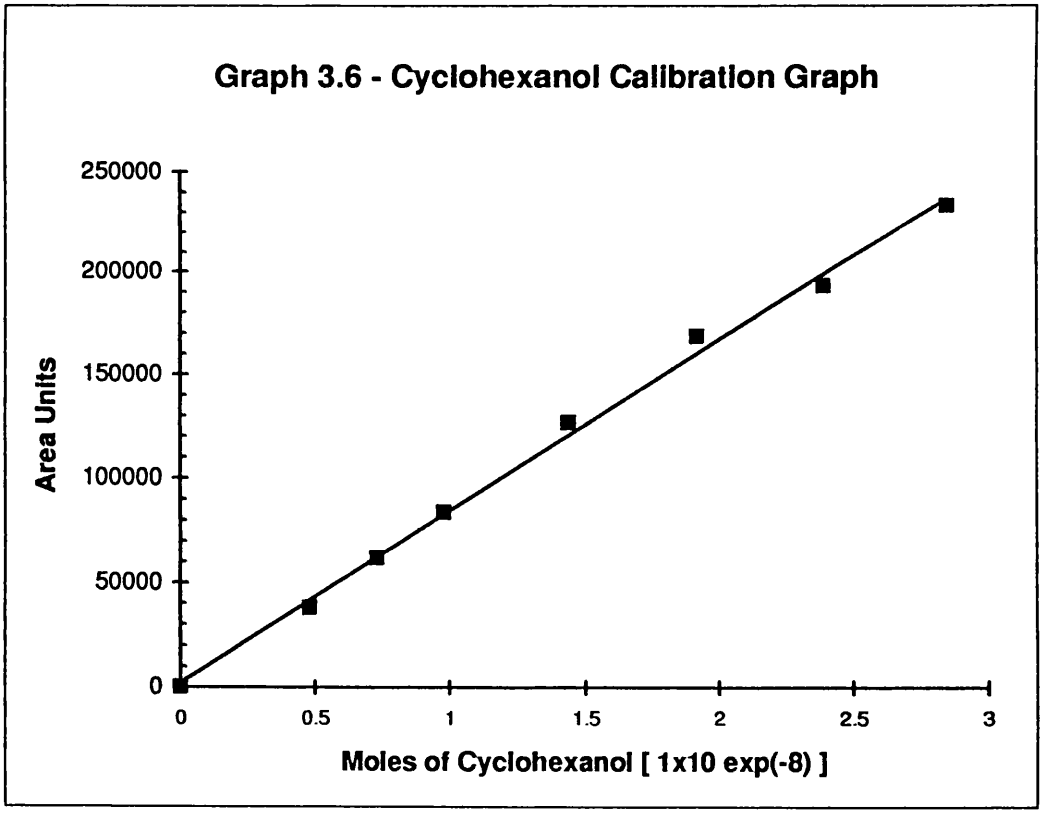
Graph 3.6 - Cyclohexanol Calibration Graph
250000
200000
150000
100000
50000
0
Area Units
0
0.5
1
1.5
2
2.5
3
Moles of Cyclohexanol [1x10 exp(-8)]

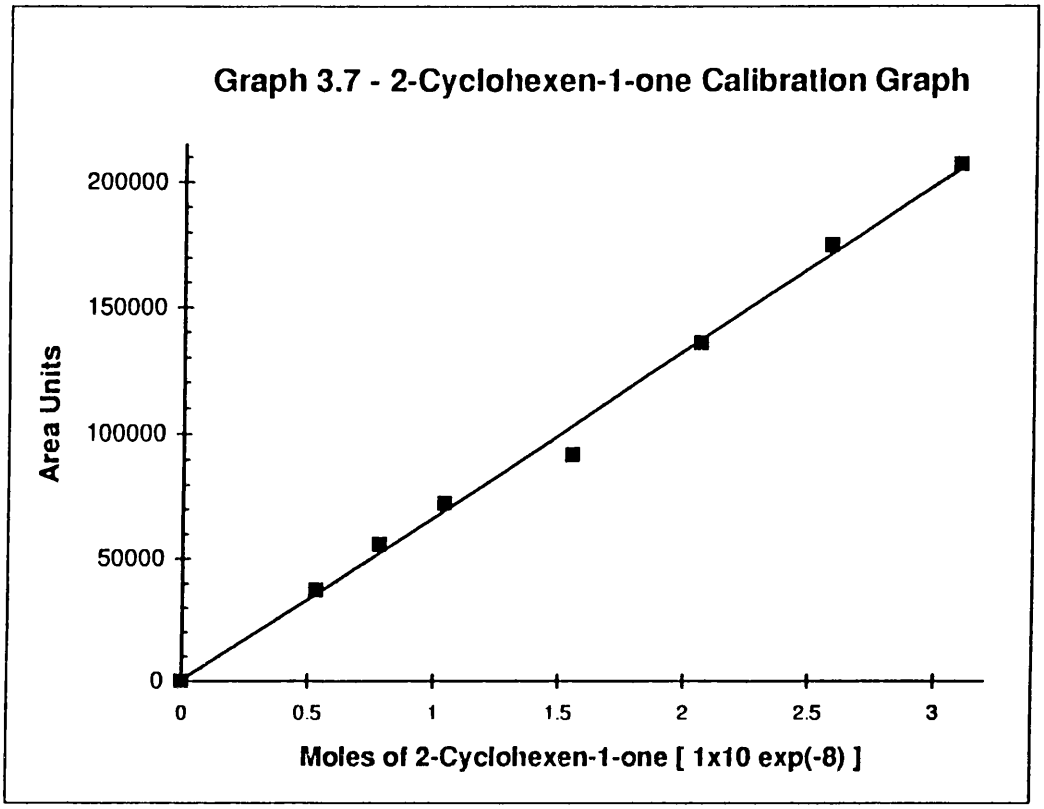
Graph 3.7 - 2-Cyclohexen-1-one Calibration Graph
Area Units
200000
150000
100000
50000
0
0
0.5
1
1.5
2
2.5
3
Moles of 2-Cyclohexen-1-one [1x10 exp(-8)]

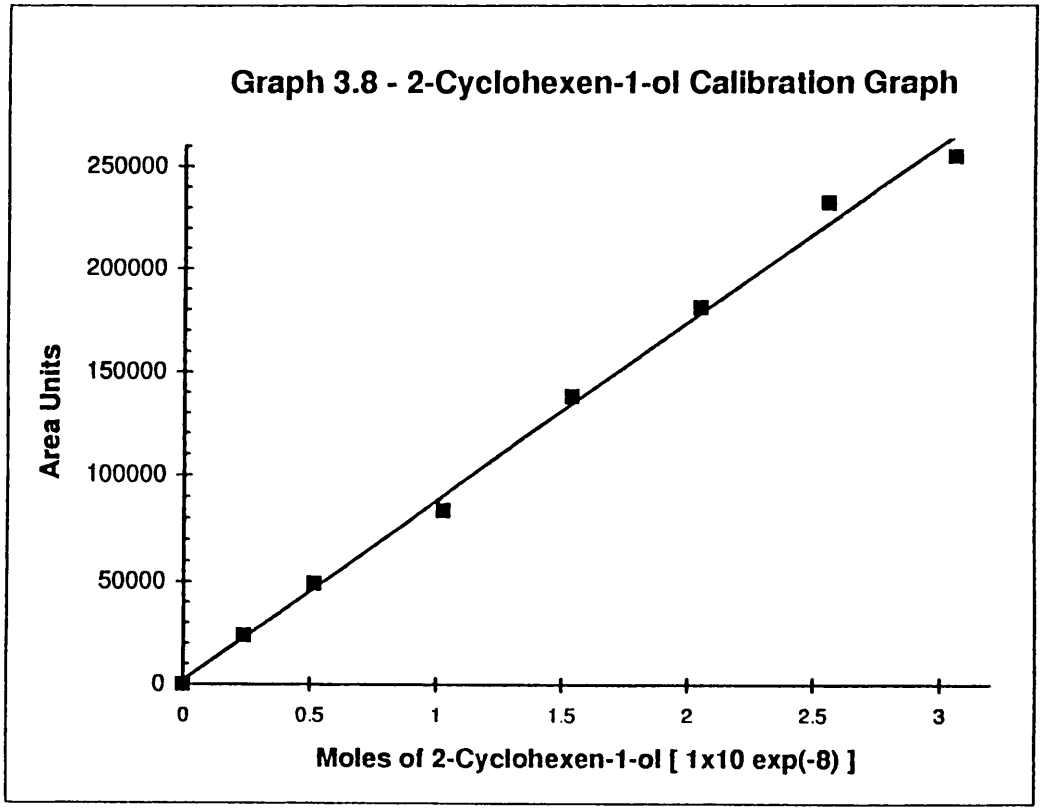
Graph 3.8 - 2-Cyclohexen-1-ol Calibration Graph
Area Units
250000
200000
150000
100000
50000
0
0
0.5
1
1.5
2
2.5
3
Moles of 2-Cyclohexen-1-ol [1x10 exp(-8)]

Chapter 4

RESULTS

RESULTS

4.1 The Hydrogenation Reaction

The hydrogenation of cinnamaldehyde, cinnamyl alcohol, hydrocinnamaldehyde or 2-cyclohexene-1-one were carried out according to the procedure detailed in section 3.5.2. 0.5 g of catalyst and 25 ml of either decalin or heptane along with 0.25 ml of substrate were reacted with hydrogen gas at temperatures of $\leq$ 135°C. Control experiments were carried out using the same experimental conditions both in the absence of catalyst and SiO_2, and also using $[PMe_3H]Br/SiO_2$. In each case, no hydrogenation products were observed after 72 hours reaction, which indicated that the reaction did not proceed uncatalysed.

Preliminary studies were carried out using a silica supported palladium catalyst prepared from $Pd(NO_3)_2.xH_2O$ as described in section 3.3.1.1. The precursor was calcined at 250°C for 3 hours in flowing air and reduced in hydrogen at 200°C for 18 hours, prior to use. After reduction, it was used in the liquid phase hydrogenation of cinnamaldehyde in decalin. Product ratios were examined at various time intervals by gas chromatography. The products obtained at reaction temperatures of 100°C and 135°C are shown in tables 4.1 and 4.2. Using this $[Pd/SiO_2]$ catalyst, cinnamaldehyde was sequentially hydrogenated, first to hydrocinnamaldehyde and then to phenylpropanol. These results were used as a standard against which the catalysts prepared from the supported palladium phosphine precursors were compared.

In addition to the supported palladium phosphine precursors, catalyst precursors prepared as a mechanical mix of $[PdCl_2/SiO_2]$ (table 4.3) and of

[$PdBr_2/SiO_2$] were examined (table 4.4). A catalyst prepared by the modification of [Pd/SiO_2] with a solution of tetra-n-butylammonium bromide, [Bu_4N]Br, was also examined (table 4.5).

In many of the reactions studied, the rate of conversion of cinnamaldehyde to other products at 135°C was so great that by the time the first sample had been extracted from the reaction vessel the reaction had essentially reached completion. For several of these reactions, therefore, the temperature was lowered to 95°C in order to follow the activities and selectivities during the important initial stages of the reaction. Tables 4.1 to 4.35 present the data for the products of all the reactions studied for the hydrogenation of cinnamaldehyde, hydrocinnamaldehyde, cinnamyl alcohol and 2-cyclohexene-1-one. Graphs numbered as 4.1 - 4.9 were also plotted for a selection of these reactions, and can be found on pages 132 - 140.

Rate constants for selected catalysts were calculated from the linear regions of graphs of % conversion plotted against time. % Conversion values = 100 x (1 - mole fraction Cinnamaldehyde). The gradient of this linear region was multiplied by the initial concentration of cinnamaldehyde to give a value for the rate constant k. Graph 4.10 (p 141) illustrates a typical % conversion against time plot for a chosen catalyst, and a list of the rate constants calculated for selected catalysts is presented in table 4.36a. In each case the conversion of cinnamaldehyde was linear with respect to time, except at high conversions (70 %+), when most of the reactants had been used up. This indicated a pseudo-zero-order reaction at low and intermediate conversions. Mass balance calculations were also carried out on a variety of catalyst systems. Differences between the

number of moles of cinnamaldehyde added and the number of moles of product formed were calculated and presented (table 3.36b).

In all of the following tables, the abbreviation CIN, stands for cinnamaldehyde, HCA stands for hydrocinnamaldehyde, PP, for phenylpropanol and CA, for cinnamyl alcohol.

Table 4.1 - Hydrogenation of 1.986×10^{-3} moles of Cinnamaldehyde, (0.5 g [Pd/SiO_2], 25 ml decalin, 100°C).

Time (hrs)	Mole Fraction			
	CIN	HCA	PP	CA
0	1.00	0.00	0.00	0.00
0.33	0.40	0.60	0.00	0.00
0.66	0.23	0.77	0.00	0.00
1.00	0.14	0.86	0.00	0.00
1.33	0.055	0.945	0.00	0.00
1.66	0.00	0.81	0.19	0.00
2.00	0.00	0.83	0.16	0.00
3.00	0.00	0.73	0.27	0.00
4.00	0.00	0.715	0.28	0.00
6.00	0.00	0.67	0.33	0.00
48.0	0.00	0.085	0.915	0.00
118.0	0.00	0.00	1.00	0.00

Table 4.2 - Hydrogenation of 1.986 x 10^{-3} moles of Cinnamaldehyde, (0.5 g [Pd/SiO_2], 25 ml decalin, 135°C).

Time (hrs)	Mole Fraction			
	CIN	HCA	PP	CA
0	1.00	0.00	0.00	0.00
0.25	0.19	0.81	0.00	0.00
0.50	0.00	0.99	0.01	0.00
0.75	0.00	0.96	0.02	0.00
1.00	0.00	0.90	0.02	0.00
2.50	0.00	0.78	0.22	0.00
3.00	0.00	0.71	0.29	0.00
4.00	0.00	0.62	0.38	0.00
24.0	0.00	0.16	0.84	0.00
48.0	0.00	0.00	1.00	0.00

The data presented in tables 4.1 and 4.2 (graphs 4.1 and 4.2) show that CIN was converted first to HCA and then to PP. 100 % PP formation required 118 hours for a reaction temperature of 100°C, although only 48 hours were required at a temperature of 135°C.

Table 4.3 - Hydrogenation of 1.986 x 10^{-3} moles of Cinnamaldehyde, (mechanical mix of 0.5g [$PdCl_2/SiO_2$], 25 ml decalin, 135°C).

Time (hrs)	Mole Fraction			
	CIN	HCA	PP	CA
0	1.00	0.00	0.00	0.00
0.5	0.832	0.148	0.02	0.00
1.0	0.551	0.326	0.123	0.00
1.5	0.341	0.425	0.234	0.00
2.0	0.187	0.363	0.45	0.00
3.33	0.066	0.307	0.627	0.00
4.0	0.00	0.205	0.795	0.00
48.0	0.00	0.00	1.00	0.00

Table 4.4 - Hydrogenation of 1.986 x 10^{-3} moles of Cinnamaldehyde, (mechanical mix of 0.5 g [$PdBr_2/SiO_2$], 25 ml decalin, 135°C).

Time (hrs)	Mole Fraction			
	CIN	HCA	PP	CA
0	1.00	0.00	0.00	0.00
0.75	0.00	0.705	0.295	0.00
2.0	0.00	0.692	0.308	0.00
24.0	0.00	0.676	0.324	0.00

Table 4.5 - Hydrogenation of 1.986 x 10^{-3} moles of Cinnamaldehyde, (0.5 g [Pd/SiO_2], modified with 4.7 x 10^{-4} moles of [Bu_4N]Br, 25 ml decalin, 135°C).

Time (hrs)	Mole Fraction			
	CIN	HCA	PP	CA
0	1.00	0.00	0.00	0.00
0.5	0.00	0.91	0.09	0.00
1.0	0.00	0.892	0.108	0.00
1.5	0.00	0.905	0.095	0.00
2.5	0.00	0.915	0.085	0.00
4.0	0.00	0.911	0.089	0.00
48	0.00	0.922	0.078	0.00

The data presented in table 4.3 (graph 4.3) refers to a catalyst prepared from a mechanical mix of [$PdCl_2/SiO_2$]. 100 % PP was produced after 48 hours reaction. PP production began at about 17 % conversion, however, compared with at almost 100 % conversion for [Pd/SiO_2].

[$PdBr_2/SiO_2$] (table 4.4) rapidly hydrogenated CIN to both HCA and PP. 70.5 % HCA and 29.5 % PP were produced after only 45 minutes. No further reaction occurred after this time.

Data regarding the performance of a [Pd/SiO_2] catalyst modified using [Bu_4N]Br is presented in table 4.5, (graph 4.4). In this case, PP production did not begin until a conversion value close to 100 % had been achieved. In this regard it behaved like the unmodified [Pd/SiO_2] catalyst, but unlike

[Pd/SiO_2], this catalyst was essentially deactivated after 1 hour. 10.8 % PP had been produced at this point.

Table 4.6 - Hydrogenation of 1.986 x 10^{-3} moles of Cinnamaldehyde (0.5 g [$PdCl_2(PMe_3)_2/SiO_2$], 25 ml decalin, 135°C).

Time (hrs)	Mole Fraction			
	CIN	HCA	PP	CA
0	1.00	0.00	0.00	0.00
0.5	0.865	0.135	0.00	0.00
1.0	0.37	0.63	0.00	0.00
1.5	0.275	0.725	0.00	0.00
2.0	0.00	1.00	0.00	0.00
3.0	0.00	1.00	0.00	0.00
4.0	0.00	1.00	0.00	0.00
24.0	0.00	1.00	0.00	0.00
48.0	0.00	1.00	0.00	0.00

Table 4.7 - Hydrogenation of 1.986 x 10^{-3} moles of Cinnamaldehyde, (0.5 g [$PdBr_2(PMe_3)_2/SiO_2$], 25 ml decalin, 135°C).

Time (hrs)	Mole Fraction			
	CIN	HCA	PP	CA
0	1.00	0.00	0.00	0.00
0.5	1.00	0.00	0.00	0.00
1.0	1.00	0.00	0.00	0.00
1.5	0.988	0.012	0.00	0.00
2.0	0.98	0.02	0.00	0.00
3.0	0.956	0.044	0.00	0.00
48.0	0.944	0.056	0.00	0.00

Table 4.8 - Hydrogenation of 1.986 x 10^{-3} moles of Cinnamaldehyde, (0.5 g [$PdI_2(PMe_3)_2/SiO_2$], 25 ml decalin, 135°C).

Time (hrs)	Mole Fraction			
	CIN	HCA	PP	CA
0	1.00	0.00	0.00	0.00
0.5	1.00	0.00	0.00	0.00
1.0	1.00	0.00	0.00	0.00
2.0	1.00	0.00	0.00	0.00
4.0	1.00	0.00	0.00	0.00
5.0	0.989	0.011	0.00	0.00
48.0	0.951	0.049	0.00	0.00

The hydrogenation of cinnamaldehyde in decalin at 135°C over the catalysts prepared from mononuclear palladium phosphine precursors, $[PdX_2(PMe_3)_2/SiO_2]$ (X=Cl, Br or I), was investigated, and the results shown in tables 4.6, 4.7 and 4.8. When X=Cl, (table 4.6) the catalyst produced was shown to be 100 % selective towards HCA. The reaction was rapid and after only 2 hours all the CIN had been converted to HCA. No further hydrogenation of HCA to PP was observed. This result was not reproducible, however, and another reaction with the same catalyst also produced phenylpropanol. When X=Br or I, selectivity was towards HCA also, but over the course of the reaction, conversion levels were low; 5.6 % for X=Br, and 4.9 % for X=I (after 48 hours). These results were reproducible.

Table 4.9 - Hydrogenation of 1.986 x 10^{-3} moles of Cinnamaldehyde, (0.5 g $[Pd_2Cl_4(PMe_3)_2/SiO_2]$, 25 ml solvent, 70°C).

Time (hrs)	Mole Fraction			
	CIN	HCA	PP	CA
0	1.00	0.00	0.00	0.00
0.5	0.97	0.03	0.00	0.00
1.0	0.959	0.041	0.00	0.00
1.5	0.955	0.045	0.00	0.00
2.0	0.927	0.073	0.00	0.00
2.5	0.89	0.11	0.00	0.00
48.0	0.17	0.68	0.15	0.00

Table 4.10 - Hydrogenation of 1.986 x 10^{-3} moles of Cinnamaldehyde, (0.5 g [$Pd_2Cl_4(PMe_3)_2/SiO_2$], 25 ml decalin, 95°C).

Time (hrs)	Mole Fraction			
	CIN	HCA	PP	CA
0	1.00	0.00	0.00	0.00
0.5	0.973	0.027	0.00	0.00
1.0	0.959	0.041	0.00	0.00
1.5	0.935	0.065	0.00	0.00
2.0	0.888	0.112	0.00	0.00
3.0	0.833	0.152	0.015	0.00
24.0	0.20	0.648	0.152	0.00

Table 4.11 - Hydrogenation of 1.986 x 10^{-3} moles of Cinnamaldehyde, (0.5 [$Pd_2Cl_4(PMe_3)_2/SiO_2$], 25 ml decalin, 135°C).

Time (hrs)	Mole Fraction			
	CIN	HCA	PP	CA
0	1.00	0.00	0.00	0.00
0.5	0.89	0.11	0.00	0.00
1.0	0.71	0.25	0.04	0.00
2.5	0.65	0.31	0.04	0.00
3.0	0.55	0.40	0.05	0.00
4.0	0.47	0.47	0.06	0.00
5.0	0.23	0.64	0.13	0.00
24.0	0.21	0.51	0.28	0.00

Table 4.12 - Hydrogenation of 1.986 x 10^{-3} moles of Cinnamaldehyde, (0.5 g [$Pd_2Cl_4(PEt_3)_2/SiO_2$], 25 ml decalin, 95 °C).

Time (hrs)	Mole Fraction			
	CIN	HCA	PP	CA
0	1.00	0.00	0.00	0.00
0.5	0.95	0.05	0.00	0.00
1.0	0.84	0.16	0.00	0.00
1.5	0.51	0.41	0.08	0.00
2.0	0.02	0.80	0.18	0.00
3.0	0.00	0.765	0.235	0.00
24.0	0.00	0.717	0.283	0.00

Table 4.13 Hydrogenation of 1.986 x 10^{-3} moles of Cinnamaldehyde, (0.5 g [$Pd_2Cl_4(PEt_3)_2/SiO_2$], 25 ml heptane, 95 °C).

Time (hrs)	Mole Fraction			
	CIN	HCA	PP	CA
0	1.00	0.00	0.00	0.00
0.33	0.977	0.023	0.00	0.00
0.66	0.943	0.057	0.00	0.00
1.0	0.867	0.133	0.00	0.00
1.33	0.614	0.386	0.00	0.00
1.66	0.21	0.549	0.24	0.00
2.0	0.04	0.71	0.25	0.00
48.0	0.00	0.70	0.30	0.00

Table 4.14 Hydrogenation of 1.986 x 10^{-3} moles of Cinnamaldehyde, (0.5 g [$Pd_2Cl_4(PEt_3)_2/SiO_2$], 25 ml decalin, 135°C).

Time (hrs)	Mole Fraction			
	CIN	HCA	PP	CA
0	1.00	0.00	0.00	0.00
0.5	0.00	0.71	0.29	0.00
1.0	0.00	0.72	0.28	0.00
1.5	0.00	0.72	0.28	0.00
2.0	0.00	0.72	0.28	0.00
3.0	0.00	0.72	0.28	0.00
24.0	0.00	0.77	0.23	0.00
48.0	0.00	0.83	0.17	0.00

The data for the binuclear chloro-palladium phosphine catalyst precursors, [$Pd_2Cl_4(PR_3)_2/SiO_2$] (R= Me, Et), used in the hydrogenation of cinnamaldehyde in decalin and heptane, at temperatures ranging from 70°C to 135°C are presented in tables 4.9 - 4.14. For every example, PP was produced in amounts ranging from 15 to 30 %.

Changing the solvent from decalin to heptane had no effect on either reaction rate or catalyst selectivity (tables 4.12 and 4.13). Changing the nature of the phosphine group from R= Me to Et, however, did have a significant effect on the rate. For [$Pd_2Cl_4(PMe_3)_2/SiO_2$], when the reaction was carried out at 135°C, 21 % of the initial starting concentration of CIN was left unreacted after 24 hours (table 4.11, graph 4.5). For [$Pd_2Cl_4(PEt_3)_2/SiO_2$], however, 100 % CIN conversion had occurred after 30 minutes. At this point the catalyst appeared to be deactivated (table

4.14, graph 4.7). In reactions where temperatures of 95°C or less were used (tables 4.9, 4.10, 4.12, 4.13 and graph 4.6), there is clear evidence of an induction period, although the length of these induction periods vary from catalyst to catalyst.

Table 4.15 - Hydrogenation of 1.986 x 10^{-3} moles of Cinnamaldehyde, (0.5 g [$Pd_2Br_4(PMe_3)_2/SiO_2$], 25 ml decalin, 95°C).

Time (hrs)	Mole Fraction			
	CIN	HCA	PP	CA
0	1.00	0.00	0.00	0.00
0.167	0.992	0.008	0.00	0.00
0.5	0.98	0.02	0.00	0.00
0.667	0.982	0.018	0.00	0.00
0.833	0.961	0.039	0.00	0.00
1.00	0.961	0.039	0.00	0.00
1.25	0.937	0.063	0.00	0.00
1.5	0.771	0.229	0.00	0.00
1.75	0.63	0.37	0.00	0.00
2.0	0.555	0.445	0.00	0.00
2.25	0.487	0.513	0.00	0.00
2.5	0.406	0.594	0.00	0.00
2.75	0.361	0.639	0.00	0.00
3.0	0.336	0.664	0.00	0.00
3.25	0.328	0.672	0.00	0.00
3.5	0.30	0.70	0.00	0.00
72.0	0.115	0.895	0.00	0.00

Table 4.16 - Hydrogenation of 1.986 x 10^{-3} moles of Cinnamaldehyde, (0.5 g [$Pd_2Br_4(PMe_3)_2/SiO_2$], 25 ml heptane, 95°C).

Time (hrs)	Mole Fraction			
	CIN	HCA	PP	CA
0	1.00	0.00	0.00	0.00
0.167	1.00	0.00	0.00	0.00
0.333	0.995	0.005	0.00	0.00
0.5	1.00	0.00	0.00	0.00
0.667	0.996	0.004	0.00	0.00
0.833	1.00	0.00	0.00	0.00
1.0	0.992	0.008	0.00	0.00
1.25	0.974	0.026	0.00	0.00
1.5	0.949	0.051	0.00	0.00
1.75	0.974	0.026	0.00	0.00
2.0	0.949	0.051	0.00	0.00
2.25	0.782	0.218	0.00	0.00

No samples were obtained after 2.25 hours since a temperature fluctuation which occurred overnight, resulted in the evaporation of the solvent.

Table 4.17 - Hydrogenation of 1.986 x 10^{-3} moles of Cinnamaldehyde, (0.5 g [$Pd_2Br_4(PMe_3)_2/SiO_2$], 25 ml decalin, 135°C).

Time (hrs)	Mole Fraction			
	CIN	HCA	PP	CA
0	1.00	0.00	0.00	0.00
0.5	0.735	0.265	0.00	0.00
1.0	0.00	1.00	0.00	0.00
1.5	0.00	1.00	0.00	0.00
2.0	0.00	1.00	0.00	0.00
3.0	0.00	1.00	0.00	0.00
4.0	0.00	1.00	0.00	0.00
5.0	0.00	1.00	0.00	0.00
24.0	0.00	1.00	0.00	0.00

Table 4.18 - Hydrogenation of 1.986 x 10^{-3} moles of Cinnamaldehyde, (0.5 g [$Pd_2Br_4(PEt_3)_2/SiO_2$], 25 ml decalin, 95°C).

Time (hrs)	Mole Fraction			
	CIN	HCA	PP	CA
0	1.00	0.00	0.00	0.00
0.17	0.998	0.002	0.00	0.00
0.33	0.961	0.039	0.00	0.00
0.5	0.912	0.088	0.00	0.00
0.66	0.884	0.116	0.00	0.00
0.83	0.841	0.159	0.00	0.00
1.0	0.779	0.221	0.00	0.00
1.33	0.521	0.48	0.00	0.00
1.66	0.212	0.788	0.00	0.00
2.0	0.076	0.924	0.00	0.00
3.0	0.00	1.00	0.00	0.00
27.0	0.00	1.00	0.00	0.00

Table 4.19 - Hydrogenation of 1.986 x 10^{-3} moles of Cinnamaldehyde, (0.5 g [$Pd_2Br_4(PEt_3)_2/SiO_2$], 25 ml decalin, 135°C).

Time (hrs)	Mole Fraction			
	CIN	HCA	PP	CA
0	1.00	0.00	0.00	0.00
0.5	0.235	0.765	0.00	0.00
1.0	0.00	1.00	0.00	0.00
1.5	0.00	1.00	0.00	0.00
3.0	0.00	1.00	0.00	0.00
24.0	0.00	1.00	0.00	0.00
48.0	0.00	1.00	0.00	0.00

Table 4.20 - Hydrogenation of 1.986 x 10^{-3} moles of Cinnamaldehyde, (mechanical mix of 0.5 g [$Pd_2Br_4(PEt_3)_2$/ SiO_2], 25 ml decalin, 135°C).

Time (hrs)	Mole Fraction			
	CIN	HCA	PP	CA
0	1.00	0.00	0.00	0.00
0.833	0.053	0.947	0.00	0.00
48.0	0.00	1.00	0.00	0.00

Table 4.21 - Hydrogenation of 1.986 x 10^{-3} moles of Cinnamaldehyde, (0.5 g [$Pd_2Br_4(PBu_3)_2/SiO_2$], 25 ml decalin, 135°C).

Time (hrs)	Mole Fraction			
	CIN	HCA	PP	CA
0	1.00	0.00	0.00	0.00
0.5	0.036	0.964	0.00	0.00
1.0	0.00	1.00	0.00	0.00
1.5	0.00	1.00	0.00	0.00
2.0	0.00	1.00	0.00	0.00
3.0	0.00	1.00	0.00	0.00
48.0	0.00	1.00	0.00	0.00

Table 4.22 - Hydrogenation of 1.986 x 10^{-3} moles of Cinnamaldehyde, (0.5 g [$Pd_2Br_4(PPr^i_3)_2/SiO_2$], 25 ml decalin, 135°C).

Time (hrs)	Mole Fraction			
	CIN	HCA	PP	CA
0	1.00	0.00	0.00	0.00
0.5	0.00	1.00	0.00	0.00
1.167	0.00	1.00	0.00	0.00
2.0	0.00	1.00	0.00	0.00
3.0	0.00	1.00	0.00	0.00
4.0	0.00	1.00	0.00	0.00
48.0	0.00	1.00	0.00	0.00

The data for the catalysts prepared from the binuclear bromo-bridged palladium phosphine precursors, $[Pd_2Br_4(PR_3)_2/SiO_2]$ (R= Me, Et, Pr^i or Bu), used in the hydrogenation of cinnamaldehyde in decalin or heptane at temperatures ranging from 95°C to 135°C are presented in tables 4.15 - 4.22.

Reactions carried out at 95°C showed clear evidence of an induction period (tables 4.15, 4.16, 4.18 and graph 4.8). This was also found with the binuclear chloro-catalysts. Unlike the chloro-catalysts, however, the selectivity for the bromo-catalysts was found to be exclusively towards HCA. The nature of the alkyl component of the phosphine ligands appeared to be in part responsible for the observed differences in reaction rate between the various bromo-catalysts. As the phosphine group became bulkier, the reaction rate was found to increase (graph 4.9). The method of catalyst preparation did not, however, appear to affect the reaction rate, and a catalyst prepared as a mechanical mix of $[Pd_2Br_4(PEt_3)_2]$ and silica proceeded with essentially the same reaction rate as a sample prepared by wet impregnation (table 4.20).

Table 4.23 - Hydrogenation of 1.986 x 10^{-3} moles of Cinnamaldehyde, (0.5 g [$Pd_2I_4(PMe_3)_2/SiO_2$], 25 ml decalin, 135°C).

Time (hrs)	Mole Fraction			
	CIN	HCA	PP	CA
0	1.00	0.00	0.00	0.00
1.0	0.99	0.01	0.00	0.00
2.5	0.97	0.03	0.00	0.00
4.0	0.96	0.04	0.00	0.00
5.0	0.955	0.045	0.00	0.00
24.0	0.94	0.06	0.00	0.00
48.0	0.913	0.087	0.00	0.00
72.0	0.896	0.104	0.00	0.00
96.0	0.885	0.115	0.00	0.00
168.0	0.887	0.113	0.00	0.00
192.0	0.882	0.118	0.00	0.00
214.0	0.852	0.158	0.00	0.00

Table - 4.24 - Hydrogenation of 1.986 x 10^{-3} moles of Cinnamaldehyde, (0.5 g [$Pd_2I_4(PEt_3)_2/SiO_2$], 25 ml decalin, 135°C).

Time (hrs)	Mole Fraction			
	CIN	HCA	PP	CA
0	1.00	0.00	0.00	0.00
0.5	1.00	0.00	0.00	0.00
1.0	1.00	0.00	0.00	0.00
1.5	0.998	0.002	0.00	0.00
2.0	0.997	0.003	0.00	0.00
3.0	0.987	0.013	0.00	0.00
4.0	0.978	0.022	0.00	0.00
24.0	0.946	0.054	0.00	0.00
48.0	0.947	0.053	0.00	0.00

The data for the catalysts prepared from the binuclear iodo-bridged palladium phosphine precursors, [$Pd_2I_4(PR_3)_2/SiO_2$] (R= Me or Et), used in the hydrogenation of cinnamaldehyde in decalin at 135°C are presented in tables 4.23 - 4.24. In both cases the catalysts formed were selective for HCA only, but conversion levels were low. For [$Pd_2I_4(PEt_3)_2/SiO_2$], only 5.3 % HCA was formed after 48 hours reaction and for [$Pd_2I_4(PMe_3)_2/SiO_2$], after an extended 'run' time of 214 hours, only 15.8 % CIN had been converted to HCA.

Table 4.25 - Hydrogenation of 1.986 x 10^{-3} moles of Cinnamaldehyde, (Unsupported $[Pd_2Cl_4(PMe_3)_2]$, (0.060 g), 25 ml decalin, 135°C).

Time (hrs)	Mole Fraction			
	CIN	HCA	PP	CA
0	1.00	0.00	0.00	0.00
0.25	0.98	0.02	0.00	0.00
0.5	0.977	0.023	0.00	0.00
0.75	0.973	0.027	0.00	0.00
1.0	0.97	0.03	0.00	0.00
1.5	0.953	0.047	0.00	0.00
3.0	0.938	0.062	0.00	0.00
4.0	0.926	0.074	0.00	0.00
24.0	0.705	0.233	0.062	0.00

The unsupported $[Pd_2Cl_4(PMe_3)_2]$ complex gave the same selectivity towards PP as its supported analogue. The reaction rate, however, was significantly lower and only 29.5 % of the total amount of CIN was converted to HCA and PP after 24 hours, compared to 79 % for the supported analogue under the same reaction conditions (table 4.11).

Table 4.26 - Hydrogenation of 1.986 x 10^{-3} moles of Cinnamaldehyde, (Unsupported $[Pd_2Br_4(PMe_3)_2]$, (0.080 g), 25 ml decalin, 135°C).

Time (hrs)	Mole Fraction			
	CIN	HCA	PP	CA
0	1.00	0.00	0.00	0.00
0.25	1.00	0.00	0.00	0.00
0.5	1.00	0.00	0.00	0.00
0.75	0.96	0.04	0.00	0.00
1.0	0.94	0.06	0.00	0.00
1.25	0.92	0.08	0.00	0.00
2.0	0.68	0.33	0.00	0.00
3.0	0.55	0.45	0.00	0.00
4.0	0.23	0.73	0.00	0.00
5.0	0.21	0.79	0.00	0.00
24.0	0.207	0.793	0.00	0.00

The unsupported $[Pd_2Br_4(PMe_3)_2]$ complex also showed the same selectivity to HCA as the supported analogue. As with the unsupported chloro-complex, however, the activity was significantly reduced. The supported catalyst gave 100 % conversion to HCA after only 60 minutes reaction, compared to 79 % conversion after 24 hours for the unsupported complex under the same reaction conditions.

In an attempt to gain further information on the reaction mechanism, reactions were carried out using selected catalyst precursors for the hydrogenation of hydrocinnamaldehyde and cinnamyl alcohol. The results of these experiments are presented in tables 4.27 - 4.30.

Table 4.27 - Hydrogenation of 1.900 x 10^{-3} moles of Hydrocinnamaldehyde, (0.5 g [Pd/SiO_2], 25 ml decalin, 135°C).

Time (hrs)	Mole Fraction			
	CIN	HCA	PP	CA
0	0.00	1.00	0.00	0.00
0.33	0.00	1.00	0.00	0.00
0.66	0.00	1.00	0.00	0.00
1.25	0.00	1.00	0.00	0.00
1.66	0.00	0.93	0.07	0.00
2.0	0.00	0.905	0.095	0.00
3.0	0.00	0.88	0.12	0.00
4.0	0.00	0.85	0.15	0.00
21.0	0.00	0.687	0.313	0.00
48.0	0.00	0.311	0.69	0.00

The [Pd/SiO_2] catalyst required an induction period of approximately 1.5 hours before hydrogenation of the HCA began. This contrasted with the reaction of CIN over the same catalyst in that, for the same conditions, CIN was hydrogenated rapidly and no induction period was observed.

Table 4.28 - Hydrogenation of 1.863 x 10^{-3} moles of Cinnamyl Alcohol, (0.5 g [Pd/SiO_2], 25 ml decalin, 95°C).

Time (hrs)	Mole Fraction			
	CIN	HCA	PP	CA
0	0.00	0.00	0.00	1.0
0.167	0.00	0.00	0.00	1.0
0.334	0.00	0.02	0.00	0.98
0.5	0.00	0.035	0.00	0.965
0.834	0.00	0.10	0.07	0.83
1.0	0.00	0.17	0.20	0.63
1.5	0.00	0.20	0.41	0.39
3.0	0.00	0.24	0.60	0.16
5.0	0.00	0.27	0.65	0.08

The [Pd/SiO_2] catalyst required an induction period of approximately 20 minutes before any reaction was observed. After this 20 minutes, rapid isomerism of the CA to HCA took place. Hydrogenation of CA to PP was also observed.

Table 4.29 illustrates the reaction of 1.900 x 10^{-3} moles of hydrocinnamaldehyde with a representative selection of catalyst precursors. Results are shown as the mole fraction of hydrocinnamaldehyde reacted after 48 hours. The reaction temperature was maintained at 135°C and in each case 0.5 g of catalyst precursor and 25 ml decalin were used.

Table 4.29

Precursor Reacted	Mole Fraction			
	CIN	HCA	PP	CA
$[PdCl_2(PMe_3)_2/SiO_2]$	0.00	1.00	0.00	0.00
$[Pd_2Cl_4(PMe_3)_2/SiO_2]$	0.00	1.00	0.00	0.00
$[Pd_2Cl_4(PEt_3)_2/SiO_2]$	0.00	1.00	0.00	0.00
$[Pd_2Br_4(PMe_3)_2/SiO_2]$	0.00	1.00	0.00	0.00
$[Pd_2Br_4(PEt_3)_2/SiO_2]$	0.00	1.00	0.00	0.00

For all of the catalyst precursors examined, none facilitated the hydrogenation of HCA.

Table 4.30 - Hydrogenation of 1.863 x 10^{-3} moles of Cinnamyl Alcohol, (0.5 g [$Pd_2Cl_4(PMe_3)_2/SiO_2$], 25 ml decalin, 135°C).

Time (hrs)	Mole Fraction			
	CIN	HCA	PP	CA
0	0.00	0.00	0.00	1.00
0.5	0.00	0.017	0.17	0.813
24.0	0.00	0.782	0.218	0.00
48.0	0.00	0.769	0.231	0.00

From the catalyst prepared from [$Pd_2Cl_4(PMe_3)_2/SiO_2$], after 48 hours all the CA had reacted. 23.1 % was converted to PP, whereas the rest was isomerised to HCA.

The same reaction was carried out using the precursor, [$Pd_2Br_4(PMe_3)_2/SiO_2$]. Under the same conditions, after 24 hours all the CA was converted to 3 % HCA and 97 % PP. This indicated that for the catalyst prepared from [$Pd_2Br_4(PMe_3)_2/SiO_2$], isomerism of CA to HCA is unlikely.

Table 4.31 - Hydrogenation of 1.986 x 10^{-3} moles of Cinnamaldehyde, (0.5 g [$Pd_2Br_4(PMe_3)_2/SiO_2$], 25 ml decalin, 135°C, reuse over 3 runs).

Reaction No	Time (hrs)	Mole Fraction			
		CIN	HCA	PP	CA
1	24.0	0.00	1.00	0.00	0.00
2	0	1.00	0.00	0.00	0.00
	1.0	0.969	0.031	0.00	0.00
	2.0	0.909	0.091	0.00	0.00
	5.0	0.928	0.072	0.00	0.00
	24.0	0.814	0.186	0.00	0.00
	48.0	0.736	0.264	0.00	0.00
3	0	1.00	0.00	0.00	0.00
	0.5	1.00	0.00	0.00	0.00
	1.0	0.993	0.007	0.00	0.00
	2.0	0.938	0.062	0.00	0.00
	24.0	0.923	0.073	0.00	0.00
	48.0	0.917	0.083	0.00	0.00

After each 'run', the solution was filtered off, and the catalyst was washed with diethyl ether and vacuum dried prior to re-use. Catalyst selectivity towards HCA was maintained but activity was significantly decreased. Only one sample was taken from the first 'run' to confirm the results obtained in previous reactions.

Experiments were carried out to see whether the timing of the addition of CIN and hydrogen was critical. The results of the two experiments performed are presented in tables 4.32 and 4.33.

Table 4.32 - Hydrogenation of 1.986 x 10^{-3} moles of Cinnamaldehyde, (0.5 g [$Pd_2Br_4(PMe_3)_2/SiO_2$], 25 ml decalin, 135°C). Cinnamaldehyde was added 30 minutes prior to the hydrogen gas. The table below records the product ratios obtained (using the point where hydrogen was introduced as 0 hours).

Time (hrs)	Mole Fraction			
	CIN	HCA	PP	CA
0	1.00	0.00	0.00	0.00
0.5	0.00	1.00	0.00	0.00
24.0	0.00	1.00	0.00	0.00

Table 4.33 - Hydrogenation of 1.986 x 10^{-3} moles of Cinnamaldehyde, (0.5 g [$Pd_2Br_4(PMe_3)_2/SiO_2$], 25 ml decalin, 135°C). Hydrogen gas was bubbled through the solvent/catalyst mixture 30 minutes prior to the addition of cinnamaldehyde. The table below displays the product ratios obtained (using the point where cinnamaldehyde was introduced as 0 hours).

Time (hrs)	Mole Fraction			
	CIN	HCA	PP	CA
0	1.00	0.00	0.00	0.00
1.0	0.649	0.351	0.00	0.00
24.0	0.386	0.614	0.00	0.00
48.0	0.306	0.694	0.00	0.00

When [$Pd_2Br_4(PMe_3)_2/SiO_2$] was pre-treated with CIN, hydrogenation occurred rapidly upon addition of the hydrogen gas to give 100 % conversion to HCA within 30 minutes. When the catalyst was pre-treated with hydrogen gas, however, after the CIN was added the reaction then proceeded at a significantly lower rate. After 48 hours, 31 % of the CIN had still not reacted.

Table 4.34 - Hydrogenation of 2.45 x 10^{-3} moles of 2-cyclohexene-1-one, (0.5 g [Pd/SiO_2], 25 ml heptane, 95°C).

In the following tables, C(eneone) stands for 2-cyclohexene-1-one, C(eneol) for 2-cyclohexene-1-ol, C(anone) for cyclohexanone and C(anol) for cyclohexanol.

Time (hrs)	Mole Fraction			
	C(eneone)	C(eneol)	C(anone)	C(anol)
0	1.0	0.00	0.00	0.00
0.25	0.854	0.00	0.146	0.00
0.5	0.628	0.00	0.372	0.00
2.0	0.550	0.00	0.45	0.00
20.0	0.377	0.00	0.623	0.00
48.0	0.00	0.00	1.00	0.00

The hydrogenation of 2-cyclohexene-1-one proceeded rapidly using [Pd/SiO_2] at 95°C, to give 100 % cyclohexanone. Further reduction to cyclohexanol was not observed.

Tables 4.35a and 4.35b refer to the reaction of 2-cyclohexene-1-one with catalysts prepared from [$Pd_2Br_4(PR_3)_2/SiO_2$] (R = Me, Pr^i). These catalysts were shown to hydrogenate cinnamaldehyde rapidly to hydrocinnamaldehyde at 95°C, and the experiments with 2-cyclohexene-1-one were carried out to determine whether activities comparable to the cinnamaldehyde system would be obtained.

Table 4.35a - Hydrogenation of 2.45 x 10^{-3} moles of 2-cyclohexene-1-one, (0.5 g [$Pd_2Br_4(PMe_3)_2/SiO_2$], 25 ml heptane, 95°C).

Time (hrs)	Mole Fraction			
	C(eneone)	C(eneol)	C(anone)	C(anol)
0	1.00	0.00	0.00	0.00
1.5	1.00	0.00	0.00	0.00
20.5	0.997	0.00	0.003	0.00
24.0	0.995	0.00	0.005	0.00

Table 4.35b - Hydrogenation of 2.45 x 10^{-3} moles of 2-cyclohexene-1-one, (0.5 g [$Pd_2Br_4(PPr^i_3)_2/SiO_2$], 25 ml heptane, 95°C).

Time (hrs)	Mole Fraction			
	C(eneone)	C(eneol)	C(anone)	C(anol)
0	1.00	0.00	0.00	0.00
0.5	1.00	0.00	0.00	0.00
1.33	1.00	0.00	0.00	0.00
2.25	1.00	0.00	0.00	0.00
4.5	1.00	0.00	0.00	0.00
6.0	1.00	0.00	0.00	0.00
21.0	0.991	0.00	0.009	0.00
45.0	0.964	0.00	0.036	0.00

The reactions of [$Pd_2Br_4(PMe_3)_2/SiO_2$] and [$Pd_2Br_4(PPr^i_3)_2/SiO_2$] with 2-cyclohexene-1-one, were very slow in both cases, and conversion levels were low. After 24 hours, using the catalyst prepared from

[$Pd_2Br_4(PMe_3)_2/SiO_2$], 0.5 % of the 2-cyclohexene-1-one was converted to form cyclohexanone and for [$Pd_2Br_4(PPr^i_3)_2/SiO_2$], this figure was 3.6 %.

Graphs 4.1 - 4.9 overleaf, show the reactions of selected catalysts for the hydrogenation of cinnamaldehyde. Graph 4.10 illustrates a typical % conversion against time plot from which a value for the rate constant was calculated.

Graph 4.1 - HYDROGENATION OF 1.986 x 10^{-3} MOLES OF CINNAMALDEHYDE

5 % [Pd/SiO_2] Catalyst, 100°C, 25 ml Decalin

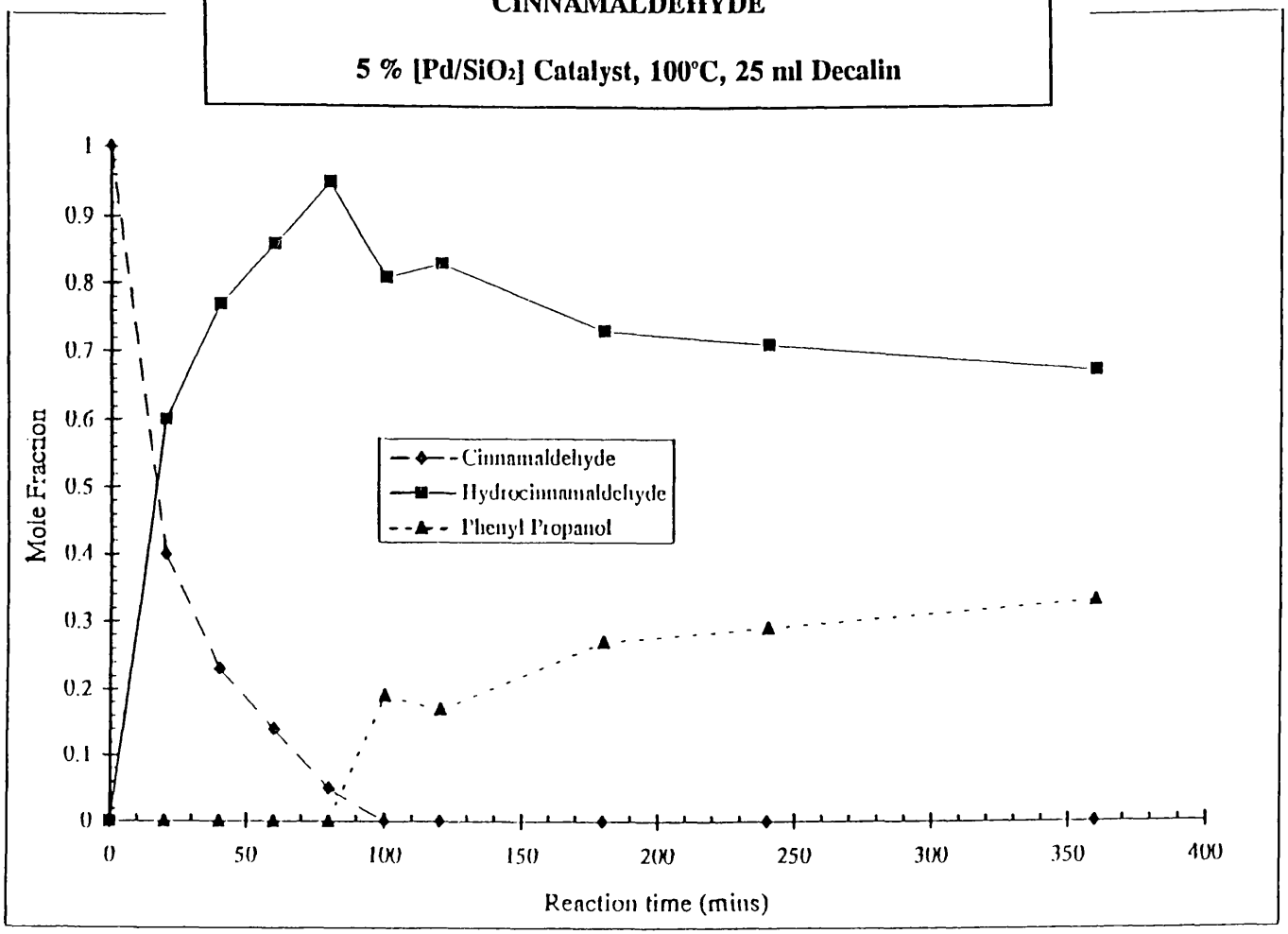

Graph 4.2 - HYDROGENATION OF 1.986 x 10^{-3} MOLES OF CINNAMALDEHYDE

5 % [Pd/SiO_2] Catalyst, 135°C, 25 ml Decalin

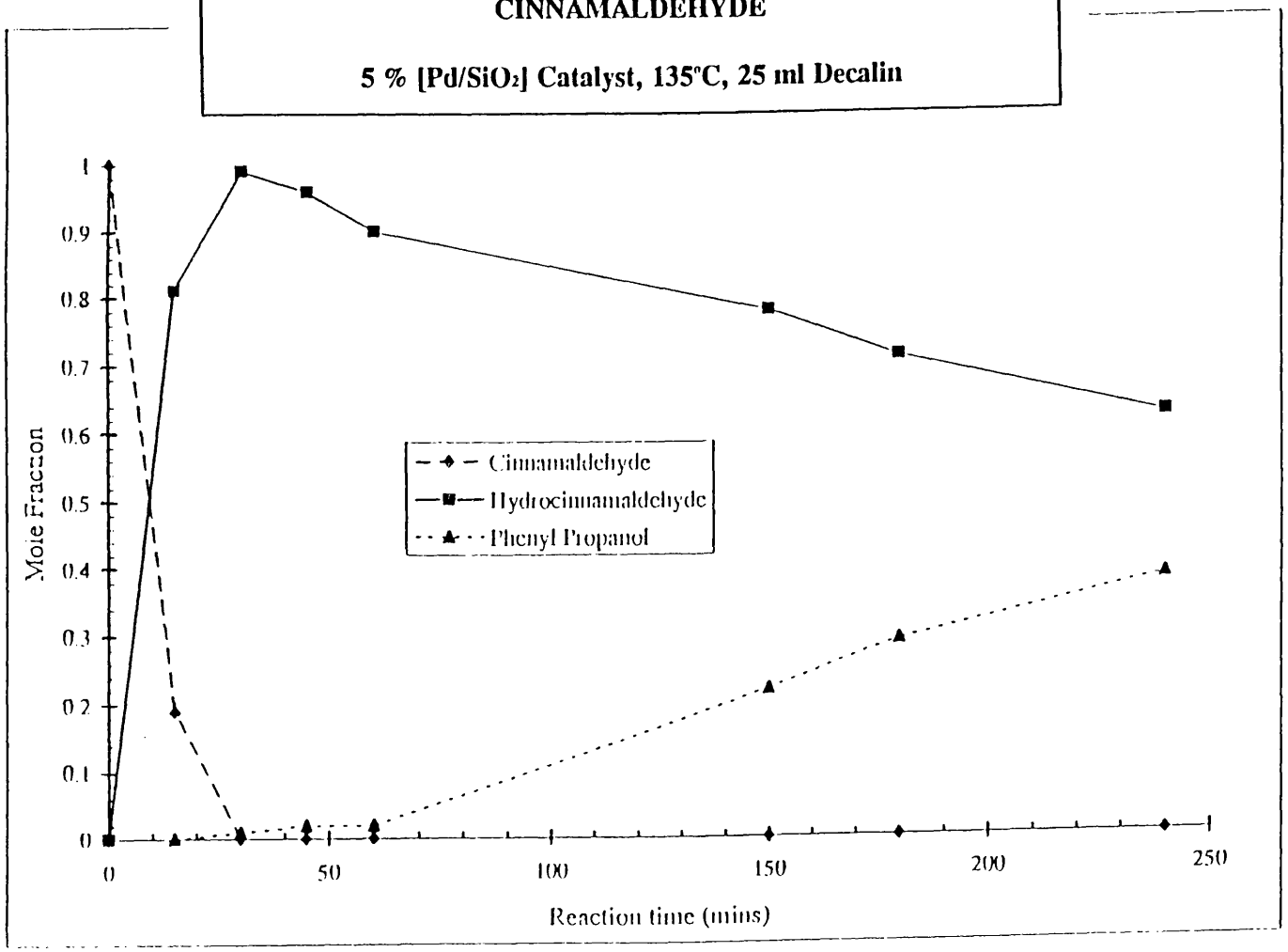

Graph 4.3 - HYDROGENATION OF 1.986 x 10^{-3} MOLES OF CINNAMALDEHYDE

[$PdCl_2/SiO_2$] Catalyst Precursor, Dry Mix, 135°C, 25 ml Decalin

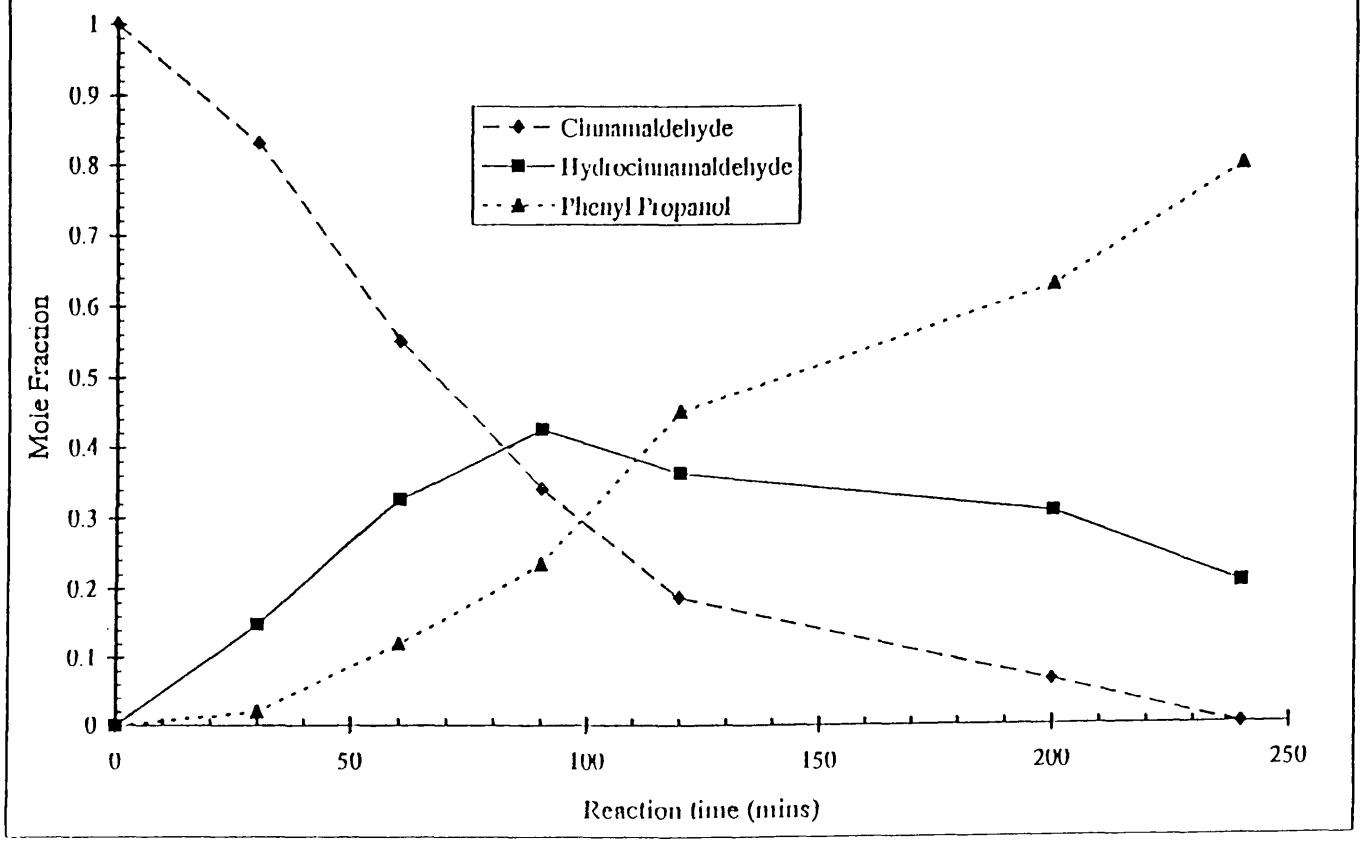

Graph 4.4 - HYDROGENATION OF 1.986 x 10^{-3} MOLES OF CINNAMALDEHYDE

5 % [Pd/SiO_2] Catalyst Modified with [Bu_4N]Br, 135°C, 25 ml Decalin

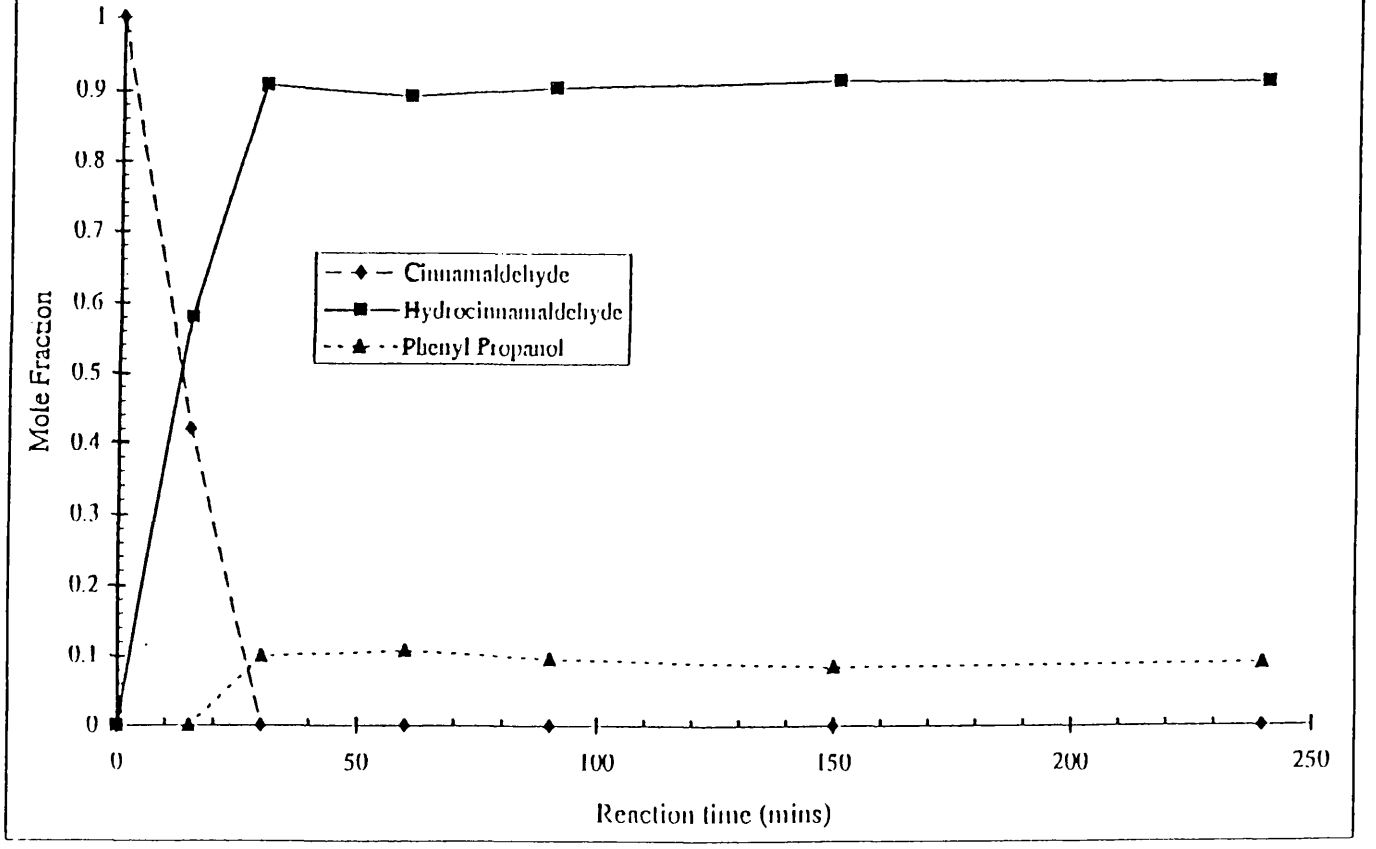

Graph 4.5 - HYDROGENATION OF 1.986 x 10^{-3} MOLES OF CINNAMALDEHYDE

[$Pd_2Cl_4(PMe_3)_2/SiO_2$] Catalyst precursor, 135°C, 25 ml Decalin

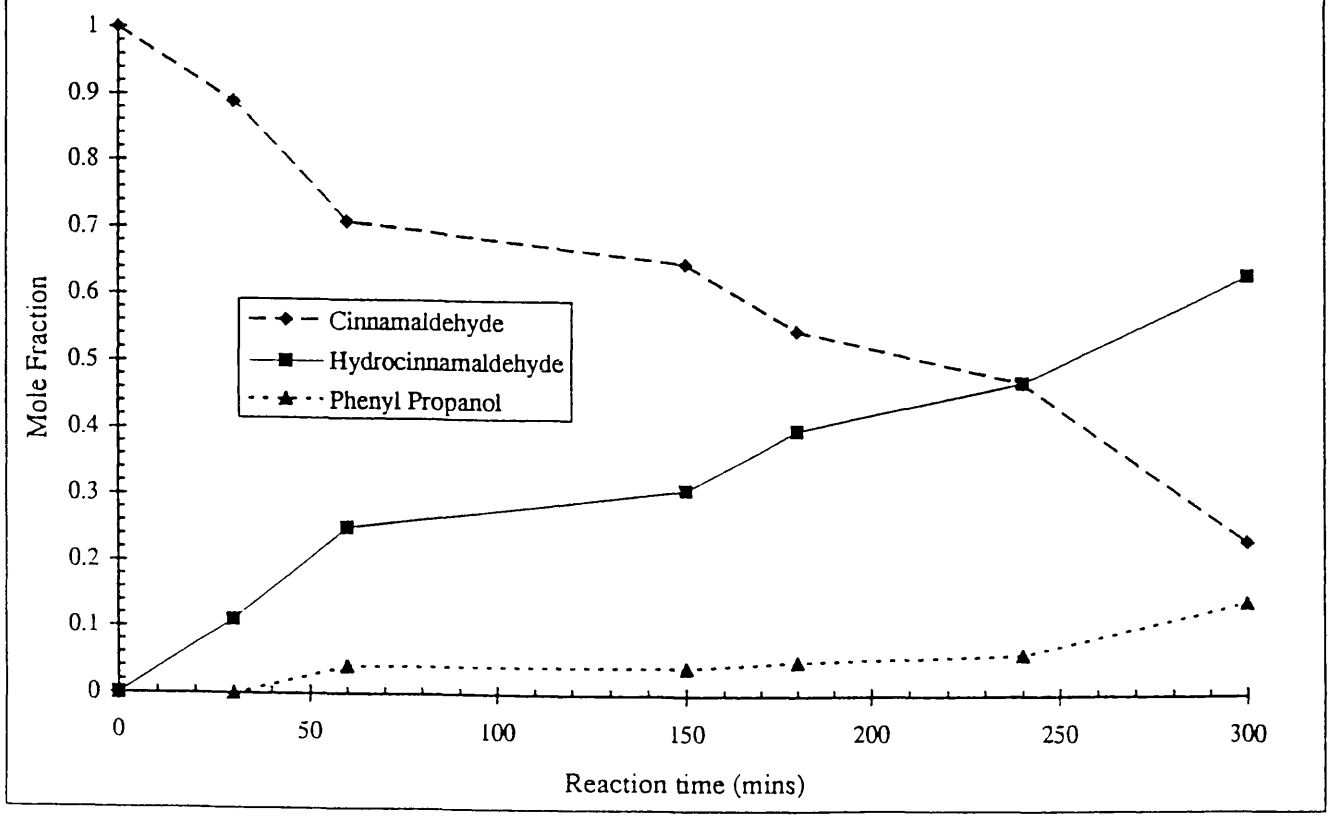

Graph 4.6 - HYDROGENATION OF 1.986×10^{-3} MOLES OF CINNAMALDEHYDE

$[Pd_2Cl_4(PEt_3)_2/SiO_2]$ Catalyst Precursor, 95°C, 25 ml Decalin

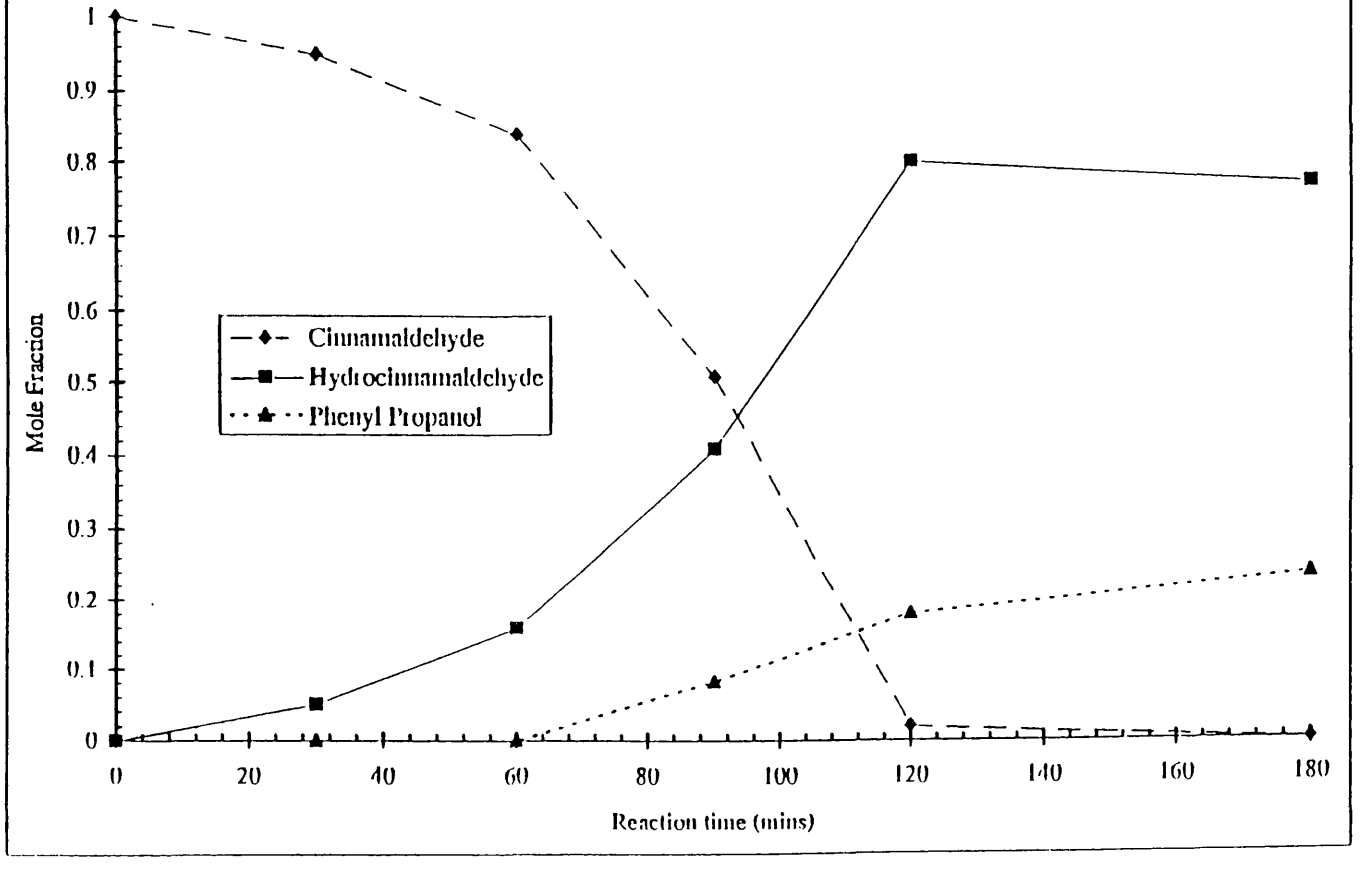

Graph 4.7 - HYDROGENATION OF 1.986 x 10^{-3} MOLES OF CINNAMALDEHYDE

[$Pd_2Cl_4(PEt_3)_2/SiO_2$] Catalyst Precursor, 135°C, 25 ml Decalin

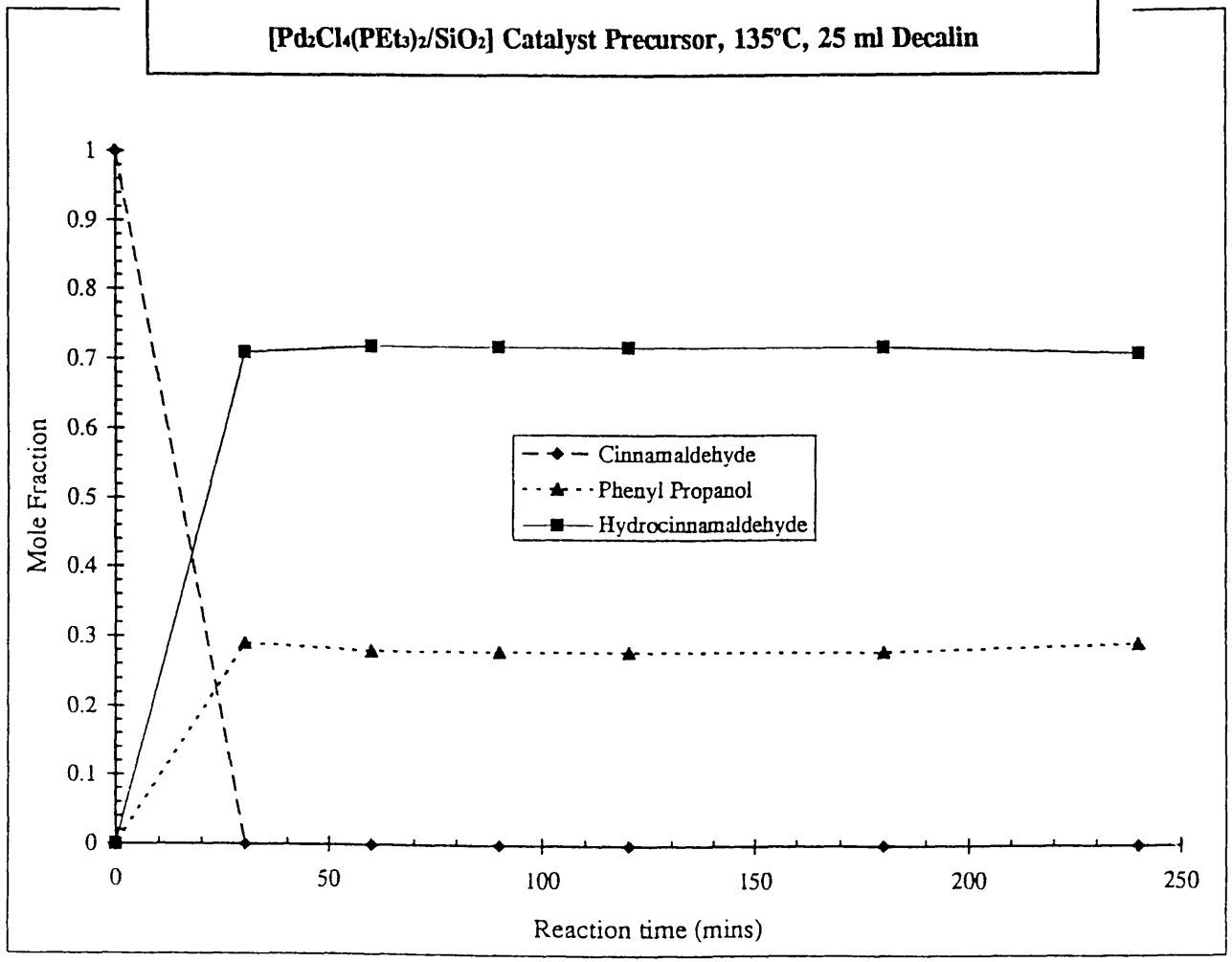

Graph 4.8 - HYDROGENATION OF 1.986 x 10^{-3} MOLES OF CINNAMALDEHYDE

[$Pd_2Br_4(PMe_3)_2/SiO_2$] Catalyst Precursor, 95°C, 25 ml Decalin

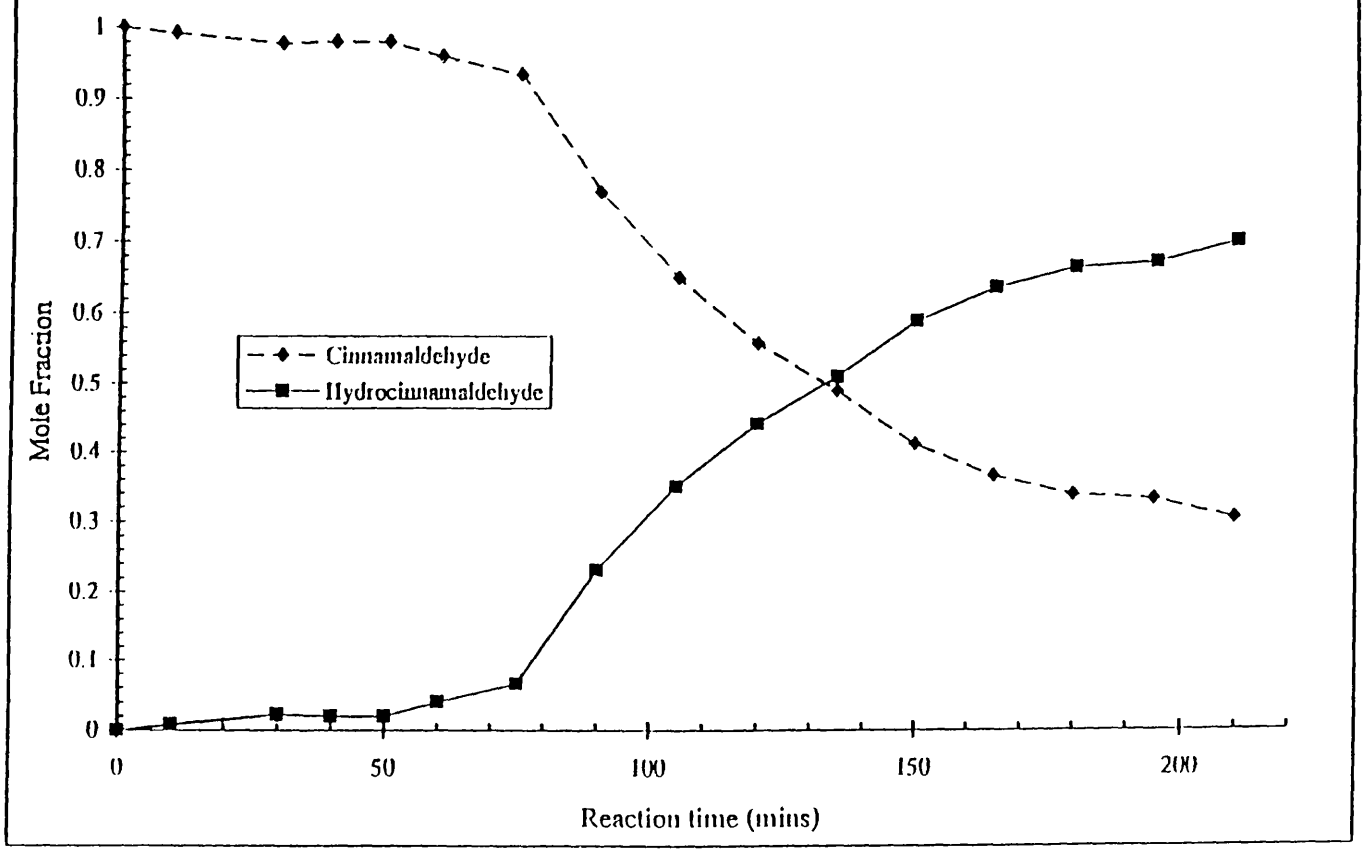

Graph 4.9 - HYDROGENATION OF 1.986 x 10^{-3} MOLES OF CINNAMALDEHYDE

[$Pd_2Br_4(PR_3)_2/SiO_2$] Catalyst Precursor, 135°C, 25 ml Decalin

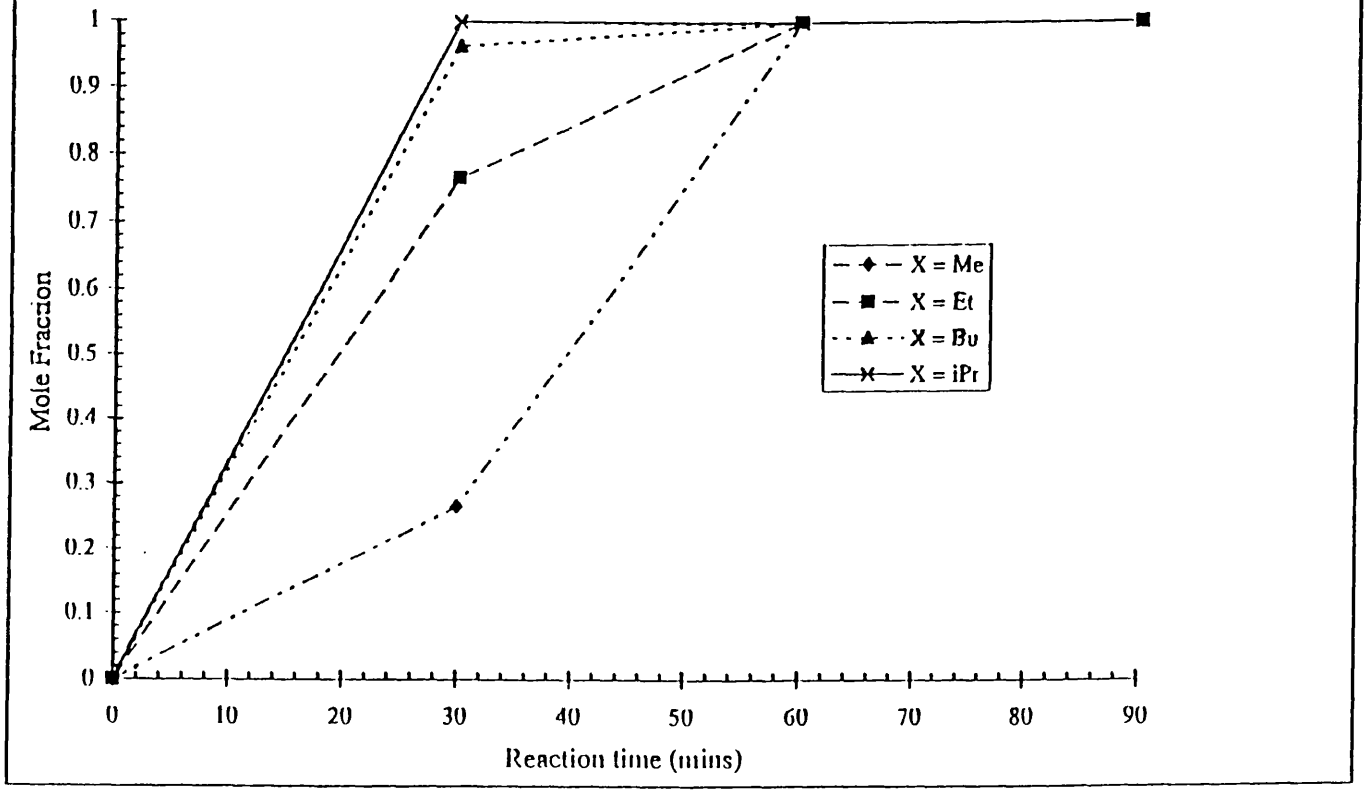

Graph 4.10 - % CONVERSION Vs TIME

[$PdCl_2/SiO_2$] Catalyst Precursor, Dry Mix, 135°C, 25 ml Decalin

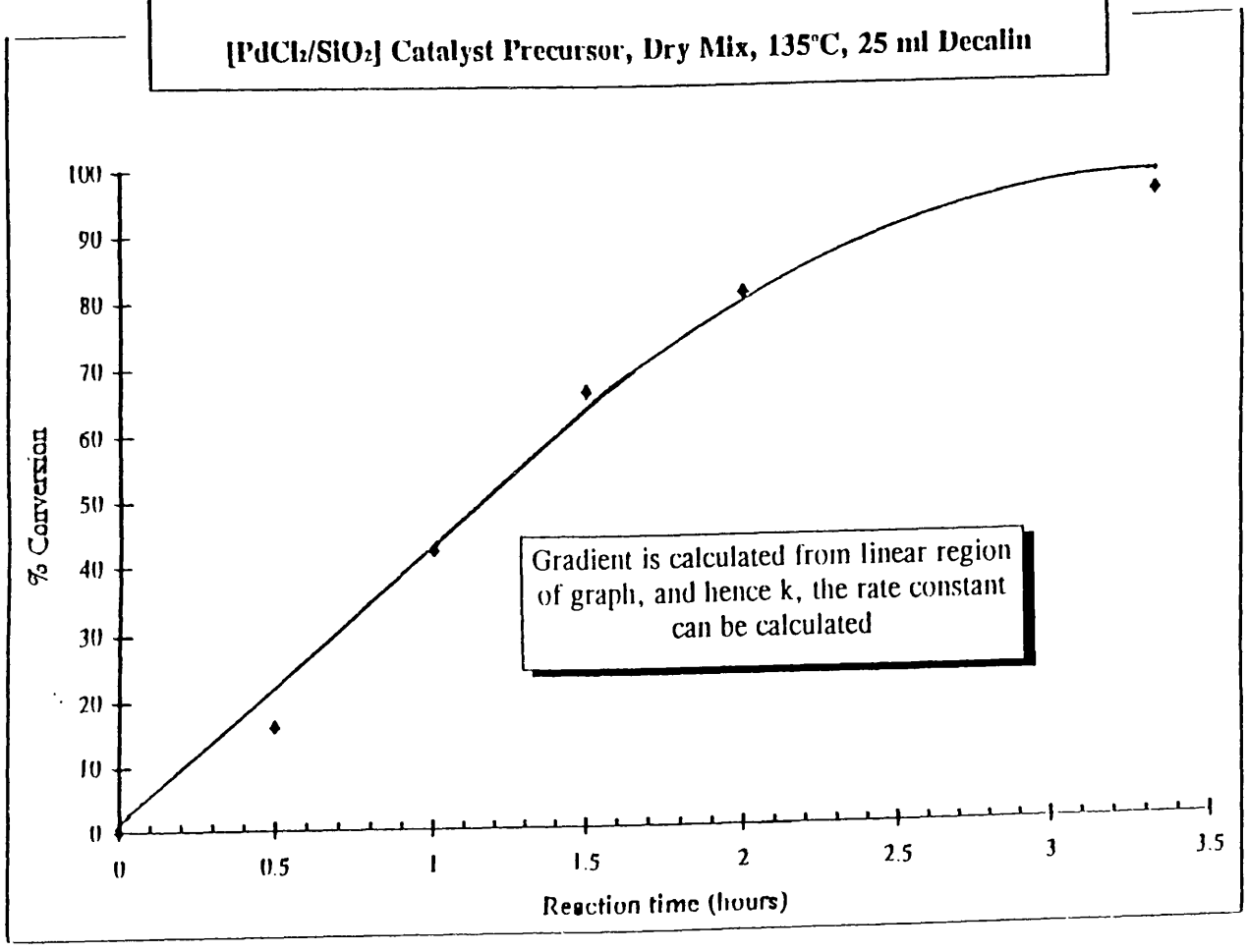

Table 4.36a - Rate Constants for the Hydrogenation of Cinnamaldehyde

(All reactions were carried out at 135°C using decalin as the solvent unless otherwise specified)

Catalyst Precursor	Rate constant k (x 10^{-2} mol $\ell^{-1}hr^{-1}$)
$[Pd/SiO_2]$ [a]	14.3 ± 1.2
$[Pd_2Cl_4(PEt_3)_2/SiO_2]$ [a]	5.7 ± 0.5
$[Pd_2Cl_4(PEt_3)_2/SiO_2]$ (heptane) [a]	5.9 ± 1.0
$[Pd_2Br_4(PMe_3)_2/SiO_2]$ [a]	4.0 ± 0.4
$[Pd_2Br_4(PEt_3)_2/SiO_2]$ [a]	6.5 ± 0.4
$[PdCl_2/SiO_2]$ [b]	3.3 ± 0.5
$[PdCl_2(PMe_3)_2/SiO_2]$	4.1 ± 0.5
$[Pd_2Cl_4(PMe_3)_2/SiO_2]$	1.3 ± 0.18
$[Pd_2Br_4(PMe_3)_2/SiO_2]$	11.5 ± 0.6
$[Pd_2Br_4(PEt_3)_2/SiO_2]$	12.2 ± 0.6
$[Pd_2Br_4(PBu_3)_2/SiO_2]$	15.3 ± 0.8
$[Pd_2Br_4(PPr^i_3)_2/SiO_2]$	15.9 ± 0.8
$[Pd_2Br_4(PMe_3)_2]$ [c]	1.9 ± 0.2

[a] Reaction carried out at 95°C

[b] Catalyst precursor prepared as a mechanical mix

[c] Complex used as an unsupported catalyst

From the table, at 95°C, the 5 % palladium-on-silica catalyst was the most active.

No difference in rate was observed for reactions carried out in both decalin and heptane over [$Pd_2Cl_4(PEt_3)_2/SiO_2$], which indicated that the solvent did not play a part in the reaction mechanism. The slowest reactions were observed for the unsupported [$Pd_2Br_4(PMe_3)_2$] complex and also for [$Pd_2Cl_4(PMe_3)_2/SiO_2$]. Interestingly, there appeared to be a correlation between the size of the attached phosphine ligand, and reaction rate for catalysts prepared from [$Pd_2Br_4(PR_3)_2/SiO_2$]. The reaction rate increased with the following ligand order. $Me < Et < Bu < Pr^i$.

Table 4.36b - Mass Balance Calculations for Selected Catalysts

(based on the difference in molar amounts between the initial starting concentration of cinnamaldehyde and the products formed after 48 hours reaction).

Catalyst Precursor	% of Cinnamaldehyde Retained at Surface
[Pd/SiO_2]	7.2 ± 0.2
[$Pd_2Br_4(PMe_3)_2/SiO_2$] [a]	7.1 ± 0.2
[$Pd_2Br_4(PBu_3)_2/SiO_2$]	11.6 ± 0.3
[$Pd_2I_4(PMe_3)_2/SiO_2$]	10.2 ± 0.3
[$Pd_2Cl_4(PMe_3)_2/SiO_2$] [a]	11.0 ± 0.3
[$Pd_2Cl_4(PEt_3)_2/SiO_2$]	8.2 ± 0.2
[$PdCl_2(PMe_3)_2/SiO_2$]	8.1 ± 0.2
[$PdBr_2(PMe_3)_2/SiO_2$]	7.9 ± 0.2
[$Pd_2I_4(PMe_3)_2/SiO_2$]	11.2 ± 0.3

[a] 24 hours reaction

These mass balance results show that between 7.1 and 11.6 % of the total concentration of cinnamaldehyde was retained on the surface of the

catalysts formed from the various precursors. No correlation was observed between the type of catalyst precursor used and the amount of cinnamaldehyde deposited.

4.2 Thermogravimetric Analysis

Table 4.37 (overleaf) shows the overall % weight loss results recorded for selected catalyst precursors. Weight loss measurements were also recorded for a $[Pd_2Br_4(PMe_3)_2/SiO_2]$ catalyst which had been exposed to hydrogen and cinnamaldehyde at 95°C. A sample of the catalyst formed from $[Pd_2Br_4(PMe_3)_2/SiO_2]$, was extracted from the reaction vessel after 30 minutes to examine the possibility of the formation of a hydrocarbonaceous residue on the surface of the catalyst.

The expected weight loss values were calculated on the assumption that there was sufficient complex on the silica to give a 5 % palladium loading. The high temperatures used in these analyses ensured that all the halide and phosphine components in the catalyst precursors were removed, leaving only palladium metal on the silica surface. The expected maximum weight loss was calculated from the ratio of palladium to carbon, hydrogen, halogen and phosphorus in each sample.

Table 4.37

Catalyst/Precursor	Weight loss obtained (%)	Weight loss expected (%)#	Difference (%)
$[PdCl_2(PMe_3)_2/SiO_2]$ [a]	13.5	10.5	+ 3.0
$[Pd_2Cl_4(PMe_3)_2/SiO_2]$ [a]	9.5	6.9	+ 2.6
$[Pd_2Cl_4(PEt_3)_2/SiO_2]$ [a]	12.8	8.9	+ 3.9
$[Pd_2Br_4(PMe_3)_2/SiO_2]$	15.3	11.1	+4.2
$[Pd_2Br_4(PEt_3)_2/SiO_2]$	15.3	13.0	+ 2.3
$[Pd_2Br_4(PBu_3)_2/SiO_2]$	21.8	17.7	+ 4.1
$[Pd_2Br_4(PPr^i_3)_2/SiO_2]$	15.5	15.0	+ 0.5
$[PdI_2(PMe_3)_2/SiO_2]$	26.8	19.5	+ 7.3
$[Pd_2I_4(PMe_3)_2/SiO_2]$	20.5	15.5	+ 5.0
$[Pd_2I_4(PEt_3)_2/SiO_2]$	22.0	17.3	+ 4.7
$[Pd_2Br_4(PMe_3)_2/SiO_2]$ [b]	15.5	11.1	+ 4.4
$[Pd_2Br_4(PMe_3)_2/SiO_2]$ (30m, 95°C)[c]	20.5	11.1	+ 9.4

[a] TGA spectra were recorded for a 100 % H_2 atmosphere

[b] Catalyst precursor was prepared as a mechanical mix

[c] Catalysts were extracted from reaction, filtered and washed with diethyl ether, prior to analysis.

Table 4.37 showed that for the catalyst precursors, the difference between the expected and obtained weight loss profiles varied between 0.5 % for $[Pd_2Br_4(PPr^i_3)_2/SiO_2]$ and 7.3 % for $[PdI_2(PMe_3)_2/SiO_2]$. This difference was believed to be due to the removal of adsorbed water and from the removal of water formed from the condensation of vicinal silanol groups on the silica surface. For the activated sample that was removed during a hydrogenation reaction at 95°C, the recorded weight loss value deviated from the value recorded for the precursor and this deviation could not be explained in terms of the loss of adsorbed water. A sample of the catalyst prepared from $[Pd_2Br_4(PMe_3)_2/SiO_2]$ extracted after 30 minutes reaction with CIN, had a weight loss value 9.4 % greater than expected, which was consistent with the lay-down of a hydrocarbonaceous over-layer on the surface. This 9.4 % value corresponded to the initial stages of the reaction when the layer was being formed. At this point the mole fraction of products formed was low and conversion was measured at only 2 % (table 4.15). After the layer had been formed, hydrogenation proceeded rapidly with 45 % conversion after 2 hours.

4.3 Transmission Electron Microscopy

TEM micrographs of catalysts prepared from $[Pd_2Br_4(PMe_3)_2/SiO_2]$ and $[Pd_2Cl_4(PMe_3)_2/SiO_2]$ were examined for samples extracted at various points during the hydrogenation of cinnamaldehyde (135°C). These two precursors were chosen because each was representative of a class of catalyst which showed marked differences in selectivity. Analyses were carried out in an attempt to investigate if differences in reaction rates and selectivities could be attributed to a difference in particle size. Micrographs were taken of the wet impregnated bromo-precursor and of a sample of the bromo-catalyst extracted after 3 hours reaction time. Micrographs were also taken for the chloro-catalyst extracted after 2 hours reaction. The particle sizes observed for the samples examined are detailed below.

1. Binuclear bromo-catalyst

Analysis of the precursor sample showed a relatively uniform distribution of metal across the surface of the silica. The mean particle size was estimated at 4.7 ± 0.2 nm based on the measurement of 100 particles. The range of particle size values varied from 2.9 - 8.1 nm, and the standard deviation of the mean value was calculated at ± 1.7 nm. After 3 hours reaction, the particles appeared to be much fewer in number and had aggregated together to give clusters, with size values varying between 10.0 nm and 39.0 nm. A rough estimate of the mean particle size was calculated based on the measurement of 25 particles in this range and found to be 20.5 ± 1.0 nm. The standard deviation on this mean was calculated at ± 8.4 nm. A separate micrograph, however, showed the existence of clusters as large as 170 ± 9 nm.

2. Binuclear chloro-catalyst

A micrograph taken of the active chloro-catalyst, which had been removed after 2 hours reaction, also showed a wide variety of particle sizes. The majority of particles fell in the range 6.1 nm - 41.5 nm, although a few isolated clusters up to 133 ± 6.7 nm were observed. A rough estimate was obtained for the mean particle size based on the measurement of 100 particles in the range discussed above and was found to be 22.5 ± 1.1 nm. The standard deviation on the mean was ± 7.0 nm.

4.4 Solid State ^{31}P MAS-NMR Spectroscopy

A selection of catalysts and precursors were examined by solid state MAS-NMR spectroscopy. The samples examined and the results obtained are detailed below.

1. $[Pd_2Br_4(PMe_3)_2/SiO_2]$.

^{31}P MAS-NMR spectra were obtained for the unreacted catalyst precursor (prepared by a wet impregnation route), for a catalyst precursor prepared by mechanically mixing $[Pd_2Br_4(PMe_3)_2]$ with silica and for the unsupported complex. Additional spectra were recorded for samples extracted at points along a typical reaction procedure. The periods at which samples were extracted from a reaction at 95°C, were carefully chosen to coincide with observed changes in activity during the catalyst's lifetime. The first sample was extracted after 30 minutes reaction, the second after 2 hours and the third after 48 hours. The table overleaf (4.38) illustrates the peak positions for the spectra recorded.

Table 4.38

Precursor/Catalyst Sample	^{31}P MAS NMR (^{1}H decoupled)
Unsupported complex	20.4 ppm (broad)
Wet Impreg precursor	14.7 ppm (sharp)
Dry mix precursor	15.2 ppm (broad, with a low field shoulder)
30 minute extraction sample	52.8 ppm (sharp)
2 hour extraction sample	53.1 ppm (sharp)
48 hour extraction sample	31.2 ppm (sharp, with a high field shoulder) 53.6 ppm (sharp)

2. $[PdBr_2(PMe_3)_2/SiO_2]$ and $[Pd_2Br_4(PEt_3)_2/SiO_2]$

Both of the catalyst precursors above were prepared by wet impregnation. Details of the spectra recorded are shown below.

Table 4.39

Catalyst Precursor	^{31}P MAS NMR (^{1}H decoupled)
$[PdBr_2(PMe_3)_2/SiO_2]$	-16.7 ppm (sharp), 0.4 ppm (broad), 4.7 ppm (broad) [a]
$[Pd_2Br_4(PEt_3)_2/SiO_2]$	54.5 ppm (sharp)

[a] Signals at 0.4 ppm and 4.7 ppm overlap and have a combined relative intensity of 60. The remaining peak has a signal intensity of 40.

The results obtained for the unsupported $[Pd_2Br_4(PMe_3)_2]$ complex show that the phosphorus atoms present exist only in one type of chemical environment. When the complex was supported on a silica surface by wet impregnation, a relatively small shift of 5.7 ppm occurred suggesting that the structure of the complex was retained on the silica surface. The ^{31}P spectrum of the catalyst precursor prepared as a dry mix of $[Pd_2Br_4(PMe_3)_2]$ and silica again showed only one signal. This signal had a similar chemical shift as that observed in the 'wet impregnated' precursor, with a difference of only 0.5 ppm between the two values.

When a catalyst prepared from $[Pd_2Br_4(PMe_3)_2/SiO_2]$ was extracted after 30 minutes reaction at 95°C, a single signal at 52.8 ppm was observed and after 2 hours there was essentially no change in the position of this signal.

After 48 hours reaction, however, 2 signals were observed. The first remained at the same approximate chemical shift as the activated sample and had a shift value of 53.6 ppm, but the second signal was observed upfield at 31.2 ppm. The ratio of the two signals was 7:3.

Table 4.39 showed the solid state ^{31}P spectra of $[Pd_2Br_4(PEt_3)_2/SiO_2]$ and $[PdBr_2(PMe_3)_2/SiO_2]$. Only one signal was observed for $[Pd_2Br_4(PEt_3)_2/SiO_2]$ and it seems likely based on the evidence for $[Pd_2Br_4(PMe_3)_2/SiO_2]$, that this complex also retained its integrity when supported on the silica. Three separate signals were, however, observed for $[PdBr_2(PMe_3)_2/SiO_2]$. The largest signal at -16.7 ppm was probably the intact trans-complex, since the unsupported complex has a solution ^{31}P NMR value of -15.96, and the signal at 0.4 ppm could conceivably be the cis-complex. The identity of the third species at 4.7 ppm was, however,

unknown. In view of the marked difference in activity between this catalyst precursor and the binuclear analogue [$Pd_2Br_4(PMe_3)_2/SiO_2$], the unidentified species may have acted as a catalyst poison.

4.5 Microanalysis Results

The technique of microanalysis was used to check that the palladium phosphine complexes were being supported intact onto the surface of the silica during impregnation, to investigate C/H lay-down on the surface of the catalysts after use and to check on halide/phosphine loss. The following carbon, hydrogen, halogen and phosphorus (C, H, X and P) microanalyses were carried out on the catalysts detailed below. The theoretical values were based on a 5 % (w/w) palladium loading.

Table 4.40 - Catalysts and precursors prepared from $[PdCl_2(PMe_3)_2]$ and $[Pd_2Cl_4(PR_3)_2]$, (R = Me, Et)

Catalyst/Precursor	Calc (%)			Found (%)		
	C	H	Cl	C	H	Cl
$[PdCl_2(PMe_3)_2/SiO_2]$	3.38	0.85	3.33	3.70	1.36	3.31
$[PdCl_2(PMe_3)_2/SiO_2]$[a] (48 h, 135°C)	3.38	0.85	3.33	7.75	1.13	-----
$[Pd_2Cl_4(PMe_3)_2/SiO_2]$[b]	1.69	0.42	3.33	1.72	0.81	3.77
$[Pd_2Cl_4(PEt_3)_2/SiO_2]$	3.38	0.85	3.33	3.78	1.31	4.22
$[Pd_2Cl_4(PMe_3)_2/SiO_2]$ (15 m, 95°C)[a]	1.69	0.42	3.33	2.67	1.14	2.80
$[Pd_2Cl_4(PMe_3)_2/SiO_2]$ (90 m, 95°C)[a]	1.69	0.42	3.33	5.81	1.16	0.95
$[Pd_2Cl_4(PMe_3)_2/SiO_2]$ (48 h, 95°C)[a c]	1.69	0.42	3.33	5.73	1.04	1.24
$[Pd_2Cl_4(PEt_3)_2/SiO_2]$ (48 h, 95°C)[a]	3.38	0.85	3.33	7.90	1.27	1.27

[a] Catalysts were extracted from reaction with 1.98 x 10^{-3} moles of cinnamaldehyde, filtered and washed with diethyl ether, prior to analysis.

[b] P M/A -Found: P, 2.11. Calc. for $C_6H_{18}Cl_4P_2Pd_2/SiO_2$: P, 1.46 %.

[c] P M/A -Found: P, 0.81. Calc. for $C_6H_{18}Cl_4P_2Pd_2/SiO_2$: P, 1.46 %.

Table 4.41 - Catalysts and precursors prepared from $[PdBr_2(PMe_3)_2]$ and $[Pd_2Br_4(PR_3)_2]$ (R = Me, Et, Pr^i or Bu)

Catalyst/Precursor	Calc (%)			Found (%)		
	C	H	Br	C	H	Br
$[PdBr_2(PMe_3)_2/SiO_2]$	3.38	0.85	7.50	3.80	1.37	7.80
$[PdBr_2(PMe_3)_2/SiO_2]$ (48 h, 135°C) ‡	3.38	0.85	7.50	5.95	0.99	6.33
$[Pd_2Br_4(PMe_3)_2/SiO_2]$ [a]	1.69	0.42	7.50	1.84	0.90	9.40
$[Pd_2Br_4(PMe_3)_2/SiO_2]$ †	1.69	0.42	7.50	1.94	1.15	-----
$[Pd_2Br_4(PEt_3)_2/SiO_2]$ [b]	3.38	0.70	7.50	3.30	0.97	7.60
$[Pd_2Br_4(PPr^i_3)_2/SiO_2]$	5.07	0.99	7.50	4.54	1.38	-----
$[Pd_2Br_4(PBu_3)_2/SiO_2]$	6.76	1.27	7.50	7.44	1.83	-----
$[Pd_2Br_4(PMe_3)_2/SiO_2]$ (2 h, 95°C)‡	1.69	0.42	7.50	3.88	0.83	-----
$[Pd_2Br_4(PMe_3)_2/SiO_2]$ (48 h, 95°C)‡ [c]	1.69	0.42	7.50	6.52	1.71	4.78

† Catalyst was prepared as a mechanical mix

‡ Catalysts were extracted from reaction with 1.98 x 10^{-3} moles of cinnamaldehyde, filtered and washed with diethyl ether, prior to analysis.

[a] P M/A -Found: P, 2.39. Calc. for $C_6H_{18}Br_4P_2Pd_2/SiO_2$: P, 1.45 %.

[b] P M/A -Found: P, 2.14. Calc. for $C_{12}H_{30}Br_4P_2Pd_2/SiO_2$: P, 1.45 %.

[c] P M/A -Found: P, 0.79. Calc. for $C_{12}H_{18}Br_4P_2Pd_2/SiO_2$: P, 1.45 %.

Table 4.42 - Catalysts and precursors prepared from $[PdI_2(PMe_3)_2]$ and $[Pd_2I_4(PR_3)_2]$ (R = Me, Et)

Catalyst	Calc (%)			Found (%)		
	C	H	I	C	H	I
$[PdI_2(PMe_3)_2/SiO_2]$	3.38	0.85	11.91	3.30	0.24	11.77
$[Pd_2I_4(PMe_3)_2/SiO_2]$ [a]	1.69	0.42	11.91	1.66	1.04	8.15
$[Pd_2I_4(PEt_3)_2/SiO_2]$	3.38	0.70	11.91	4.49	1.30	11.84
$[PdI_2(PMe_3)_2/SiO_2]$ (48h, 135°C)‡	3.38	0.85	11.91	6.56	1.39	-----
$[Pd_2I_4(PMe_3)_2/SiO_2]$ (48h, 135°C)‡	1.69	0.42	11.91	8.94	1.93	7.20
$[Pd_2I_4(PEt_3)_2/SiO_2]$ (48h, 135°C)‡	3.38	0.70	11.91	8.84	1.41	-----

‡ Catalysts were extracted from reaction with 1.98 x 10^{-3} moles of cinnamaldehyde, filtered and washed with diethyl ether, prior to analysis.

[a] P M/A -Found: P, 1.46. Calc. for $C_6H_{18}I_4P_2Pd_2/SiO_2$: P, 1.82 %.

In all cases, the catalyst precursors examined showed a higher than expected hydrogen content. The maximum H % recorded was + 0.73 % shown for $[Pd_2Br_4(PMe_3)_2/SiO_2]$. This was believed to be due to the presence of surface hydroxyl groups on the silica. Microanalysis on silica

itself showed a hydrogen content of 0.5 % which is consistent with these results.

The catalysts prepared from $[Pd_2Cl_4(PR_3)_2/SiO_2]$ (R = Me or Et), showed a significant decrease in chloride content with reaction time. In the reactions investigated, $[Pd_2Cl_4(PMe_3)_2/SiO_2]$ and $[Pd_2Cl_4(PEt_3)_2/SiO_2]$ showed a decrease in chloride content of approximately two thirds over the course of a 48 hour reaction at 95°C and the phosphorus content of $[Pd_2Cl_4(PMe_3)_2/SiO_2]$ was shown to decrease by 61.6 %. Catalysts prepared from $[PdBr_2(PMe_3)_2/SiO_2]$ and $[Pd_2X_4(PR_3)_2/SiO_2]$ (X=Br or I; R=Me, Et, Pr^i or Bu), however, appeared to retain a significantly higher proportion of halide. The catalyst prepared from $[Pd_2Br_4(PMe_3)_2/SiO_2]$ retained over 50.0 % bromide at 95°C, whereas, at 135°C $[PdBr_2(PMe_3)_2/SiO_2]$ retained 81.2 % bromide and $[Pd_2I_4(PMe_3)_2/SiO_2]$ retained over 88.0 % iodide over the course of a 48 hour reaction. The phosphorus content of $[Pd_2Br_4(PMe_3)_2/SiO_2]$ was similarly analysed after 48 hours reaction at 95°C and found to decrease by 63.1 %.

4.6 Neutron Activation Analysis (NAA)

Fig 4.4 illustrates the packing sequence of the samples within the 'rabbit' described in section 1.8.2. Two standards with known amounts of palladium were included on both levels for calibration. Samples of $[Pd_2Br_4(PMe_3)_2/SiO_2]$ were extracted during a typical reaction procedure and examined in order to determine the palladium content. The unreacted catalyst precursor as well as samples of the activated catalyst extracted after 30 minutes reaction, 2 hours and 48 hours, were examined.

Fig 4.1

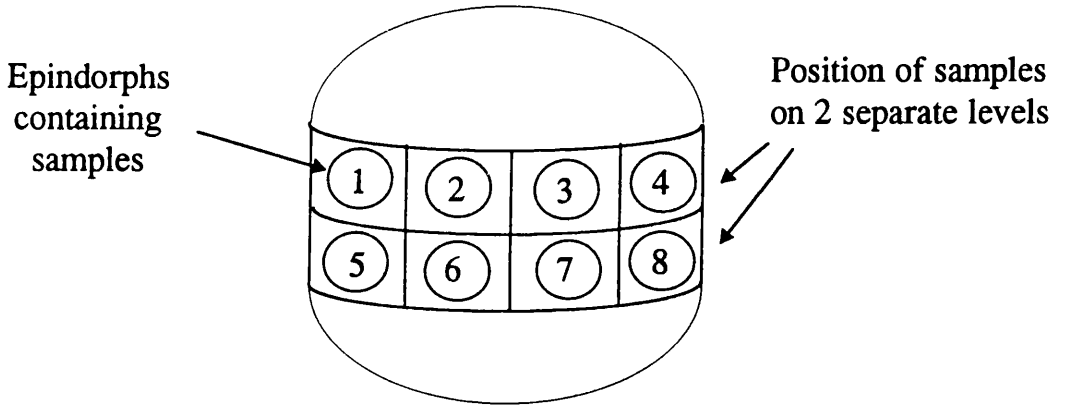

Sample 1 = Sample extracted after 2 hours reaction (135°C, decalin)

Sample 2 = Sample extracted after 0.5 hours reaction (95°C, decalin)

Sample 3 = 1st standard, containing 12.9 mg Pd (5.2 %)

Sample 4 = 2nd standard, containing 13.6 mg Pd (5.4 %)

Sample 5 = Unreacted, wet impregnated catalyst

Sample 6 = Sample extracted after 48.0 hours reaction (135°C, decalin)

Sample 7 = 3rd standard, containing 2.5 mg Pd (1.0 %)

Sample 8 = 4th standard, containing 12.6 mg Pd (5.0 %)

From the weight measurements and packing sequence on the previous page and from the equations detailed in section 1.8.1, the palladium content of each sample was calculated. The results are shown below.

Table 4.43

Sample No	Activity at time of counting (A_t) (cps)	Decay time (seconds)	Decay Corrected Activity (A_o) (cps)	% Pd
1	85.2 ± 0.6	76481	251.0 ± 1.8	3.89 ± 0.03 [b] 3.53 ± 0.03 [c]
2	66.0 ± 0.6	77268	195.9 ± 1.8	3.04 ± 0.03 [b] 2.76 ± 0.03 [c]
3 (1st std)	115.8 ± 0.6	74844	332.9 ± 1.6	5.15 ± 0.02
4 (2nd std)	132.9 ± 0.6	75618	386.6 ± 1.7	5.40 ± 0.02
5 [a]	12.1 ± 0.4	80859	38.0 ± 1.1	4.65 ± 0.17 [d] 4.39 ± 0.14 [e]
6	21.8 ± 0.3	80052	67.6 ± 0.8	3.45 ± 0.08 [d] 3.25 ± 0.05 [e]
7 (3rd std)	6.4 ± 0.1	79287	19.5 ± 0.4	1.00 ± 0.02
8 (4th std)	34.4 ± 0.3	78516	104.1 ± 0.9	5.04 ± 0.04

[a] 0.1048 g of sample analysed. [b] % Pd calculated with respect to sample 3 (1st standard) ; [c] with respect to sample 4 (2nd standard); [d] with respect to sample 7 (3rd standard); [e] with respect to sample 8 (4th standard).

In each case, counting of the palladium γ radiation signal (88.0 KeV in energy) was carried out at a set distance from the detector over a 600 second time period and the data was processed using an Ortec software programme.

Scheme 4.1

$$^{108}_{46}Pd + ^{1}_{0}n \longrightarrow ^{109}_{46}Pd \longrightarrow ^{109}_{47}Ag + ^{0}_{-1}e + \gamma$$

The activity of each sample was determined approximately one day after irradiation (A_t). By calculating the time that elapsed between irradiation and counting, the samples were decay corrected to give the initial activity value (A_o). By comparing the activities of standards with known palladium content with samples containing an unknown amount, the % palladium content was then calculated. A sample calculation is included below.

Sample 5. Wet-Impregnated $[Pd_2Br_4(PMe_3)_2/SiO_2]$ catalyst precursor

To calculate the activity immediately after irradiation,

$A = A_oe^{-\lambda t}$, therefore, 12.1 = Ao $e^{(-1.44 \times 10\text{-}5 \times 80859)}$ = 38.0 cps initial activity. Wt of sample used = 0.1048 g, therefore for a typical sample weight of 0.2500g, activity would equal 90.6 cps. With respect to the 3rd sample, decay corrected activity is calculated at 19.5 cps. Since this corresponds to a palladium content of 2.5 mg in 0.2500 g of sample, and since 2.5 mg = 1.0 % Pd, 90.6/19.5 = 4.65 %.

For each sample analysed, an average value for palladium content was obtained based on the use of both calibration samples. In this way the palladium content for the catalyst precursor was calculated to be 4.5 % (w/w), which was reasonably consistent with the expected value of 5.0 %. The 0.5 % deviation may in part be due to the uptake of water on the silica surface or due to a non uniform dispersion of palladium in the standard samples.

After the catalyst had been exposed to hydrogenation conditions and a sample extracted after 30 minutes reaction, the palladium content is seen to decrease markedly to 2.9 %. A small part of this reduction may simply be due to the presence of a hydrocarbonaceous layer on the catalyst surface since the technique is very sensitive to deviations in weight. Interestingly, however, the result obtained for the sample extracted after 2 hours reaction showed an increase in palladium content to 3.7 %. After 48 hours the value was 3.35 %. At a glance, the decrease in the observed palladium content seemed to indicate a leeching of the metal from the complex. However, the variance in the results suggested some sort of sample contamination.

Further analysis showed that a considerable amount of decalin solvent was retained on the active catalyst samples. As a consequence, the retained decalin significantly affected the % palladium content of the samples being analysed which would account for the observed results.

4.7 X-Ray Photoelectron Spectroscopy (XPS)

Selected catalysts and precursors were analysed by XPS using the method described in section 1.7.1.2. Pd 3d$_{5/2,3/2}$, Br 3d$_{5/2}$, and Cl 2p$_{3/2}$ signals were investigated. In certain cases, peak fitting computer software was used to de-convolute secondary shoulder peaks present in the spectra.

The tables below illustrate the chemical shift values of the peaks recorded. Linear and Shirley background subtraction methods were used.

1. $[Pd_2Cl_4(PMe_3)_2/SiO_2]$ *

Table 4.44

Method of Preparation/time of extraction	XPS Signal (eV)	
	Pd 3d $_{5/2}$ $_{3/2}$	Cl 2p $_{3/2}$
Wet impregnation	337.6, 342.8 335.7, 340.9	198.2
Active catalyst phase [a]	337.1, 342.3 335.1, 340.4	198.8
Deactivated catalyst phase [b]	336.6, 341.9 334.6, 339.9	No signal observed

[a] Sample was extracted after 2 hours, from a reaction mixture operating at 135°C, filtered, and washed with diethyl ether .

[b] Catalyst was extracted after 48 hours reaction, and treated as above.

In each case, the separation between the two palladium signals (Δ value), was observed to be 5.26 ± 0.01 eV.

For each of the 3 spectra recorded, the second palladium signal was observed as a shoulder on the first. The exact position of this secondary peak was calculated using a peak fitting software package. The peak fitted spectra for the palladium signals are shown below.

Fig 4.2 - $[Pd_2Cl_4(PMe_3)_2/SiO_2]$ (wet impregnated precursor)

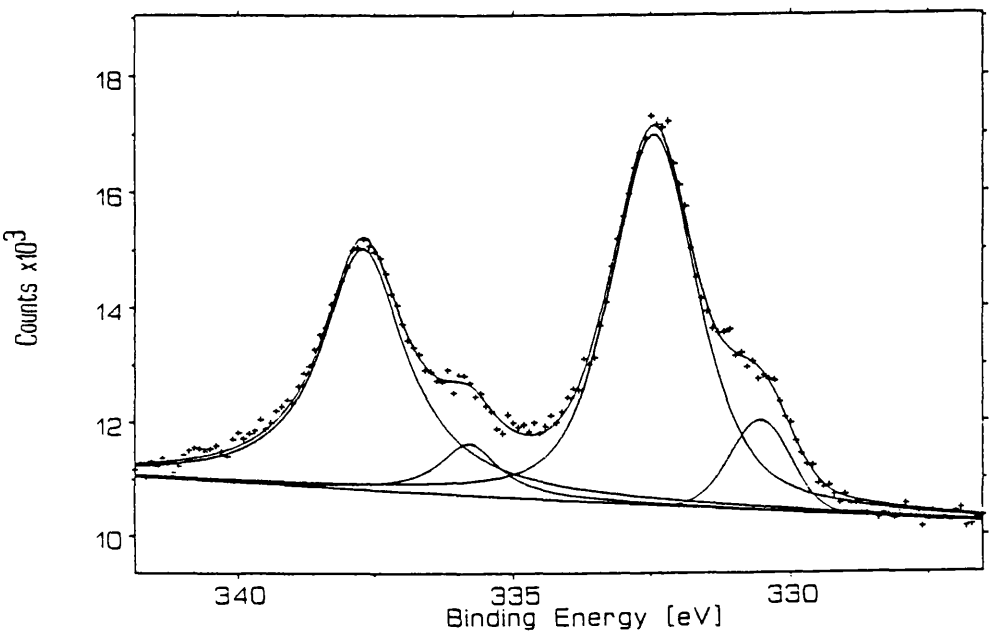

* The maximum peak binding energy values were corrected in each case to take account of surface charging. The corrected values are displayed in tables 4.44 - 4.46.

Fig 4.3 - [$Pd_2Cl_4(PMe_3)_2/SiO_2$] (active catalyst sample, 2 hour extraction, 135°C)

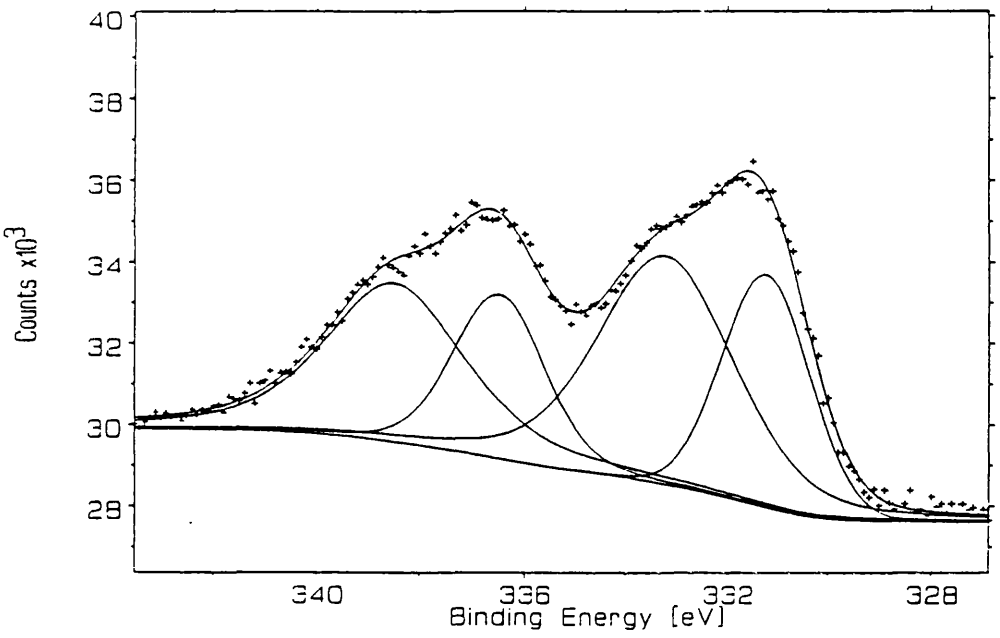

Fig 4.4 - [$Pd_2Cl_4(PMe_3)_2/SiO_2$] (deactivated catalyst, 48 hour extraction, 135°C)

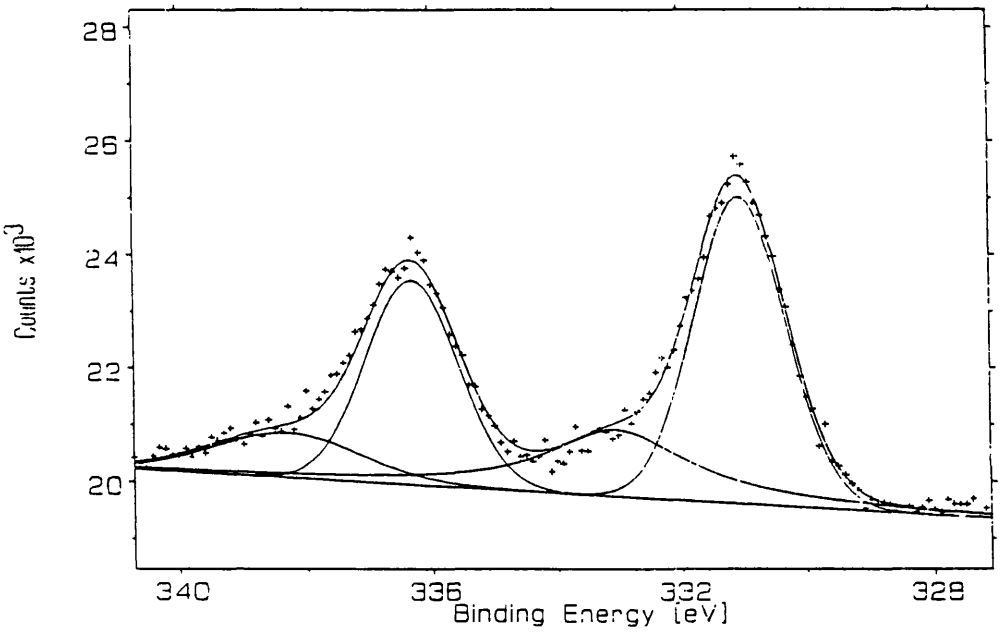

2. $[Pd_2Cl_4(PEt_3)_2/SiO_2]$

Table 4.45

Method of Preparation / time of extraction	XPS Signal	
	Pd 3d ½, ⅜	Cl 2p ⅜
Wet impregnation	337.2, 342.4 335.6, 340.8	198.3

($\Delta = 5.26 \pm 0.06$)

Fig 4.5 illustrates the peak fitted spectra of the wet impregnated precursor - $[Pd_2Cl_4(PEt_3)_2/SiO_2]$

Fig 4.5

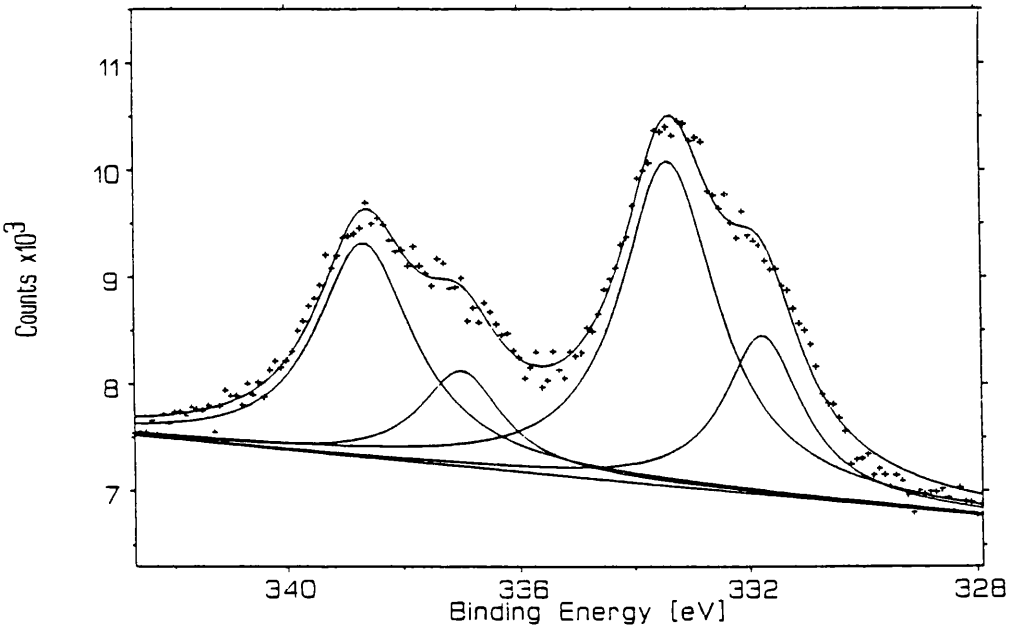

3. $[Pd_2Br_4(PMe_3)_2/SiO_2]$

Table 4.46

Method of Preparation/time of extraction	XPS Signal (eV) Pd 3d ½ ⅜	Br 3d (av)
Wet impregnation	337.7, 343.0	69.4
Dry mix	337.7, 343.0	69.4
Active catalyst phase [a]	336.7, 342.1	69.2
Deactivated catalyst phase [b]	337.4, 342.6 335.6, 337.4	69.1

[a] catalyst is extracted after 2 hours, from reaction mixture operating at a temperature of 95°C, filtered, and washed with diethyl ether.

[b] catalyst is extracted after 48 hours reaction, and treated as above.

The catalysts prepared from $[Pd_2Cl_4(PMe_3)_2/SiO_2]$ and $[Pd_2Cl_4(PEt_3)_2/SiO_2]$ both showed two signals in the palladium region of the recorded XPS spectra. For $[Pd_2Cl_4(PMe_3)_2/SiO_2]$, the Pd $3d^5/_2$ signal at 337.6 eV corresponded to Pd(II), whereas the signal at 335.7 was indicative of Pd(0) (86, 87), and the ratio of the two signals was 87:13, which indicated that although the complex was largely intact when supported on the silica, there did appear to be some decomposition. The same situation is observed for $[Pd_2Cl_4(PEt_3)_2/SiO_2]$, although the ratio of the signals was 71:29.

After 2 hours reaction at a temperature of 135°C, a sample of $[Pd_2Cl_4(PMe_3)_2/SiO_2]$ was extracted from the reaction vessel and examined.

Analysis of the Pd region of the XPS spectrum of this sample, again showed two signals. The signals were in the same position as for the wet impregnated catalyst, although their ratios had now changed to 63:37. The same was true for a sample of the catalyst extracted after 48 hours reaction, although at this point the proportion of the two signals was now 31:69. This indicated a conversion of Pd(II) to Pd(0) with reaction time. The chloride region of the XPS spectra recorded was also examined for the two catalysts discussed above. For both catalyst precursors, only one Cl 2p signal was observed. The position of this signal was observed at 198.2 eV for $[Pd_2Cl_4(PMe_3)_2/SiO_2]$ and at 198.3 eV for $[Pd_2Cl_4(PEt_3)_2/SiO_2]$. The Cl $2p_{3/2}$ signal for $[Pd_2Cl_4(PMe_3)_2/SiO_2]$ shifted by 0.6 eV at the activated stage and no signal was observed after 48 hours reaction.

For $[Pd_2Br_4(PMe_3)_2/SiO_2]$, only one Pd $3d^5/_2$ signal was observed for both the wet impregnated example and the catalyst prepared as a mechanical mix. The position of the signal was identical in both cases (337.7 eV) which indicated that the integrity of the complex was maintained on impregnation. This signal was found to shift by 1.0 eV, to 336.7eV upon activation. After 48 hours reaction, however, two signals were evident; one at 337.4 eV and the second at 335.6 eV. The ratio of the two signals was 63:37.

With regard to the bromide region, only one signal was observed for the $[Pd_2Br_4(PMe_3)_2/SiO_2]$ precursor and only a small shift in signal position was observed upon activation. The signal was observed at 63.4 eV for the precursor and moved 0.3 eV after 48 hours reaction. The recorded signal intensity at this point had decreased to almost a fifth of that observed in the wet impregnated precursor.

Chapter 5

DISCUSSION

5.1 INTRODUCTION

In this chapter the effects of catalysts prepared from silica supported palladium phosphine complexes - $[PdX_2(PMe_3)_2/SiO_2]$ (X=Cl, Br or I); and $[Pd_2X_4(PR_3)_2/SiO_2]$ (X=Cl, Br or I; R=Me, Et, Pr^i or Bu), on the hydrogenation of cinnamaldehyde, hydrocinnamaldehyde, cinnamyl alcohol and 2-cyclohexene-1-one are discussed. The reactions considered refer to the hydrogenation of 0.25 ml of substrate at reaction temperatures ranging from 70°C to 135°C in 25 ml of either decalin or heptane.

Comparisons were made between the products formed from the hydrogenation of cinnamaldehyde over a $[Pd/SiO_2]$ catalyst, with the products formed from use of the supported palladium phosphine catalysts.

The hydrogenation of cinnamaldehyde gives rise to three likely products, namely hydrocinnamaldehyde, cinnamyl alcohol and phenyl propanol. No cinnamyl alcohol was detected as a product for any of the catalysts studied. The SiO_2 itself and $[PMe_3H]Br$ on silica were confirmed to be catalytically inactive under the same conditions.

The hydrogenation of cinnamaldehyde over a series of silica supported copper and modified copper catalysts has been investigated by Chambers (38). In these studies, cinnamyl alcohol, hydrocinnamaldehyde and phenyl propanol were all formed. The proportions of the products formed were shown to depend on the nature of the catalyst. In all cases cinnamaldehyde was hydrogenated exclusively to hydrocinnamaldehyde during the initial stages of reaction and it was believed that the hydrocinnamaldehyde molecules thus formed were retained in part at the catalyst surface. As a result of this retention, it was argued that the catalyst surface may have

been modified in such a way as to promote the hydrogenation of unreacted cinnamaldehyde molecules to cinnamyl alcohol. This was ascribed to the result of steric effects by which cinnamaldehyde molecules were forced to adsorb through the C=O and also through a modifying ligand effect in which the charge density on the active site was increased, thus reducing the propensity of C=C bond activation.

These effects were not observed in the course of this study and any surface modification occurring on the catalysts prepared from $[PdX_2(PMe_3)_2/SiO_2]$ and $[Pd_2X_4(PR_3)_2/SiO_2]$ was different from that of the copper catalysts.

5.2 Catalyst Behaviour Profiles

The catalysts prepared from $[Pd_2X_4(PR_3)_2/SiO_2]$, fall into three distinct behaviour categories on the basis of their composition, reactivity and selectivities in the hydrogenation of cinnamaldehyde. These are:

1. Palladium/silica catalyst,

2. Catalysts prepared from the supported binuclear bromo- and iodo-palladium phosphine complexes, and

3. Catalysts prepared from the supported binuclear chloro-palladium phosphine complexes

The activities and selectivities of the catalysts prepared from the supported mononuclear complexes, $[PdX_2(PMe_3)_2/SiO_2]$, and the behaviour of catalysts prepared from the reaction of supported binuclear bromo-complexes with 2-cyclohexene-1-one are also discussed. Each category is addressed in turn.

5.3 Palladium/Silica Catalyst

The hydrogenation of cinnamaldehyde, hydrocinnamaldehyde and cinnamyl alcohol have each been studied. Cinnamaldehyde reacted sequentially to form hydrocinnamaldehyde and then phenylpropanol, probably at the same sites and with no induction period observed even at the lower reaction temperature of 100°C (table 4.1). 100 % phenylpropanol was formed after 48 hours reaction at 135°C (table 4.2). Cinnamyl alcohol reacted after an induction period of approximately 30 minutes (at 95°C) to form both hydrocinnamaldehyde by isomerisation and phenylpropanol by hydrogenation (table 4.28). During the early stages of reaction, the rate of production of hydrocinnamaldehyde exceeded that of phenylpropanol. The rate of production of hydrocinnamaldehyde from cinnamyl alcohol declined after about 1 hour (95°C) and the remaining cinnamyl alcohol was slowly but steadily converted to phenylpropanol. The hydrogenation of hydrocinnamaldehyde to phenylpropanol over a [Pd/SiO_2] catalyst required a long induction period before the reaction slowly proceeded (table 4.27), and no hydrogenation was observed up to 80 minutes (at 135°C) after the cinnamaldehyde and hydrogen gas were introduced to the reactor system. The difference in induction period for the hydrogenation of hydrocinnamaldehyde can be understood in terms of the greater affinity of palladium for C=C bonds than for C=O. As a result, strong interactions with $PhCH{=}CHCHO$ and $PhCH{=}CHCH_2OH$ can lead to rapid surface activation. This activation process is thought to occur through the formation of a hydrocarbonaceous over-layer. Modification of metal surfaces by the formation of such layers has been postulated by Webb (84). A sample of the used catalyst (reacted at 135°C), after being washed in diethyl ether and dried, was found to contain 3.91 % C and 0.82 % H,

which showed that some of the cinnamaldehyde must have been deposited on the surface of the catalyst. Mass balance calculations showed that 7.2 ± 0.2 % of the total amount of cinnamaldehyde was used to form this layer (table 4.36b).

The active sites formed from the contact of a [Pd/SiO_2] catalyst and hydrocinnamaldehyde appear to be different from those formed on contact with cinnamaldehyde. This may occur due to a weaker hydrocinnamaldehyde-metal interaction, although there is also the possibility that the sites thus formed are simply fewer in number, resulting in a lower rate of reaction.

The isomerisation and hydrogenation reactions undergone by cinnamyl alcohol appear to proceed at different sites. The two processes began after a similar induction period, but the formation of hydrocinnamaldehyde declined whilst the production of phenylpropanol continued. This indicated that the isomerisation sites were rapidly deactivated. The high rate of formation of phenylpropanol from the hydrogenation of cinnamyl alcohol indicated that the formation of cinnamyl alcohol followed by its subsequent rapid isomerism to hydrocinnamaldehyde was not an intermediary step in the hydrogenation of cinnamaldehyde. The possibility of the interaction of cinnamyl alcohol with palladium leading to the production of active sites which are different from those formed from the interaction of cinnamaldehyde could not be ruled out, however.

The type of palladium precursor used in the production of the [Pd/SiO_2] catalyst did not seem to be critical. A catalyst formed from the calcination at 250°C of [$Pd_2Cl_4(PMe_3)_2/SiO_2$] followed by reduction at 200°C, showed similar activities and selectivities in the hydrogenation of cinnamaldehyde

to a [Pd/SiO_2] catalyst prepared from [$Pd(NO_3)_2/SiO_2$]. This indicated that under the calcination/reduction conditions used, all the phosphine and chloride were removed. Microanalysis of the used catalyst confirmed the absence of chloride, and thermogravimetric measurements confirmed that the total weight loss from a [$Pd_2Cl_4(PMe_3)_2/SiO_2$] precursor (in a 100 % hydrogen atmosphere) occurred prior to the maximum calcination temperature of 250°C. A catalyst prepared from [$PdCl_2/SiO_2$] also behaved in the same way towards the hydrogenation of cinnamaldehyde (table 4.3).

The preferential hydrogenation of C=C bonds by palladium was expected since palladium catalysts have long been used to adsorb selectively and reduce alkenes. Cinnamaldehyde has been shown to co-ordinate through C=C only in the platinum(0) complex [$Pt(PhCH=CHCHO)(PPh_3)_2$] (85), and it is likely that palladium would behave in a similar manner.

Rate constants k, were measured for several of the reactions (table 4.36a), and the fastest reaction rate (at 95°C), was obtained from the palladium-on-silica catalyst. The reason for the difference in reaction rate may possibly be attributed to a particle size effect, although care must be exercised with this assumption, however, as data regarding palladium particle sizes of the [Pd/SiO_2] catalyst was not obtained. It is also likely that the observed rate occurs as a result of the absence of catalyst poisons such as halide ions and phosphines.

5.4 Catalysts Prepared from Supported Binuclear Bromo- and Iodo-Palladium Phosphine Complexes

This class of catalyst was highly selective in the hydrogenation of cinnamaldehyde to hydrocinnamaldehyde in the liquid phase, with the bromo-catalysts proving to be particularly active. No phenylpropanol was produced from any of these catalysts at reaction times up to 72 hours.

5.4.1 Supported Binuclear Bromo- and Iodo-Catalyst Precursors

The precursors were prepared by a wet impregnation technique, to give a 5 % palladium loading. The experimental procedure is detailed in section 3.3. Atomic absorption analysis proved to be ineffective as an analytical method of confirming the palladium loading. Heating a representative selection of catalyst precursors at temperatures up to 70°C for 24 hours in concentrated nitric acid appeared to extract less than half of the palladium into solution. Analysis of the extracted solution by atomic absorption gave a palladium concentration of just 2 %. Neutron activation analysis was therefore used to estimate the palladium content. $[Pd_2Br_4(PMe_3)_2/SiO_2]$ was chosen as a representative precursor and the analysis indicated a palladium content of 4.5 % (table 4.43). The 0.5 % deviation from the expected value was possibly due to the presence of adsorbed water on the silica surface as well as a non uniform distribution of palladium in the samples used for standardisation.

X-ray photoelectron spectroscopy (XPS), solid state ^{31}P magic angle spinning NMR spectroscopy (MAS-NMR) and microanalysis (M/A) confirmed that the complexes were retained intact upon impregnation onto silica.

The palladium region of the XPS spectra was recorded for the catalyst precursor [$Pd_2Br_4(PMe_3)_2/SiO_2$], prepared both by wet impregnation and by mechanically mixing the complex with silica (table 4.46). A single Pd $3d^5/_2$ signal was observed in both cases. The position of this signal was recorded at 337.7 eV in both examples and was indicative of a Pd(II)-containing material (86, 87). Investigation of the bromide region showed a single Br $3d^5/_2$ signal, again for both samples. This signal was observed at 69.4 eV.

Solid state ^{31}P MAS-NMR spectra were then recorded for [$Pd_2Br_4(PMe_3)_2/SiO_2$]. No differences were observed between the precursor prepared by wet impregnation and the precursor prepared as a mechanical mixture. In each case only one signal was recorded, and this was observed at chemical shift values of 14.7 ppm and 15.2 ppm respectively. In each case the presence of a single resonance indicated that the phosphorus atoms were present in only one type of chemical environment. In view of the close proximity of these signals, it appeared that the complex retained its integrity upon impregnation, and, in the absence of any other resonances, it appeared to do so with no decomposition. The catalyst precursor [$Pd_2Br_4(PEt_3)_2/SiO_2$] prepared by wet impregnation was also investigated. A single signal was observed at 54.5 ppm, and it appeared therefore that this complex also retained its integrity when supported on silica.

The colours of all the complexes examined varied from light yellow to deep orange and the same colours were observed in the precursors upon impregnation. Microanalyses on these yellow or orange materials showed C, H, halogen, and phosphorus values consistent with a 5 % palladium loading (table 4.41). The analytical values for hydrogen were all about 0.5 % higher than calculated and these discrepancies were attributed to the

presence of surface silanol groups on the silica. Transmission electron micrographs (TEM) of a $[Pd_2Br_4(PMe_3)_2/SiO_2]$ precursor showed that, based on the measurement of 100 particles, the mean particle size was 4.7 ± 0.2 nm and the standard deviation on this measurement was 1.7 nm The range of sizes examined varied between 2.9 nm and 8.1 nm.

5.4.2 Catalyst Activation - Supported Binuclear Bromo- and Iodo-Catalysts

The active catalysts were produced by the hydrogen reduction of $[Pd_2Br_4(PR_3)_2/SiO_2]$ and $[Pd_2I_4(PR_3)_2/SiO_2]$ in the presence of cinnamaldehyde at temperatures between 70° and 135°C. An induction period was observed, however, prior to hydrogenation. This induction period was related to the formation of a hydrocarbonaceous over-layer on the catalyst surface. Mass balance calculations indicated that for catalysts prepared from $[Pd_2Br_4(PMe_3)_2/SiO_2]$ and $[Pd_2Br_4(PBu_3)_2/SiO_2]$, 7.1 ± 0.2 % and 11.6 ± 0.3 % respectively, of the cinnamaldehyde substrate contributed to the formation of this layer (table 4.36b). Elevated C and H % values obtained by microanalysis for a sample of $[Pd_2Br_4(PMe_3)_2/SiO_2]$ extracted after 2 hours reaction at 95°C, were consistent with the formation of such a hydrocarbonaceous over-layer.

The catalyst precursors did not change in appearance with the introduction of the solvent or cinnamaldehyde at temperatures up to 135°C. The introduction of hydrogen gas, however, immediately caused the materials to turn black, even at temperatures as low as 70°C, producing the active catalysts. The sequence of addition of cinnamaldehyde and hydrogen was critical. Experiments testing the sensitivity of this timing were carried out using a catalyst prepared from $[Pd_2Br_4(PMe_3)_2/SiO_2]$. When the catalyst was

pre-treated for 30 minutes with hydrogen (table 4.33), a marked reduction in catalyst activity was observed. No reduction in activity was observed when the catalyst was pre-treated with cinnamaldehyde (table 4.32). This indicated that cinnamaldehyde was required to modify the surface of the catalyst and that pre-reduction with hydrogen in the absence of cinnamaldehyde led to the formation of a less active catalyst.

The method of precursor preparation did not seem to affect either the rate of reaction or its selectivity. A $[Pd_2Br_4(PEt_3)_2/SiO_2]$ precursor prepared by wet impregnation (table 4.19) and one prepared by mechanically mixing the complex with silica (table 4.20), were both found to be 100 % selective to hydrocinnamaldehyde only and had comparable reaction rates at 135°C. When an unsupported $[Pd_2Br_4(PMe_3)_2]$ complex was used, however, the catalyst formed, whilst still retaining its selectivity towards hydrocinnamaldehyde (table 4.26), was found to be much less active than the supported analogue (table 4.17). The unsupported complex changed colour from orange to black upon activation, but the solution itself remained colourless and fine particles of the catalytic material were observed at the end of the reaction. This indicated that no homogeneous catalytic reaction was occurring. The catalytic material formed from the unsupported complex was therefore acting as a heterogeneous catalyst only and the difference in activity can be compared with the 'heterogenisation' of homogeneous catalysts (11). By supporting the 'free' complexes onto a variety of high surface area inorganic supports, considerable increases in catalyst activity have be achieved (18).

In an attempt to elucidate the nature of the mechanism responsible for the selectivity observed, a series of experiments was performed in which hydrocinnamaldehyde and cinnamyl alcohol were used. The precursors examined are detailed in table 4.29. In each case no reaction occurred with the hydrocinnamaldehyde. Cinnamyl alcohol, however, was rapidly converted to phenylpropanol (table 4.30-footnote), so the formation of cinnamyl alcohol followed by isomerism to hydrocinnamaldehyde does not contribute to the mechanism.

Upon catalyst activation, the colour of the catalyst precursors changed from orange/yellow to black. The difference in selectivity between the catalysts resulting from supported binuclear bromo- and iodo-complexes and the palladium-on-silica catalyst described previously, indicated that although the chemical identity of these precursors was clearly altered, decomposition of the palladium(II) complex to form palladium metal would not explain the reaction products formed, or fit the analytical evidence.

X-ray photoelectron spectroscopy (XPS) was used primarily to investigate changes in the oxidation state of palladium with reaction time. A catalyst prepared from $[Pd_2Br_4(PMe_3)_2/SiO_2]$ was examined. After 2 hours reaction at 95°C, the Pd $3d^5/_2$ signal was found to shift from the precursor value of 337.7 eV to 336.7 eV. Since palladium(I) species are rare and since the new value recorded was 1.0 eV away for the value expected for Pd(0), it is very likely that at this stage the oxidation state of palladium in the activated catalyst sample was still +2 (86, 87). The 1.0 eV downward shift may therefore be the result of a decrease in electron density at the metal. The intensity of this signal was recorded at 25 % of the value obtained in the wet-impregnated precursor. Since XPS is a surface sensitive technique, this

result was consistent with the formation of a hydrocarbonaceous over-layer which covered the catalyst. For the bromide region, a single Br $3d^5/_2$ signal was recorded. The position of this signal at 69.2 eV, remained essentially unmoved from the value observed in the precursor, but there was a dramatic reduction in signal intensity which was again consistent with the formation of an over-layer. By this stage it had dropped to 11.2 % of the initial recorded value. A solid state ^{31}P MAS-NMR spectrum of a similar activated catalyst system was obtained for a sample which had been extracted from the reaction mixture after 30 minutes. A single signal was observed at 52.8 ppm, 32.4 ppm upfield from the wet-impregnated precursor value. Analysis of a second sample extracted after 2 hours showed a single signal at 53.1 ppm. This indicated that after the initial activation process there was essentially no change in the chemical identity of the associated phosphorus species after several hours reaction. The procedure resulting in the activation of the $[Pd_2Br_4(PMe_3)_2/SiO_2]$ precursor, whilst clearly altering the chemical identity of the phosphine, did so 'cleanly' at this stage with 100 % conversion of the precursor to the active species and with only one type of phosphorus present.

Microanalysis has shown that over the course of a reaction a considerable amount of phosphorus was lost. Some of the phosphorus being lost may be in the form of the free phosphine. Minor peaks were observed in the gas chromatographic trace of the products and these peaks were shown to correspond to the retention times of R_3P (R= Me or Et).

Transmission electron microscopy (TEM) was used to analyse a sample of a catalyst prepared from $[Pd_2Br_4(PMe_3)_2/SiO_2]$, which had been extracted after 3 hours reaction at 135°C. The micrographs obtained showed

clustering of metal particles to form aggregates, with particle sizes ranging between 10.0 - 39.0 nm. The mean value was calculated at 20.5 ± 1.0 nm based on the measurement of 25 particles, with a standard deviation of 8.4 nm. Clusters up to 170 ± 9 nm were also observed.

When comparing catalysts prepared from the supported and unsupported precursors, considerable differences in activity were observed. The supported precursors made far more active catalysts than their unsupported analogues. This may be due to several reasons. Impregnation of the complex onto a high surface area support such as silica would result in a greater dispersion of the complex. The large surface area may also help provide a template on which the hydrocarbonaceous over-layer may form. Separate experiments have shown silica to be catalytically inactive under the conditions used in this study and the support can be said to play a passive rather than an active role.

Silica can be thought of as a covalent solid and the contribution of the electrostatic energy to the total crystal energy is negligible. In short, the surface has a homopolar character, which means any interactions which may occur between the surface and substrate molecules are generally weak. The use of ionic supports such as TiO_2 and alumina, have shown that the support can act as a 'sink' for catalytic poisons (88). For less polar oxides such as silica this likely to occur to a lesser extent. The activities of all the catalysts examined in this study were all the more remarkable therefore, in view of the ability of phosphines and halogens to act as catalyst poisons (89).

5.4.3 Catalyst Deactivation - Supported Binuclear Bromo- and Iodo-Catalysts

All of the catalysts examined in this study appeared to be deactivated with prolonged or repeated use (table 4.31). A representative selection of the catalysts examined in this study were analysed after 48 hours reaction to investigate the nature of this process.

Microanalysis of some of the silica-supported catalysts showed that a substantial proportion of the bromide and phosphorus available in the precursors was retained by the catalysts after several hours reaction. A catalyst prepared from $[Pd_2Br_4(PMe_3)_2/SiO_2]$ retained 51 % bromide and 37 % phosphorus after 48 hours reaction at 95°C (table 4.42), whereas a catalyst prepared from $[Pd_2I_4(PMe_3)_2/SiO_2]$, retained over 88 % of its iodide content after 48 hours reaction at 135°C (table 4.44). The percentage of retained halide for the catalysts prepared from both these precursors was considerably higher than for the chloro-analogue. This difference may reflect the higher nucleophilicity of bromide and iodide ions for palladium (90).

XPS analysis of a catalyst prepared from $[Pd_2Br_4(PMe_3)_2/SiO_2]$ showed that after 48 hours reaction at 135°C, two Pd $3d^5/_2$ signals were evident; one at 337.4 eV and the second at 335.6 eV. The first signal was again indicative of a Pd(II)-containing material, whereas the second signal position corresponded to Pd(0) (86, 87). This second signal was not observed in the activated catalyst. The ratio of these two signals was 63:37. On the basis of this evidence it seemed likely therefore, that Pd(II) was being converted to Pd(0) as the reaction progressed. The total intensity of the palladium signals recorded at this point had reduced to 17.9 %. Presumably, this

reduction in overall signal intensity (from 25 % in the active sample to 17.9 % in the deactivated sample) resulted from a non uniform coverage of the surface by the hydrocarbonaceous over-layer. The bromide region of the XPS spectrum again showed a single Br $3d^5/_2$ signal with a shift value of 69.1 eV. This was essentially unchanged from the values found for both the precursor and the active catalyst. The signal, however, only possessed 10.1 % of its initial intensity, again as the result of the hydrocarbonaceous over-layer. A Solid State ^{31}P MAS-NMR spectrum was recorded for the same sample. Two ^{31}P signals were observed. The first at 53.6 ppm corresponded to the 52.8 ppm signal of the active catalyst. The second signal observed at 31.2 ppm, did not correspond to any of the signals recorded for either the precursor or the active sample. It was possible that hydrogen reduction of the supported complexes had produced a phosphonium species of the type $[PR_3H]^+$. The ratio of the two signals observed for the deactivated catalyst sample, was shown to be 7:3, which indicated that the catalyst, over a period of time was being converted, first into an active species, and, as the reaction proceeded, surface restructuring, or modification of the active site resulted in the deactivation of this site with a corresponding change in the chemical identity of the associated phosphorus atoms. Some of this retained phosphorus is therefore likely to be in the form of $[PR_3H]^+$ (or a derivative thereof), shown to be inactive by itself.

From these results, it appeared that there was only one type of phosphorus in the active catalyst and that the phosphonium species (or derivative) observed in the deactivated catalyst originated from this active species. This, along with the XPS evidence would suggest that at the active stage at least some of the phosphine and halide ligands were still attached to

palladium. Catalysts prepared from the iodo-complexes show the same selectivity as the bromo-complexes but were much less active. This reinforces the idea that some of the ligands remain in contact with the active site. The lower activity of the iodo-complexes was possibly due to the fact that iodide ligands are known to be stronger catalyst poisons than either bromide or chloride (91), although it may also reflect the larger amount of halide retained. There is also some evidence that the organic substituents were retained on the phosphorus since the reaction rates varied in the sequence $Pr^i > Bu > Et > Me$ (table 4.36). This was a steric rather than an electronic effect, since the electronic parameters of the four phosphine ligands vary only slightly (92). Therefore, upon catalyst activation, removal of some of the bulkier phosphine ligands may allow for easier approach of cinnamaldehyde molecules and provide less hindrance to desorbing hydrocinnamaldehyde molecules. Interestingly, the large steric effects exerted by the halide ligands appear to operate in the opposite direction with the larger ions slowing the reactions.

It is likely therefore, that these catalysts operate through one type of active site which was capable of converting cinnamaldehyde to hydrocinnamaldehyde and cinnamyl alcohol to phenylpropanol, although it was possible that the sites formed upon interaction with cinnamaldehyde were different from those formed with cinnamyl alcohol. Whilst this again demonstrates the preference of palladium for C=C bond co-ordination and reduction, these sites are clearly different from those of the [Pd/SiO_2] catalyst discussed previously, which were also able to convert hydrocinnamaldehyde to phenylpropanol. The presence of phosphine appeared to be required for selectivity to be maintained, since catalysts formed from the reduction of [$PdBr_2/SiO_2$], although differing in activity to

those produced from [Pd/SiO_2] or [$PdCl_2/SiO_2$], produced some phenylpropanol as well as hydrocinnamaldehyde (table 4.4).

Given the nature of the system, the formation of an intermediary palladium hydride species seemed to be likely. Hydridopalladium complexes are not very robust and any palladium hydride species formed on treatment of the [$Pd_2X_4(PR_3)_2/SiO_2$] precursors with hydrogen would be unlikely to remain intact under the reaction conditions used. The Pd-H species thus formed, would be able to 'insert' into the C=C functionality of the cinnamaldehyde molecule, effectively reducing it. Upon decomposition of this hydridopalladium species, HX and/or $[PR_3H]^+X^-$ are likely to be the initial elimination products, which would result in the formal reduction of palladium.

5.5 Catalysts Prepared from the Supported Binuclear Chloro-Palladium Phosphine Complexes

This class of catalyst produced phenylpropanol as well as hydrocinnamaldehyde in the liquid phase hydrogenation of cinnamaldehyde. In this regard the supported binuclear chloro-catalysts behaved in the same way as [Pd/SiO_2]. Reaction rates over these catalysts were slower than for [Pd/SiO_2], however, and the ratio and sequence of product formation also differed.

5.5.1 Supported Binuclear Chloro-Catalyst Precursors

The supported binuclear chloro-catalyst precursors were prepared in the same way as for the bromo- and iodo- analogues by wet impregnation methods. Details of the preparation method are given in section 3.3. The

precursors were analysed by X-ray photoelectron spectroscopy (XPS), and microanalyses (M/A).

XPS analysis of the precursors prepared from [$Pd_2Cl_4(PMe_3)_2/SiO_2$] and [$Pd_2Cl_4(PEt_3)_2/SiO_2$] indicated that some decomposition occurred upon impregnation. The complexes themselves were air stable, and no decomposition was observed when they were prepared and analysed. Each precursor exhibited two Pd $3d^5/_2$ signals (table 4.45). With respect to [$Pd_2Cl_4(PMe_3)_2/SiO_2$], the Pd $3d^5/_2$ signals were observed at 337.6 eV and 335.7 eV and corresponded to Pd(II) and Pd(0) respectively (86, 87). The ratio of areas of the two signals was 87:13. A similar situation was observed for [$Pd_2Cl_4(PEt_3)_2/SiO_2$], with two Pd $3d^5/_2$ signals observed at 337.2 eV and 335.6 eV (table 4.46). In this case the ratio of the signals was 71:29. This decomposition to Pd(0) upon impregnation did not occur for the supported bromo-catalyst precursors. A narrow energy scan was performed on the chloride region of both supported chloro-catalyst precursors (table 4.45). In each case only one signal was observed. The Cl $2p^3/_2$ peak was observed at 198.2 eV for [$Pd_2Cl_4(PMe_3)_2/SiO_2$], and at 198.3 eV for [$Pd_2Cl_4(PEt_3)_2/SiO_2$)].

Microanalysis of the catalyst precursors did not show decreased levels of C, H or halide and the colour of the precursors did not indicate any decomposition. Presumably therefore, any decomposition products were retained on the support. The preservation of the colour of the complexes appeared to indicate that any metallic palladium formed must have been finely dispersed over the surface.

5.5.2 Catalyst Activation - Supported Binuclear Chloro-Catalysts

The active catalysts were formed from the hydrogen reduction of the precursors [$Pd_2Cl_4(PR_3)_2/SiO_2$)], at temperatures ranging from 70-135°C in the presence of cinnamaldehyde. Hydrogen reduction was accompanied by a change in the colour of the precursor from yellow/orange to black. In this regard, the activation process mirrored that of the supported bromo-catalysts. Both of the binuclear-chloro catalyst precursors examined also required an induction period prior to hydrogenation. This again indicated the formation of a hydrocarbonaceous over-layer. Mass balance calculations showed that 8.2 ± 0.2 % of the initial amount of cinnamaldehyde for the catalyst prepared from [$Pd_2Cl_4(PMe_3)_2/SiO_2$)], and 11.0 ± 0.3 % for the catalyst prepared from [$Pd_2Cl_4(PEt_3)_2/SiO_2$)] contributed to the formation of this layer at 135°C (table 4.36b). Microanalyses of samples of a catalyst prepared from [$Pd_2Cl_4(PMe_3)_2/SiO_2$)] at 95°C, indicated that the proportion of carbon on the catalyst surface steadily increased during the first 90 minutes of reaction (table 4.41). A sample extracted after 48 hours, however, showed no further increase in the C %. The initial increase occurred presumably as a result of the formation of the hydrocarbonaceous over-layer, which was completed after 90 minutes. After this layer was formed the hydrogenation rate appeared to accelerate.

A catalyst prepared from unsupported [$Pd_2Cl_4(PMe_3)_2$] also required an induction period. This induction period took several hours longer than for the supported analogue, however, even at the higher reaction temperature of 135°C. This was presumably due to the absence of a support which could have acted as a template for the formation of the hydrocarbonaceous over-layer. The supported and unsupported chloro-catalysts produced both

hydrocinnamaldehyde and phenylpropanol. In each case a substantial amount of hydrocinnamaldehyde formed before any phenylpropanol was observed and formation of the phenylpropanol stopped before hydrogenation of cinnamaldehyde was complete. New catalysts did not reduce hydrocinnamaldehyde to phenylpropanol (table 4.29), although this may be the result of a different surface modification in the absence of cinnamaldehyde. Cinnamyl alcohol, however, was partially hydrogenated to phenylpropanol using a catalyst prepared from $[Pd_2Cl_4(PMe_3)_2/SiO_2]$ at 135°C (table 4.30), but most was isomerised to hydrocinnamaldehyde. This was different from a catalyst formed by the reaction of $[Pd/SiO_2]$ at 95°C with cinnamyl alcohol in which the hydrogenation of cinnamyl alcohol to form phenylpropanol was the major reaction (table 4.28). Although differences in the rates of reaction for these two catalyst systems can perhaps be ascribed to differences in temperature, it is likely that the presence of chloride also had an effect in view of the fact that metal halides such as ferric chloride and stannic chloride, and strong acids such as $HCl/AlCl_3$ are known to promote isomerism reactions (93, 94).

X-ray photoelectron spectroscopy (XPS) was used to examine a sample of a catalyst prepared from $[Pd_2Cl_4(PMe_3)_2/SiO_2]$ after 2 hours reaction at 135°C. Analysis of the palladium region showed the presence of two Pd $3d^5/_2$ signals at 337.1eV and 335.1eV, which corresponded to Pd(II) and Pd(0) respectively (86, 87). The ratio of Pd(II) to Pd(0) was shown to be 63:37. This was significantly different from the ratio observed in the precursor and the proportion of Pd(0) was shown to increase considerably with reaction time. The intensity of the palladium signals, however, had decreased to 56.6 %. A narrow energy scan performed on the chloride region showed the presence of only one Cl $2p^3/_2$ signal. This was observed

at 198.8 eV. The 0.6 eV shift from the precursor signal was attributed to the low signal intensity and irregular peak shape which made determination of the mean signal position difficult. The Cl $2p^3/_2$ signal intensity was 37.8 % of the precursor value. This fall in intensity was again attributed to the catalyst being 'buried' under a hydrocarbonaceous over-layer.

In an attempt to investigate particle sizes of a typical chloro-catalyst, transmission electron microscopy (TEM) was used. A sample of $[Pd_2Cl_4(PMe_3)_2/SiO_2]$ was extracted from a reaction mixture after 2 hours at 135°C and micrographs were obtained. Metal particles in the range of 6.1 - 41.5 nm were observed. Measurement of 100 such particles gave a mean value of 22.5 ± 1.1 nm with a standard deviation of 7.03 nm. Clusters of particles of up to 133 ± 7 nm were, however, also observed. This particle aggregation was also observed for the analogous supported bromo-catalyst, with a similar wide range of particle sizes observed after activation. It appeared therefore, that the differences in rate between the catalysts prepared from the supported binuclear bromo- and chloro-catalysts were attributable to differences in chemical composition and not particle size.

5.5.3 Catalyst Deactivation - Supported Binuclear Chloro-Catalysts

Samples were obtained from the hydrogenation reactions of the catalysts prepared from $[Pd_2Cl_4(PMe_3)_2/SiO_2]$ and $[Pd_2Cl_4(PEt_3)_2/SiO_2]$ with cinnamaldehyde at 95°C. After 48 hours reaction, microanalysis showed that the catalysts had retained 32.9 % and 30.1 %, respectively of their original Cl content (table 4.41). This compared with 50.9 % bromide retention from $[Pd_2Br_4(PMe_3)_2/SiO_2]$ and 88.3 % iodide retention from $[Pd_2I_4(PMe_3)_2/SiO_2]$ (after reaction at 135°C). The phosphorus content for

the catalyst prepared from $[Pd_2Cl_4(PMe_3)_2/SiO_2]$ was, however, similar to that observed from $[Pd_2Br_4(PMe_3)_2/SiO_2]$. Microanalyses showed the % P retained for the chloro-catalyst was 38.4 %, whereas for the same reaction, the bromo-catalyst retained 33.1 %. The lower chloride content observed for this class of catalysts might be expected, as chloride is a poorer nucleophile towards palladium than bromide or iodide (90).

XPS was used to examine a catalyst prepared from $[Pd_2Cl_4(PMe_3)_2/SiO_2]$, after 48 hours reaction at 135°C. Two Pd $3d^5/_2$ signals were again observed, which corresponded to Pd(II) and Pd(0) respectively (86, 87). The chemical shift values of the signals were 336.6 eV and 334.6 eV, and the signal ratio was now observed to be 31:69. These palladium signals were observed at 38.8 % of the original intensity recorded for the precursor and extended scans failed to detect the presence of chloride. Once again the decrease in observed signal intensity is due to the hydrocarbonaceous over-layer. The complete absence of the Cl $2p^3/_2$ signal, however, was probably connected to the lower percentage of chloride retained in the used chloro-catalyst samples.

Given the nature of the system, it was likely that the halide was being lost as HX, and the phosphine as $[PR_3H]^+$ in the same way as for the analogous bromo- and iodo-catalysts. The catalysts formed from the chloro-precursors appeared to be less stable than the bromo-analogues, however. For a catalyst precursor prepared from $[Pd_2Cl_4(PMe_3)_2/SiO_2]$, partial decomposition to Pd(0) was shown to occur upon impregnation and halide/phosphine loss during the reaction led to the formation of an increasing amount of Pd(0) with time. Pd(0) was not observed until much later in the reaction for the analogous bromo-catalyst. An interesting

comparison can be made to the work of Drago *et al* (95), where a series of metal complexes with the formulae $[(C_6H_5CN)_2PdCl_2]$ were supported on polystyrene-2,2-bipyridine, to give $[[P]\text{-}bpyPdCl_2]$ and these precursors were used in the hydrogenation of substrates including 1-hexene, p-benzoquinone and nitrobenzene. The conclusions of this work indicated that the hydrogenation of these reactants occurred as a result of catalysis by a mixture of ($[P]\text{-}bpyPdCl_2$) and palladium metal. This was consistent with the observations regarding cinnamaldehyde hydrogenation for the binuclear chloro-catalysts used in this study.

It is likely therefore, that at least two types of active sites operate in these chloro-catalysts in the presence of cinnamaldehyde. One type was probably analogous to that which operates selectively in the bromo- and iodo-catalysts and was responsible for the production of most (although perhaps not all) of the hydrocinnamaldehyde. The second type was responsible for the production of phenylpropanol. This site required a longer induction period than the first before becoming active and was deactivated more rapidly. There are three possible modes of operation for this second site. It may produce phenylpropanol directly from cinnamaldehyde from a single visit to the catalyst. The diminished amount of halide in the catalyst may permit the simultaneous co-ordination of a cinnamaldehyde molecule through both the C=C and C=O, which was then hydrogenated prior to desorption. Secondly, this site type may produce cinnamyl alcohol, some of which is rapidly further hydrogenated and the rest of which is isomerised to hydrocinnamaldehyde. Third, the sites could be the same as those produced on $[Pd/SiO_2]$.

Pd(0) was presumably the active species in the catalyst [Pd/SiO_2], therefore, the formation of Pd(0) itself was not responsible for the loss of activity in the binuclear catalysts. The relative stability of the binuclear catalysts and the extent to which displaced halide and phosphine ligands act as poisons must, therefore, determine the activity and selectivity instead. From the TEM studies, it also appears likely that the extensive metal particle aggregation which was observed for catalysts prepared from [$Pd_2Cl_4(PMe_3)_2/SiO_2$] and [$Pd_2Br_4(PMe_3)_2/SiO_2$] over the course of a typical reaction with cinnamaldehyde at 135°C, was also responsible for their deactivation.

5.6 Catalysts Prepared from the Supported Mononuclear Complexes

The catalysts formed from the supported mononuclear complexes were selective for hydrocinnamaldehyde, although differences in activity were observed. In each case no phenylpropanol was produced.

5.6.1 The Supported Mononuclear Precursors

The supported mononuclear catalyst precursors were prepared by wet impregnation in the same way as for the binuclear analogues. Details of the preparation method are given in section 3.3.

Microanalyses of the catalyst precursors indicated that the amount of C, H and halogen present was consistent with expected values. For the precursor [$PdBr_2(PMe_3)_2/SiO_2$], however, solid state ^{31}P MAS-NMR spectroscopy indicated the presence of three phosphorus-containing species. The largest signal at - 16.7 ppm corresponded with the ^{31}P value obtained from the complex in solution. However, other signals were also observed at 0.4 ppm and 4.7 ppm. One of these values could conceivably be the cis complex which has a solution ^{31}P signal at -1.7, but the other appeared to be a

phosphorus containing decomposition product. Thermogravimetric analysis (TGA) on the catalyst precursors $[PdCl_2(PMe_3)_2/SiO_2]$ and $[PdI_2(PMe_3)_2/SiO_2]$ showed that total weight loss values were consistent with the formation of a 5 % palladium-on-silica catalyst from the supported complexes, which confirmed that the expected palladium loading was attained. Under the conditions used to record the TGA spectra, all the phosphine and halide were removed.

5.6.2 Catalyst Activation/Deactivation - Supported Mononuclear Catalysts

Active catalysts were produced by the hydrogen reduction of $[PdX_2(PMe_3)_2/SiO_2]$ in the presence of cinnamaldehyde. Reactions were carried out at 135°C. Upon addition of hydrogen gas, the precursors again rapidly changed in appearance to form a black material. It is interesting to note that for a similar system in which polyolefins were hydrogenated using $PdCl_2$ supported on phosphinated polystyrene, a colour change from yellow in the precursor to grey/green was observed during the reaction. No explanation was offered for this behaviour and when the system was examined to determine whether the active catalyst was the palladium(II) complex or palladium metal, the authors established that any Pd(0) formed was catalytically inactive (18).

With regards to the cinnamaldehyde system, the monomer catalysts were shown to be selective for hydrocinnamaldehyde, although differences in activity were observed. In each case no phenylpropanol was produced. The hydrogenation of cinnamaldehyde over the mononuclear catalysts proceeded after the formation of a hydrocarbonaceous over-layer. The same situation was also observed for the binuclear catalysts. The

percentage of C and H laid down on the surface was established by mass balance calculations. 8.1 ± 0.2 % of the total amount of cinnamaldehyde contributed to the hydrocarbonaceous over-layer for the chloro-catalyst, 7.3 ± 0.2 % for the bromo-catalyst and 11.2 ± 0.3 % for the iodo-catalyst (table 4.36b).

Preliminary studies on a catalyst prepared from $[PdBr_2(PMe_3)_2/SiO_2]$ showed that the reaction occurred extremely slowly at 95°C, with only 3 % conversion to hydrocinnamaldehyde after 48 hours. In view of this lower activity with respect to the binuclear analogue, the reactions for this class of catalyst were carried out at 135°C. This increase in temperature did not significantly affect the rate of reaction for the mononuclear bromo- or iodo-catalysts, however, and both showed cinnamaldehyde conversion levels of less than 6 %, after 48 hours at 135°C. Microanalysis of a mononuclear bromo-catalyst sample extracted after 48 hours reaction, showed that 81.2 % of the bromide was retained. This was considerably more than for the 50.9 % retained on the binuclear analogue. In view of the higher nucleophilicity of iodide ions towards palladium, and with regard to the microanalysis results obtained on the binuclear bromo- and iodo-catalysts, it was likely that at least as much iodide as bromide would be retained on the mononuclear iodo-catalyst. In addition to the higher observed halide content, the 2:1 phosphorus to palladium ratio observed for the mononuclear complexes versus the 1:1 ratio for the binuclear analogues may also be significant.

The catalyst produced from the mononuclear chloro-catalyst was an enigma. The selectivity of this catalyst was towards hydrocinnamaldehyde, and 100 % conversion of cinnamaldehyde to hydrocinnamaldehyde

occurred after 2 hours reaction. This selectivity deviated from that observed for the binuclear chloro-catalysts. Several early experiments using the mononuclear chloro-catalyst resulted in the production of phenylpropanol as well as hydrocinnamaldehyde, however, and there was some difficulty in obtaining reproducible results. It may be, therefore, that the percentage of halide and phosphine retained for this catalyst varied from reaction to reaction resulting in the observed differences in selectivity.

It appeared likely that the mononuclear catalysts formed the same type of active site as those formed for the binuclear bromo- and iodo-catalysts. Furthermore, these catalysts retained a significantly higher proportion of halide than their binuclear analogues. It is possible therefore that the extra halide retained may simply have hindered C=C co-ordination, resulting in a decrease in reaction rate. No microanalysis data for the phosphorus content of the used mononuclear catalysts were obtained, but in view of the similar chemical nature of the monomers with regard to the binuclear precursors, it seems likely that a significant proportion would also be lost. Therefore, it is possible that the difference in the observed selectivity between the mononuclear chloro catalyst and the binuclear analogue was due to the 'spilling over' of $[PR_3H]^+$ elimination products onto the sites responsible for phenylpropanol formation. In this regard the 2:1 phosphine to palladium ratio may be significant.

5.7 Reaction of Catalysts Prepared from Supported Binuclear Bromo-Palladium Phosphine Complexes with 2-Cyclohexene-1-one

The hydrogenation of 2-cyclohexene-1-one using a [Pd/SiO_2] catalyst (table 4.34), showed that the unsaturated C=C double bond was rapidly and completely hydrogenated. Cyclohexanone was formed in 100 % yield after approximately 48 hours reaction at 95°C and no cyclohexanol was observed. The reaction proceeded without an induction period. In this regard its behaviour mirrored the reaction of [Pd/SiO_2] with cinnamaldehyde, although, unlike the cinnamaldehyde reaction, no hydrogenation of the C=O function was observed.

Catalysts prepared from the precursors [$Pd_2Br_4(PR_3)_2/SiO_2$] (R=Me, Pr^i), were then used in the liquid phase hydrogenation of 2-cyclohexene-1-one, at 95°C. Preparation of the precursors is described in section 3.3.

Investigation of the hydrogenation activities and selectivities of the catalysts prepared from [$Pd_2Br_4(PR_3)_2/SiO_2$] (R=Me, Pr^i), towards 2-cyclohexene-1-one, were carried out to investigate how the nature of the substrate affected the reaction. The rates of reaction, however, were very slow. The catalyst prepared from [$Pd_2Br_4(PMe_3)_2/SiO_2$], gave less than 1 % conversion to the saturated ketone after 24 hours (table 4.35b), whereas for [$Pd_2Br_4(PPr^i_3)_2/SiO_2$], only 4 % of the saturated ketone was formed after 45 hours (table 4.35). The small difference in rate may have been the result of differences in the bulkiness of the associated phosphine groups. A similar rate effect was observed for the binuclear catalysts used in the cinnamaldehyde reactions.

Interestingly, the introduction of hydrogen gas and 2-cyclohexene-1-one, did not result in immediate catalyst activation and approximately 21 hours were required before the precursor turned black. For the same conditions, but in the presence of cinnamaldehyde instead of 2-cyclohexene-1-one, rapid catalyst activation was observed. It appeared therefore, that the 2-cyclohexene-1-one was stabilising the active catalyst intermediate. The platinum atom in the complex $[Pt(PhCH=CHCHO)(PPh_3)_2]$, co-ordinated to cinnamaldehyde through the C=C functionality. 2-cyclohexene-1-one has a cis geometric configuration, whereas cinnamaldehyde is found only in the trans form. For olefins, the cis isomers are more strained than the trans analogues and some of this strain is released upon complex formation (96). The actual bonds formed between cis olefins and metals are also stronger, as a result of the minimisation of non bonded interactions. Similar interactions may lead to the stabilisation of the active intermediate formed from the reaction of 2-cyclohexene-1-one with the catalyst precursors $[Pd_2Br_4(PR_3)_2/SiO_2]$ (R=Me, Pr^i), resulting in the observed activity. It appeared, therefore, that the catalyst system associated with the binuclear bromo-and iodo-precursors was sensitive to the geometric configuration of the substrate. The selectivity observed for $[Pd/SiO_2]$ and for the catalysts prepared from $[Pd_2Br_4(PR_3)_2/SiO_2]$ (R=Me, Pr^i) was expected in view of the low hydrogenation activity of palladium towards aliphatic ketones (97).

5.8 General Conclusions

The initial hydrogen activation of the supported binuclear catalyst precursors [$Pd_2X_4(PR_3)_2/SiO_2$] resulted in the formation of an active catalyst material which was visibly different from the precursor. The oxidation state of palladium in the bromo-catalyst precursor was +2 and no change in this oxidation state was observed after activation. Several hours reaction were required before Pd(0) was observed. The chloro-catalyst precursor, however, was less stable and partial decomposition to Pd(0) occurred when the complex was impregnated onto the support. Further reduction of Pd(II) to Pd(0) occurred upon activation and the majority of the material prepared from the chloro-catalyst was in the form of Pd(0) after 48 hours reaction.

The hydrogenation of cinnamaldehyde using catalysts prepared from the binuclear catalyst precursors [$Pd_2X_4(PR_3)_2/SiO_2$], therefore, gradually led to the conversion of Pd(II) to Pd(0) containing materials, although, for all the catalysts examined some X and P was retained.

The supported mononuclear precursors [$PdX_2(PMe_3)_2/SiO_2$], in view of their similar chemical nature and reactivity, were also likely to operate in a similar manner.

The liquid phase hydrogenation activities of these solid materials were dependent on the presence or absence of a support and on the physical nature of the precursors. The hydrogenation of cinnamaldehyde took place in the presence of a hydrocarbonaceous over-layer, the formation of which was shown to coincide with induction periods observed for all the catalysts prepared from supported palladium phosphine complexes studied at reaction temperatures of 95°C or less. Mass balance calculations indicated

that between 7 % and 12 % of the initial concentration of cinnamaldehyde contributed to the formation of this layer. Elevated C and H % values measured by microanalysis for the used catalysts were also observed.

Cinnamyl alcohol may adsorb to form a similar over-layer in the case of the catalysts formed from $[Pd_2Cl_4(PMe_3)_2/SiO_2]$ and $[Pd/SiO_2]$ but hydrocinnamaldehyde does not contribute to the activation process since only $[Pd/SiO_2]$ showed any activity in the hydrogenation of hydrocinnamaldehyde and even then this reaction was found to proceed at a very slow rate. The failure to detect an induction period over $[Pd/SiO_2]$ indicated that the hydrocarbonaceous over-layer was formed on this catalyst more rapidly than on catalysts formed from $[Pd_2X_4(PR_3)_2/SiO_2]$ and this was reflected in the rate constant value (k) for the reaction of cinnamaldehyde over $[Pd/SiO_2]$ at 95°C. It appeared that partial loss of halide and/or phosphine, or surface restructuring was occurring on the catalysts formed from $[Pd_2X_4(PR_3)_2/SiO_2]$ during the induction period and it was likely that the same processes were occurring for the catalysts formed from $[PdX_2(PR_3)_2/SiO_2]$. Furthermore, it was likely that the catalysts thus formed, unlike the $[Pd/SiO_2]$ catalyst, were continuously changing during the course of the reactions since they were slowly being deactivated during use. The retained halides and phosphines which were shown to control the activities and selectivities of the catalysts, may become labile under reaction conditions and interact with other active sites to promote further restructuring, which ultimately may be responsible for catalyst deactivation. Deactivation of the catalysts may also occur as a result of extensive metal clustering.

In Summary

The hydrogenation of cinnamaldehyde using [Pd/SiO_2] leads to the formation of hydrocinnamaldehyde and phenylpropanol at Pd(0) sites. The active sites responsible for the formation of hydrocinnamaldehyde on the supported binuclear bromo- and iodo-catalyst precursors, appeared, however, to be associated with Pd(II). This Pd(II) containing material was slowly converted to Pd(0) as the reaction proceeded. No phenylpropanol was formed on the Pd(0) sites formed on the bromo- and iodo-catalysts, however, presumably as a result of poisoning by the phosphine and/or halide ligands displaced in the reaction. For the supported binuclear chloro-precursors, some decomposition occurred at the impregnation stage to form both Pd(II) and Pd(0) and the proportion of Pd(0) steadily increased with reaction time. The proportion of Pd(0) found in the used chloro-catalysts was considerably greater than that observed in the analogous bromo-catalysts, which accounted for the formation of phenylpropanol. The formation of hydrocinnamaldehyde on the chloro-catalysts was much quicker initially than that of phenylpropanol, however, which reflected the initial low availability of these Pd(0) sites. The selectivities of the catalysts formed from the mononuclear precursors mirrored that of the supported binuclear bromo- and iodo-catalysts. The lower activity, however, can possibly be ascribed to the increased proportion of retained halide.

The low activity of the catalysts prepared from [$Pd_2Br_4(PR_3)_2/SiO_2$] (R=Me, Pr^i) in the hydrogenation of 2-cyclohexene-1-one was attributed to the increased stability of the reactive metal-olefin intermediate.

REFERENCES

REFERENCES

1. J. Tropfast., *Chem. Britain.* **26**, 432 (1990).

2. C. G. Bernhard., "Through France with Berzelius: live scholars and dead volcanoes", Pergamon Press, New York (1989).

3. S. J. Thomson and G. Webb., "Heterogeneous Catalysis", Oliver and Boyd, Edinburgh (1968).

4. P. W. Atkins., "Physical Chemistry, 4th Edition", Oxford University Press", Oxford, 477 (1990).

5. V. Ponec and G. C. Bond., "Catalysis by Metals and Alloys", Elsevier, Amsterdam, Vol **95**, 477 (1990).

6. S. A. Goddard, R. D. Cortright and J. A. Dumesic., *J. Catal.* **137**, 186 (1992).

7. P. Sabatier and J. B. Sendersons., *Compt. Rend.* **135**, 87 (1902).

8. R. Hubaut, J. P. Bonnelle and M. Daage., *Appl. Catal.* **22**, 231 (1986).

9. J. Jenck and J. E. Germain., *J.Catal.* **65**, 141 (1980).

10. P. N. Rylander., "Catalytic Hydrogenation over Platinum Group Metals", Academic Press, New York and London, 4 (1967).

11. M. L. Bender., "Mechanism of Homogeneous Catalysis - from Protons to Proteins", Wiley-Interscience, New York (1971).

12. L. H. Pignolet (Ed)., "Homogeneous Catalysis with Metal Phosphine Complexes", Plenum Press, New York and London (1983).

13. P. K. Santra and C. R. Saha., *J. Mol. Catal.* **39**, 279 (1987).

14. D. K. Mukherjee, B. K. Palit and C. R. Saha., *Indian J. Chem., Sect. A.* **31**, 243 (1992).

15. A. A. Naiini, H. M. Ali and C. H. Brubaker., *J. Mol. Catal.* **67**, 47 (1991).

16. H. Brunner, W. Pieronczyk, B. Schönhanmer, K. Streng, I. Bernal and J. Korp., *Chem. Ber.* **114**, 1137 (1981).

17. B. M. Choudary, K. Ravi. Kumar and M. L. Kantam., *J. Catal.* **130**, 41 (1991).

18. H. Bruner and J. C. Bailar., *Inorg. Chem.* **12**, 1465 (1973)

19. G. Braca, A. M. Raspolli Galletti, M. Di. Girolamo, G. Sbrana, R. Silla, P. Farrarini., *J. Mol. Catal. A (Chemical).* **96**, 203 (1995).

20. K. G. Allum, R. D. Hancock, I. V. Howell, S. McKenzie, R. C. Pitkethly and P. J. Robinson., *J. Organomet. Chem.* **87**, 203 (1975).

21. D. G. H. Ballard., *Adv. Catal.* **23**, 263 (1973).

22. J. Blümel., *Inorg. Chem.* **33**, 5050 (1994).

23. P. N. Rylander., "Catalytic Hydrogenation over Platinum Group Metals", Academic Press, New York and London, Ch 14 (1967).

24. P. N. Rylander., "Catalytic Hydrogenation in Organic Synthesis", Academic Press, New York, San Fransisco and London, Ch 5 (1979).

25. E. B. Maxted and S. Akhtar., *J. Chem. Soc.* 3130 (1959).

26. W. H. Carothers and R. Adams., *J. Am. Chem. Soc.* **45**, 1071 (1923).

27. S. Galvagno, A. Donato, G. Neri, R. Pietropaolo and D. Pietropaolo., *J. Mol. Catal.* **49**, 223 (1989).

28. O. A. Moe, D. T. Warner, M. I. Buckley., *J. Am. Chem. Soc.* **73**, 1062 (1951).

29. V. Voorhees and R. Adams., *J. Am. Chem. Soc.* **44**, 1397 (1922).

30. V.I. Sharkov., *Angew. Chem., Int. Ed. Engl.* **2**, 405 (1963).

31. J. G. E. Cohn., German Patent 1,082,245, May 25 (1960).

32. R. W. Meschke, W. H. Hartung., *J. Org. Chem.* **25**, 137 (1960).

33. R. L. Shriner, and R. Adams., *J. Am. Chem. Soc.* **46**, 1683 (1924).

34. N. Campbell, W. Anderson and J. Gilmore., *J. Chem. Soc.* 819 (1940).

35. W. H. Carothers and R. Adams., *J. Am. Chem. Soc.* **46**, 1675 (1924).

36. A. A. Ponamarev, A. S. Cheyola., *Dokl. Akad. Nauk SSSR*, **145**, 812 (1962).

37. B. Coq, P. S. Kumbhar, C. Moreau, P. Moreau and M. G. Warawdekar., *J. Mol. Catal.* **85**, 215 (1993).

38. A. Chambers, PhD Thesis., " The Hydrogenation of Cinnamaldehyde over Silica Supported Copper and Modified Copper Catalysts", University of Glasgow (1994).

39. J. Phillips, P. Gallezot and G. Bergeret., *J. Mol. Catal.* **78**, 295 (1993).

40. M. Arai, K. Usui and Y. Nishiyama., *J. Chem. Soc., Chem. Commun.* **2**, 1853 (1993).

41. Y. Nitta, K. Ueno and T. Imanaka., *Appl. Catal.* **56**, 9 (1989).

42. S. Galvagno, A. Donato, G. Neri, R. Pietropaolo and G. Capannalli., *J. Mol. Catal.* **78**, 227 (1993).

43. M. T. Bogert and G. Powell., *J. Am. Chem. Soc.* **53**, 2747 (1931).

44. F. Straus, H. Grindel., *Ann. Chem. Liebigs*. **439**, 276 (1924).

45. R. Hubaut, J. P. Bonnelle and M. Daage., *J. Mol. Catal.* **55**, 170 (1989).

46. P. Gallezot, A. Giroir-Fendler and D. Richard., "Heterogeneous Catalysis and Fine Chemicals", M. Guisnet, J. Barrault, C. Bouchoule, D. Perez, C. Montassier and G. Perot (Eds), Elsevier, Amsterdam, 171 (1988).

47. J. Kaspar, M. Graziani, G. P. Escobar, A. Trovarelli., *J. Mol. Catal.* **72**, 243 (1992).

48. F. Coloma, A. Sepúlveda-Escribano, F. Rodríguez-Reinoso., *Appl. Catal A. (General).* **123**, L1 (1995).

49. M. A. Vannice and B. Sen., *J. Catal.* **115**, 65 (1989).

50. G. J. Hutchings, F. King, I. P. Okoye and C. H. Rochester., *Appl. Catal A. (General).* **83**, L7 (1992).

51. D. Burn, G. Cooley, M. T. Davies, J. W. Ducker, B. Ellis, P. Feather, A. K. Hiscock, D. N. Kirk, A. P Leftwick, V. Petrow, D. M. Williamson., *Tetrahedron*, **20**, 597 (1964).

52. V. Ponec and G. C. Bond., "Catalysis by Metals and Alloys", Elsevier, Amsterdam, Vol **95**, 512 (1990).

53. G. W. Roberts., "Catalysis in Organic Synthesis", P. N. Rylander, H. Greenfield (Eds), Academic Press, London, 1 (1976).

54. D. L. Trimm, "Design of Industrial catalysts", Elsevier, Amsterdam, 91 (1980).

55. R. K. Iler, "The Chemistry of Silica", Wiley Interscience, New York (1979).

56. A. V. Kiselev., Kolloidn. Zh. **2**, 17 (1936).

57. C. J. Brinker, G. W. Scherer, "Sol Gel Science" Academic Press, New York, Ch 10.

58. R. Ugo (ed), "Aspects of Homogeneous Catalysis", Kluwer Academic Publishers, Netherlands, Vol **7**, 85 (1990).

59. A. Zecchina, C. O. Arean., *Catal. Rev.-Science. Eng.* **35(2)**, 261 (1993).

60. H. H. Lamb, B. C. Gates and H. Knozinger., *Angew. Chem., Int. Ed. Engl.* **27**, 1127 (1988).

61. D. C. Bailey and S. H. Langer., *Chem. Rev.* **81**, 109 (1981).

62. A. N. Patil, M. A. Bañares, X. Lei, T. P. Fehlner and E. E. Wolf., *J. Catal.* **159**, 458 (1996).

63. F. J. Karol, C. Wu, W. T. Reichle and N. J. Maraschin., *J. Catal.* **60**, 68 (1979).

64. G. Braca, G. Sbrana, A. M. Raspolli-Galletti, A. Altomare, G. Arribas, M. Michelotti and F. Ciardelli., *J. Mol. Catal. A (Chemical).* **107**, 113 (1996).

65. M. D. Ward and J. Schwartz., *J. Mol. Catal.* **11**, 397 (1981).

66. Y. Iwasawa, K. Asakura, H. Ishii and H. Kuroda., *Z. Phy. Chem. (N.F).* **144**, 105 (1985).

67. B. Didillon, J. P. Candy, F. Le Peletier, O. A. Ferretti and J. M. Basset, "Heterogeneous Catalysis and Fine Chemicals III", M. Guisnet *et al* (Eds), Elsevier Science, 147 (1993).

68. B. Didillon, J. P. Candy, A. El. Mansour, C. Houtmann and J. M. Basset., *J. Mol. Catal.* **74**, 43 (1992).

69. J. F. Moulder, "Handbook of X-ray Photoelectron Spectroscopy", Perkin Elmer Corporation, New York (1992).

70. D. Briggs and M. P. Seah, (Eds)., "Practical Surface Analysis, by Auger and X-ray Photoelectron Spectroscopy", Wiley and Sons Ltd, New York (1983).

71. W. D. Ehmann, D. E. Vance, "Radiochemistry and Nuclear Methods of Analysis", Wiley and Sons Inc, Vol **116** (1991).

72. G. Choppin, J. Rydberg, J. O. Liljenzin, " Radiochemistry and Nuclear Chemistry, 2nd Ed", Butterworth-Heinemann Ltd, Oxford, (1995).

73. J. G. Evans, P. L. Goggin, J. G. Smith., *J. Chem. Soc. A*. 464 (1968).

74. R. J. Goodfellow, S. R. Haddock, J. R. Knight, F. J. S. Reid and B. F. Taylor., *J. Chem. Soc., Dalton Trans*. 523 (1974).

75. D. A. Duddell, J. G. Evans, P. L. Goggin, R. J. Goodfellow, A. J. Rest and J. G. Smith., *J. Chem. Soc. A*. 2134 (1969).

76. J. G. Verkade and L. D. Quin, (Eds)., "Methods in Stereochemical Analysis", VCH Publishers, Florida, **8**, 506 (1987).

77. N. W. Alcock, T. J. Kemp and F. L. Wimmer., *J. Chem. Soc., Dalton Trans*. 635 (1981).

78. B. E. Mann, B. L. Shaw and R. M. Slade., *J. Chem. Soc. A*. 2976 (1971).

79. J. E. Ferguson and P. R. Heveldt., *Inorg. Chim. Acta.* **31**, 145 (1978).

80. J.Chatt and L.M. Venanzi., *J. Chem. Soc. A.* **2**, 2351 (1957).

81. R. Uson, J. Fornies and F. Martinez., *J. Organomet. Chem.* **132**, 429 (1977).

82. S. O. Grim and R.L. Keiter., *Inorg. Chim. Acta.* **4**, 56 (1970).

83. F. R. Hartley., *J. Organomet. Chem. Rev. A.* **6**, 119 (1970).

84. G. Webb., *Catal. Today.* **7**, 137 (1990).

85. S. Cenini, R. Ugo and G. La Monica., *J. Am. Chem. Soc. A.* 409 (1971).

86. G. Kumar, J. R. Blackburn, R. G. Albridge, W. E. Moddeman and M. M. Jones., *Inorg. Chem.* Vol **11**, 296 (1972).

87. V. I. Nefedov. Ya, V. Salyn, I. I. Moiseev, A. P. Sadovskii, A. S. Berenbljum, A. G. Knizhnik and S. L. Mund., *Inorg. Chim. Acta.* **35**, L343 (1979).

88. H. Windawi, Z. C. Zhang., *Catal. Today.* **30**, 99 (1990).

89. J. A. Mieth and J. A. Schwartz., *J. Catal.* **118**, 218 (1989); D. W. Goodman and J. E. Houston., *Science.* **236**, 403 (1987).

90. e.g. J. D. Atwood, "Inorganic and Organometallic Reaction Mechanisms", Brooks-Cole, Monterey, 1985.

91. R. Baltzly., *J. Org. Chem.* **41** , 928 (1976).

92. C. A. Tolman., *Chem. Rev.* **77**, 313 (1977).

93. B. C. Gates, J. R. Katzer and G. C. A Schunt., "Chemistry of Catalytic Processes", McGraw-Hill, New York (1971).

94. H. Pines., "The Chemistry of Catalytic Hydrocarbon Conversions", Academic Press, New York, 6 (1981).

95. R. S. Drago, E. D. Nyberg and E. G. El A'mma., *Inorg. Chem.* **20**, 2461 (1981).

96. F. R. Hartley., "The Chemistry of Platinum and Palladium", Applied Science Publishers, London, 377 (1973).

97. P. N. Rylander., "Catalytic Hydrogenation over Platinum Group Metals", Academic Press, New York and London, Ch 15 (1967).